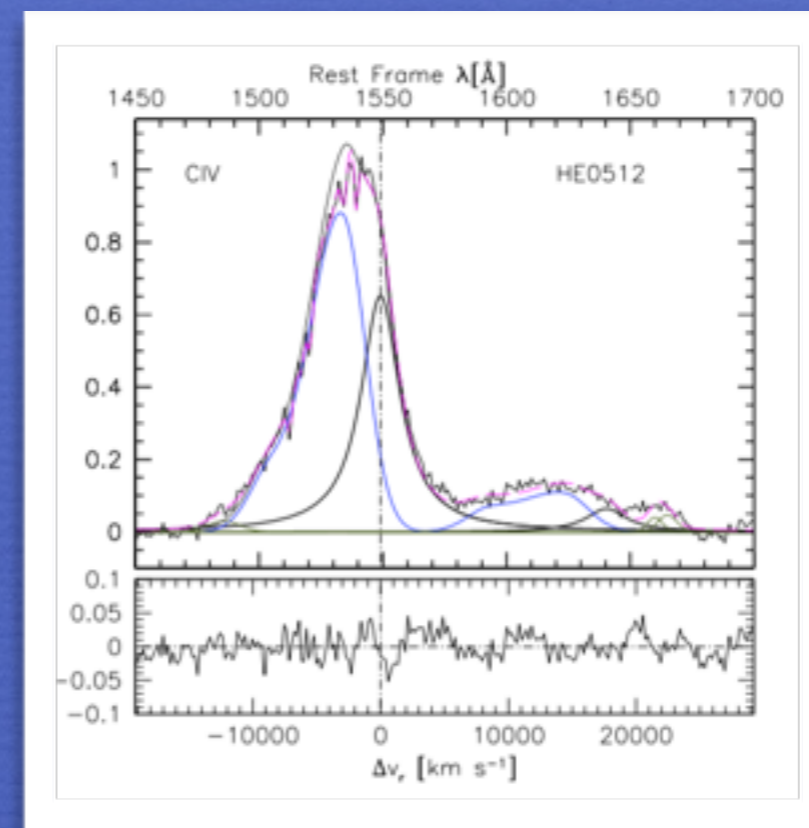
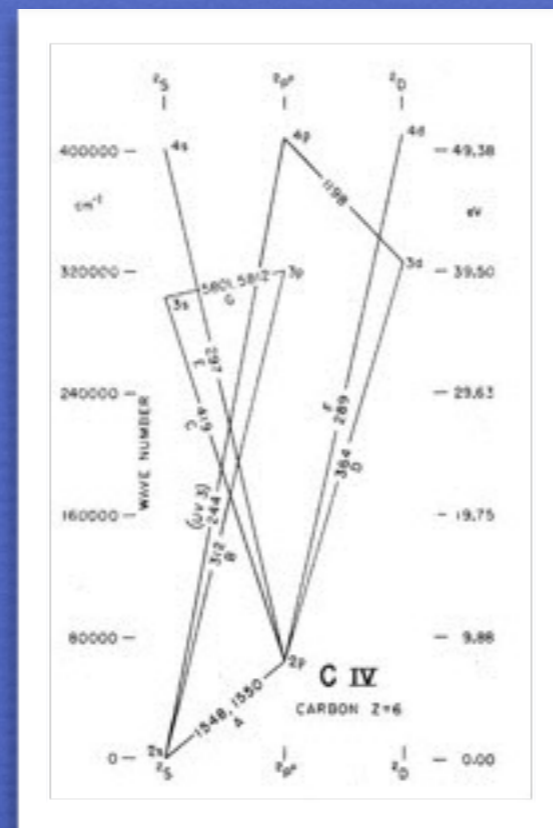


THE MOST POWERFUL QUASAR OUTFLOWS AS SEEN FROM THE CIV $\lambda 1549$ RESONANCE LINE (in emission)



Paola Marziani

INAF, Osservatorio Astronomico di Padova, Italia

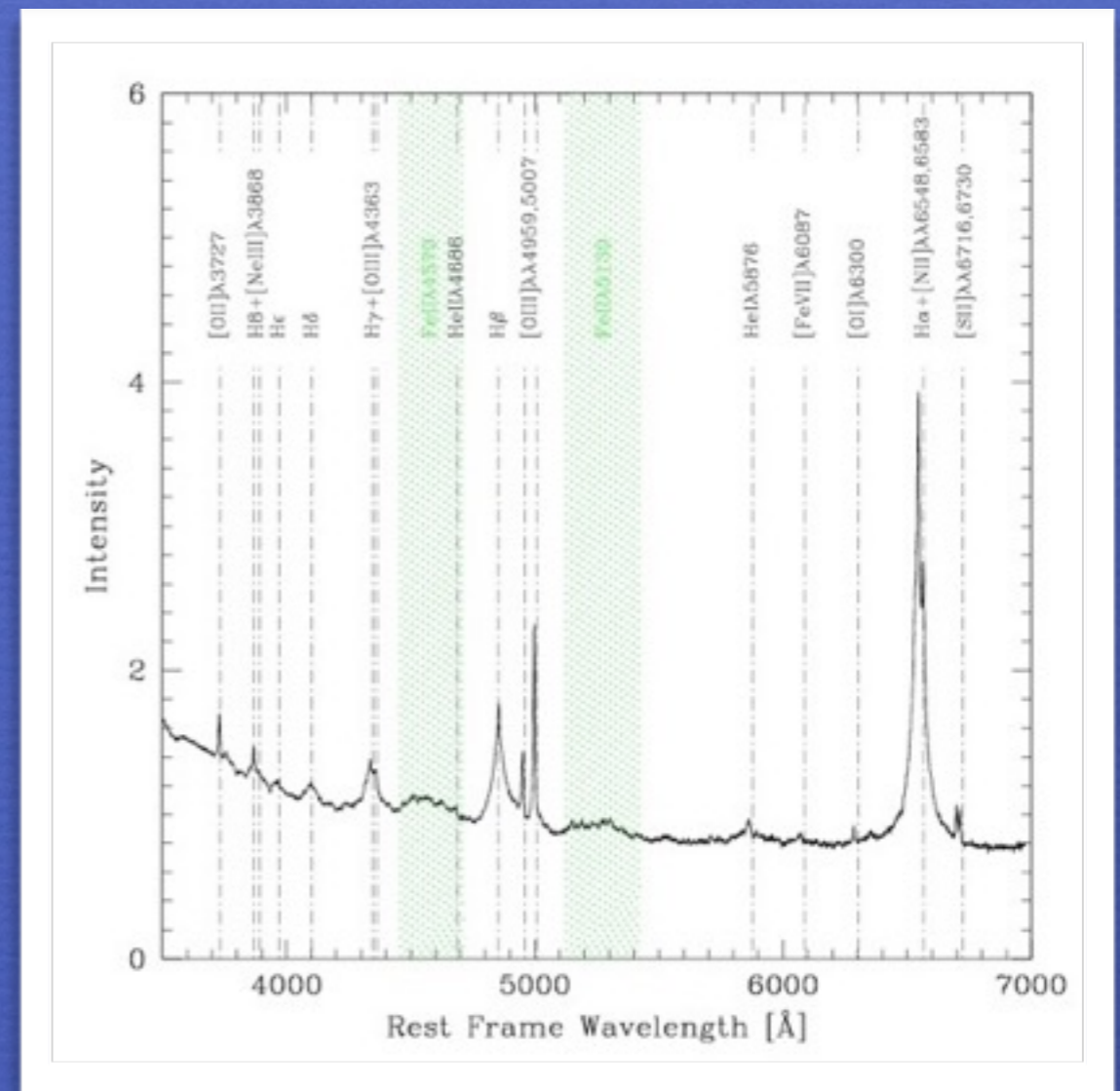
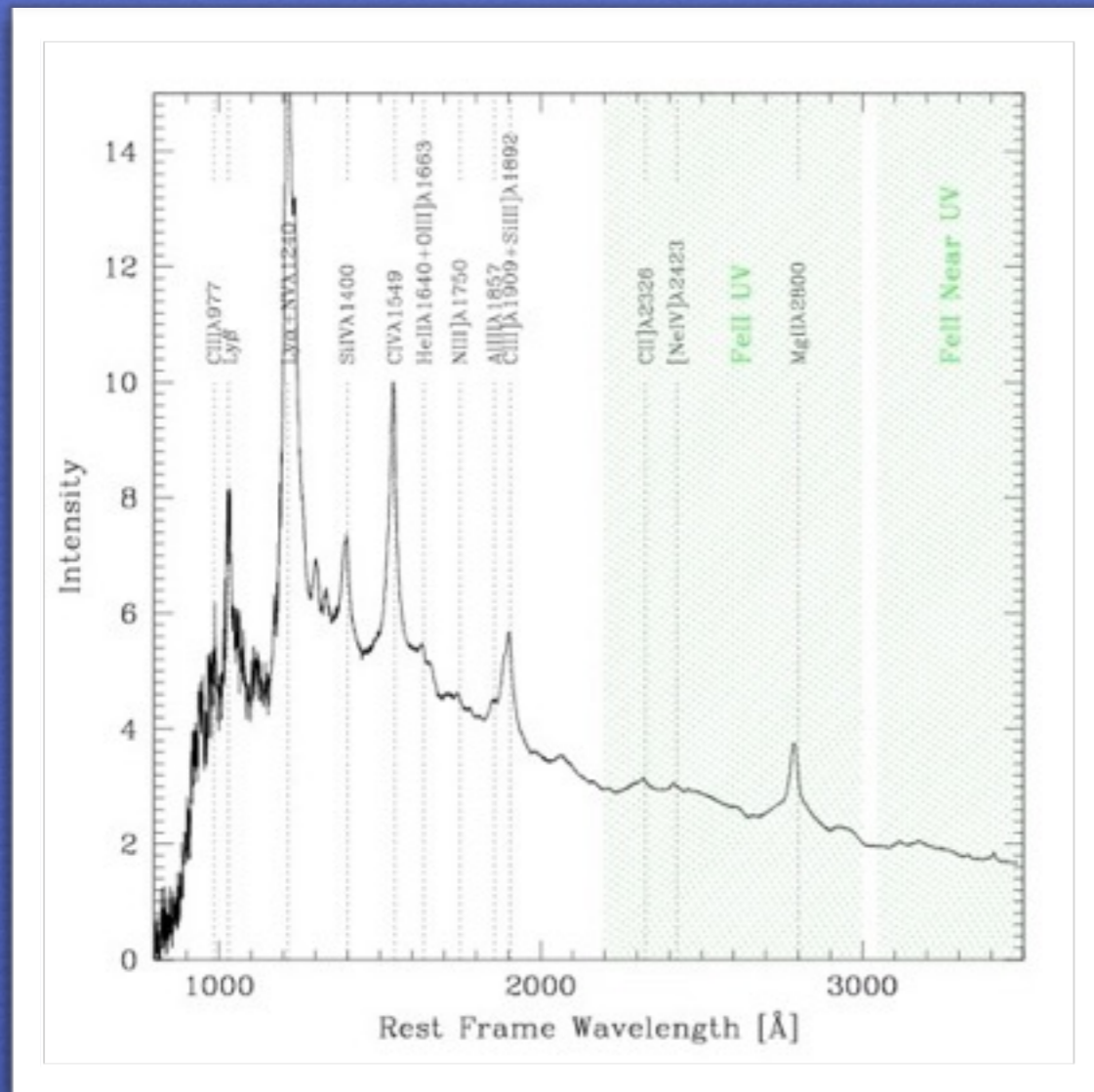
Jack W. Sulentic, Ascensión del Olmo, M. A. Martínez-Carballo

IAA (CSIC), España, Giovanna M. Stirpe, INAF, Osservatorio Astronomico di Bologna, Italia

Quasars' optical and UV spectrum

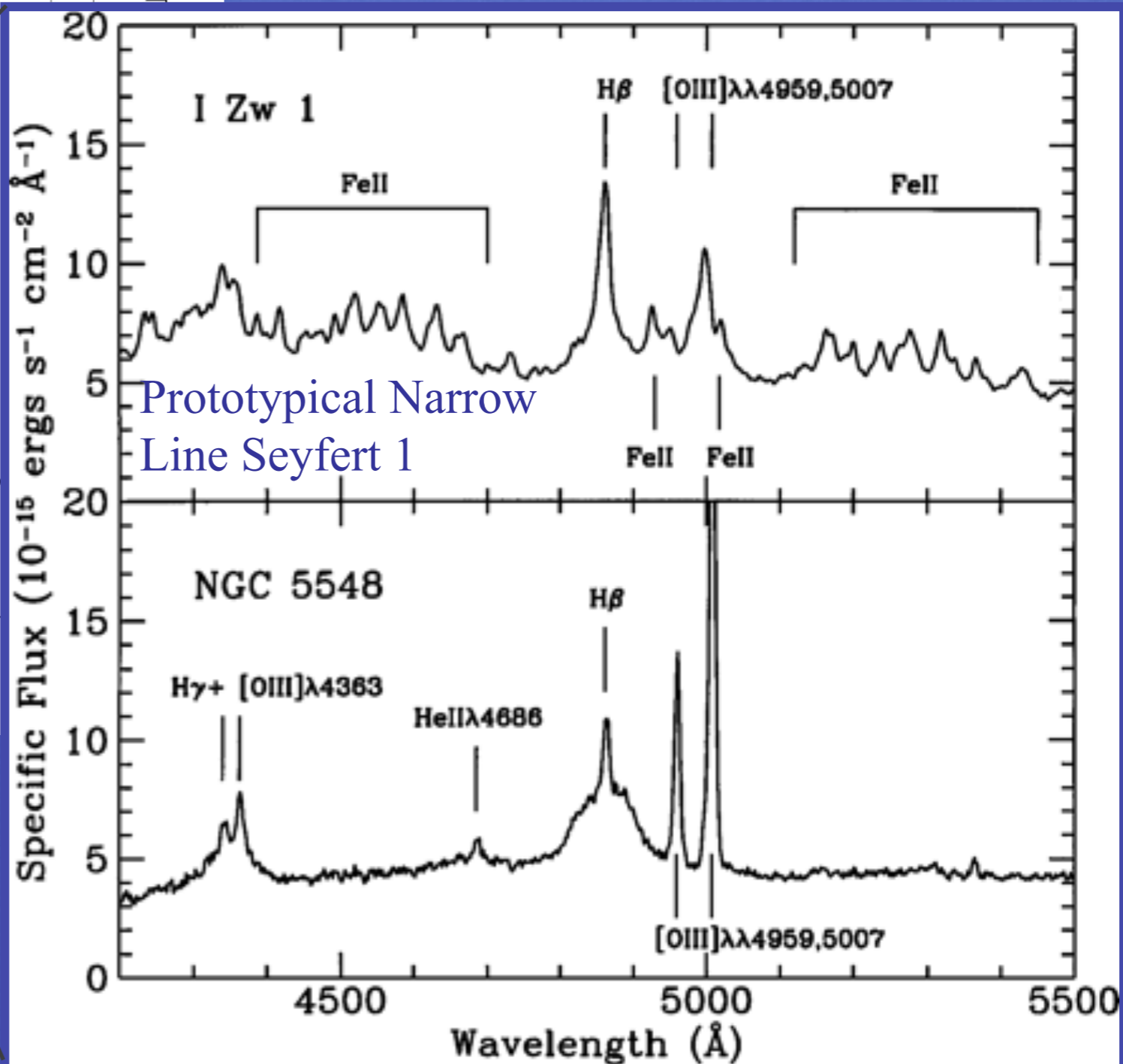
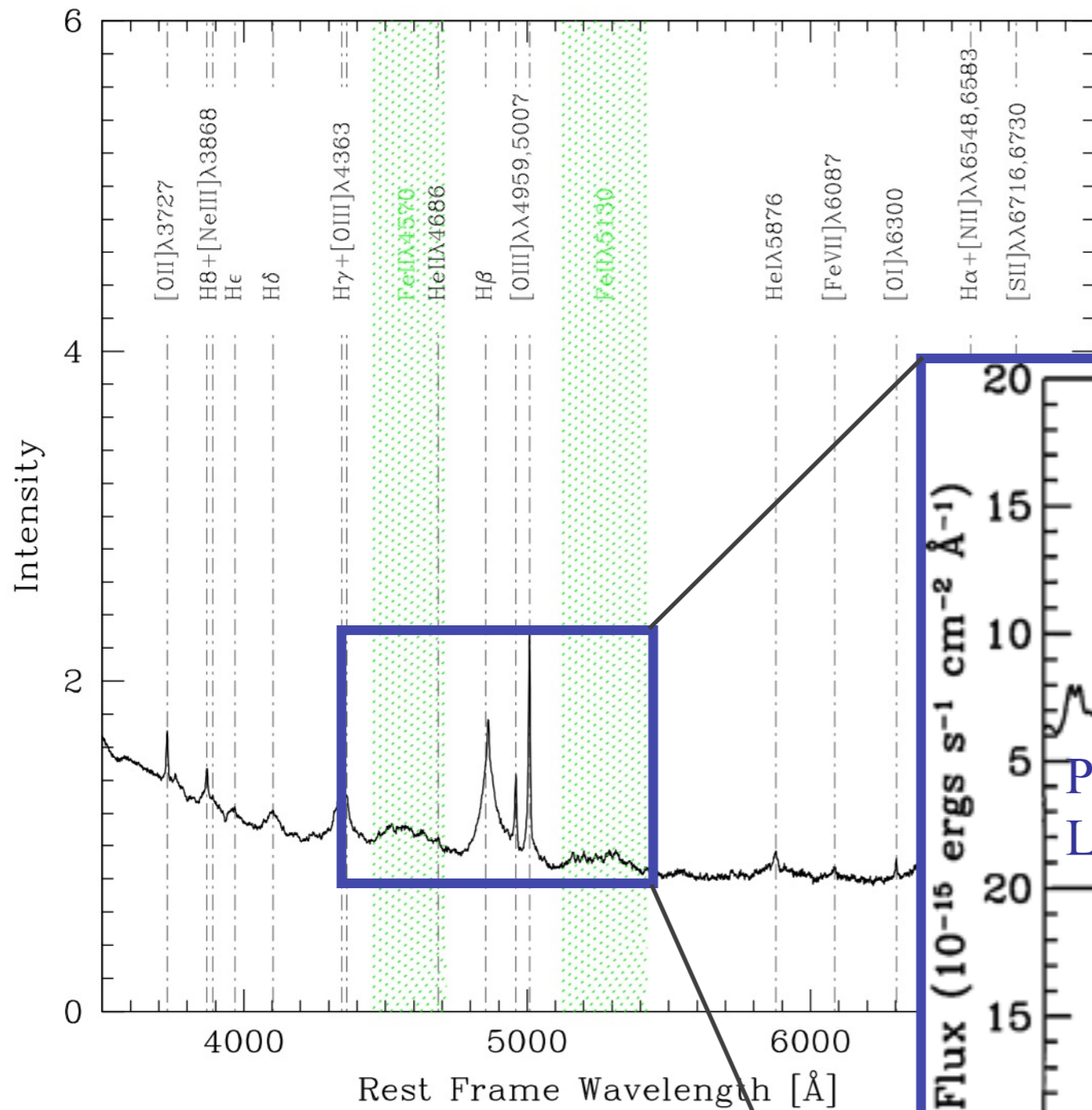
broad and narrow lines emitted by ionic species over a wide range of IPs

	Broad	Narrow
High Ionization	CIV λ 1549, HeII	[OIII] λ 4959,5007, HeII,NeIII
Low Ionization	Balmer (H β), FeII, MgII λ 2800, CaII IR Triplet)	Balmer, [OI] λ 6300,



The composite quasar spectrum from the Sloan DSS (Van den Berk et al. 2001; Marziani et al. 2006)

Quasars do not all show the same spectrum!

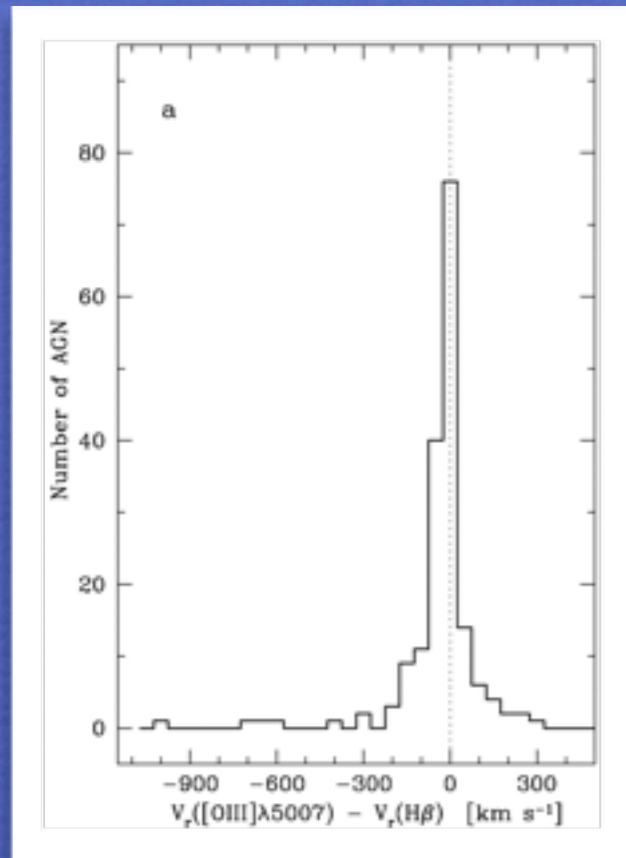


Prototypical Narrow Line Seyfert 1

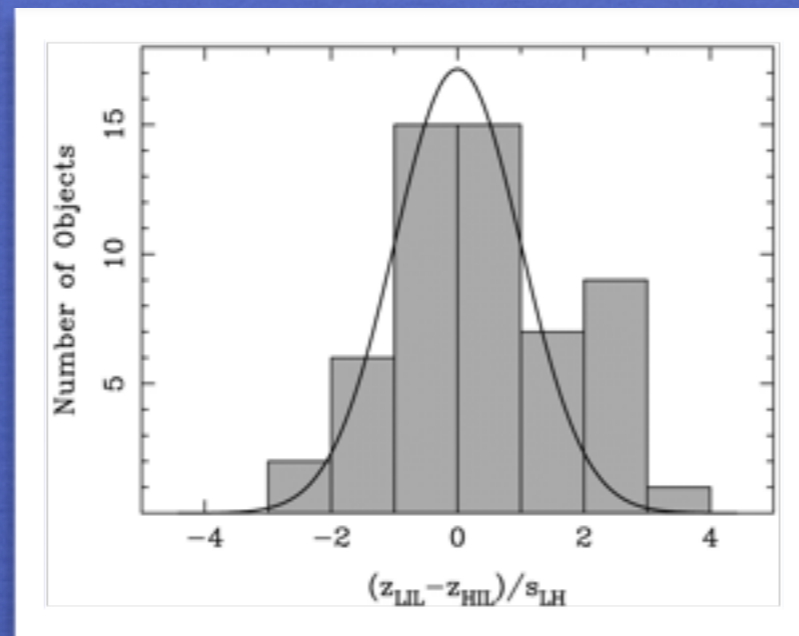
Widely different line profiles, intensity ratios, ionization level

Lines do not all show the same profiles!

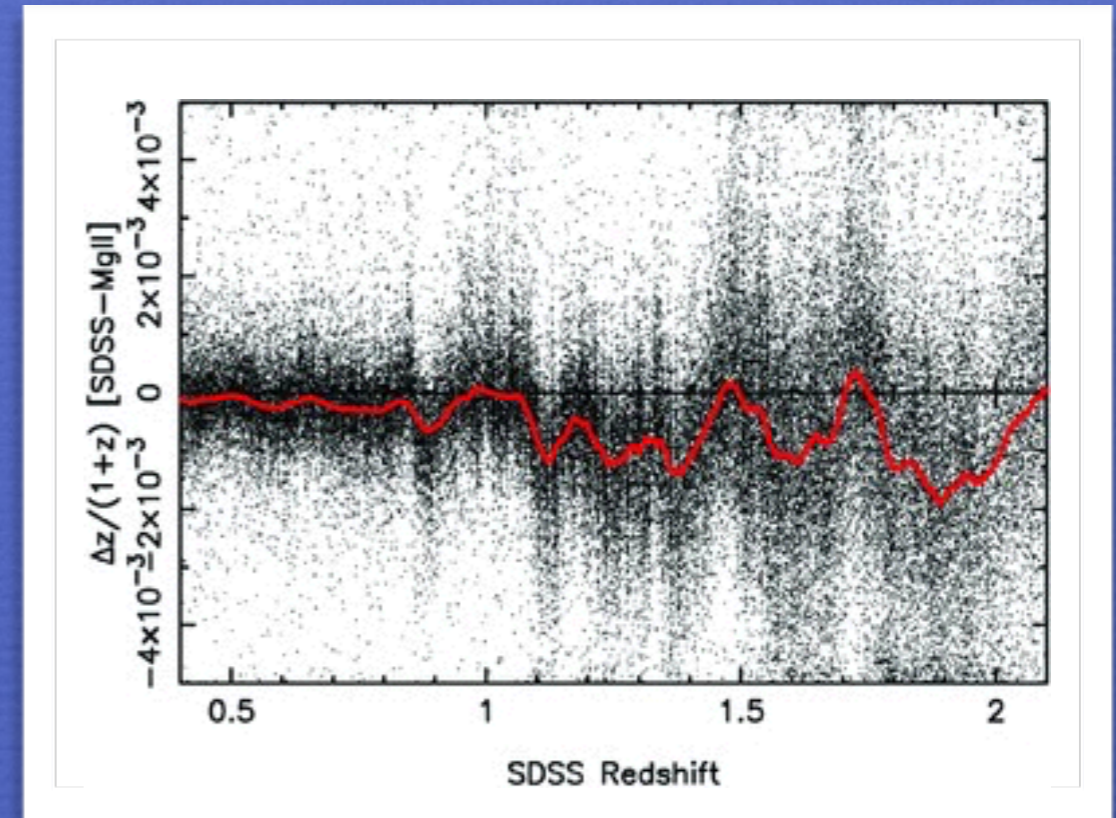
Internal emission line shifts
involve both broad and narrow lines!



Zamanov et al. 2002



Eracleous & Halpern 2003
c.f. Hu et al. 2008



Hewett and Wild 2010

Narrow low-ionization lines such as narrow H β and [OII] λ 3727
best for systemic redshift

Quasar systemic redshift more uncertain if $z > 1$

Internal emission line shifts

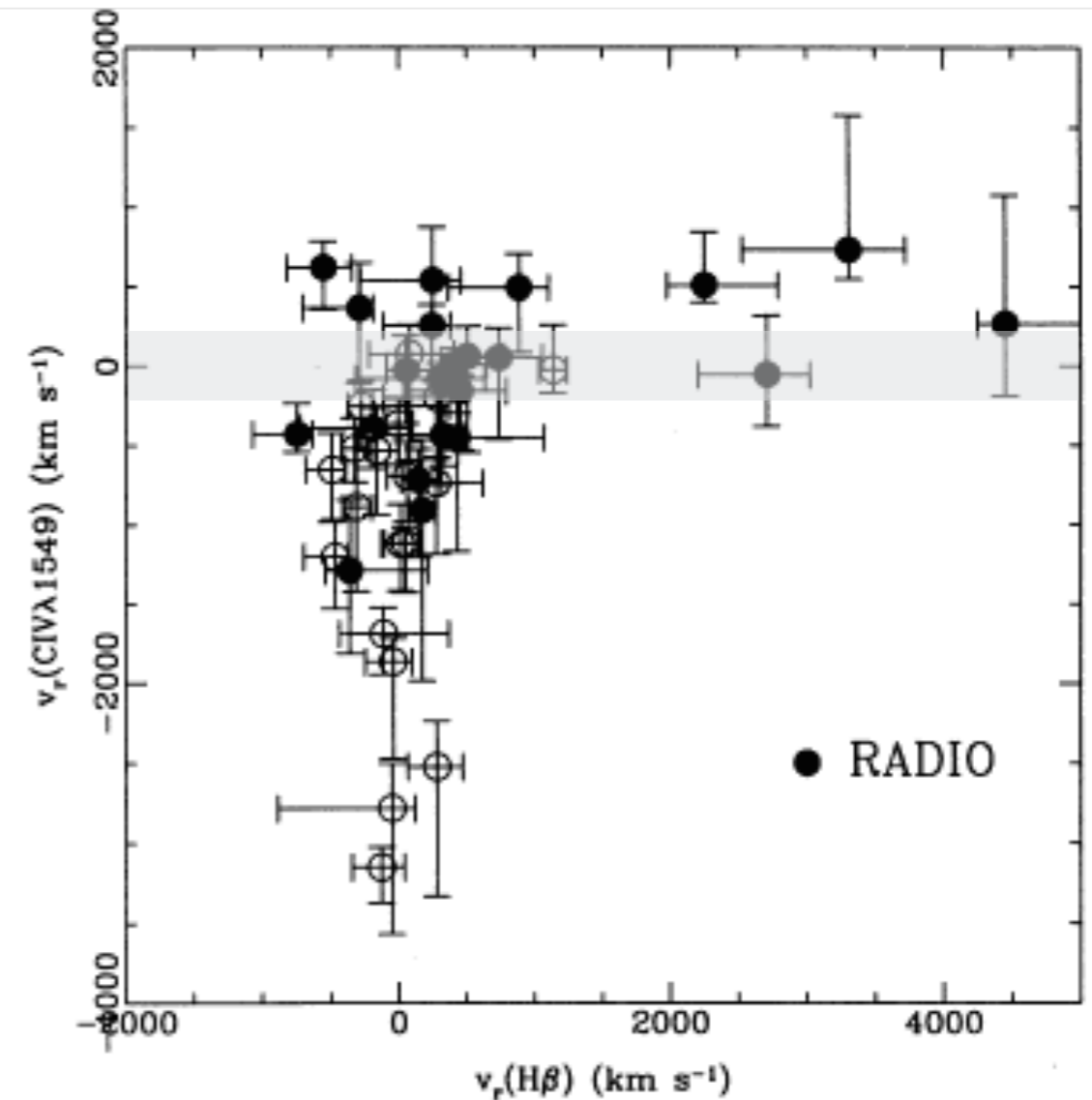
HIL blueshifts provide evidence of outflow
require rest frame knowledge and proper contextualisation

A first contextualisation
(radio quiet vs. radio loud)

TABLE 1
PUBLISHED EMISSION-LINE VELOCITY SHIFTS

Line - Reference Line	Velocity ^a (km s ⁻¹)	N ^b	σ (km s ⁻¹)	Reference
High Ionization - Low Ionization				
C IV - [O III] λ 3727	-40 ± 70	13	230	1
C IV - H α	-1140 ± 290	17	1180	2
C IV - O I λ 1304	-560 ± 120	23	...	3
C IV - O I λ 1304	-1290 ± 180	19	800	4
C IV - C II λ 1335	-1320 ± 400	7	1046	4
C IV - Mg II	-565 ± 100	17	...	3
C IV - Mg II	-460 ± 110	15	410	1
C IV - Mg II	-980 ± 180	26	930	5
C III - Mg II	-600 ± 90	44	600	4
C III - H α	-880 ± 230	16	920	2
Ly α - H α	-1770 ± 370 ^d	11	1230	2
High Ionization - High Ionization				
C IV - C III	120 ± 150	65	1200	4
C IV - C III	-530 ± 110	25	570	5
C IV - Ly α	-400 ± 100	55	...	3
C IV - N V	-170 ± 100	26	...	3
Low Ionization - Low Ionization				
Mg II - [O II]	-200 ± 170	22	810	4
Mg II - [O II]	380 ± 80	12	270	1
Mg II - H α	-140 ± 120	17	510	2
O I - H α	-390 ± 470	4	930	2
[O III] - H β	-220 ± 150	23	730	4
[O II] - [O III]	100 ± 130	6	310	4

^a Mean velocity of first ion in the reference frame of the z given by second ion, $\pm \sigma/\sqrt{N}$.
^b Number of QSOs.
^c Reduces to -780 when two QSOs with -4400 and -2500 are excluded.
^d Reduces to -1420 when one outlier value of -5200 is excluded.
 REFERENCES.—(1) Junkkarinen 1989; (2) Espey et al. 1989; (3) Gaskell 1982; (4) Wilkes 1986; (5) Corbin 1990—excluding BAL QSOs.



(4D) Eigenvector 1 quasar contextualization at low- z

Interpretation of the CIV λ 1549 emission line profile
evidence of outflows

analysis of the CIV λ 1549 line at high- z and very high L
with coverage of H β -spectral range

extreme outflows

(weak lined quasars, (WLQ)s, extreme Pop. A quasars)

feedback on host galaxy?

Organizing quasar spectral diversity — Quasars' (4D) Eigenvector 1

Boroson & Green 1992; see also Gaskell et al. 1999

Originally defined by a Principal Component Analysis of PG quasars, and associated with an anticorrelation between **strength of FeII λ 4570** and **width of H β**

Found in several independent samples

(Dultzin-Hacyan et al. 1997; Shang et al. 2003, Yip et al. 2004, Sulentic et al. 2000, 2007, Kruzcek et al 2011 Tang et al. 2012); Recently confirmed by an analysis of SDSS data (Shen & Ho 2014, Sun & Ho 2015)

Found for multi-dimensional parameter spaces

(Kuraszkiewicz et al. 2008; Mao et al. 2009; Grupe 2004, Wang et al. 2006; Bachev et al. 2004; Sulentic et al. 2007)

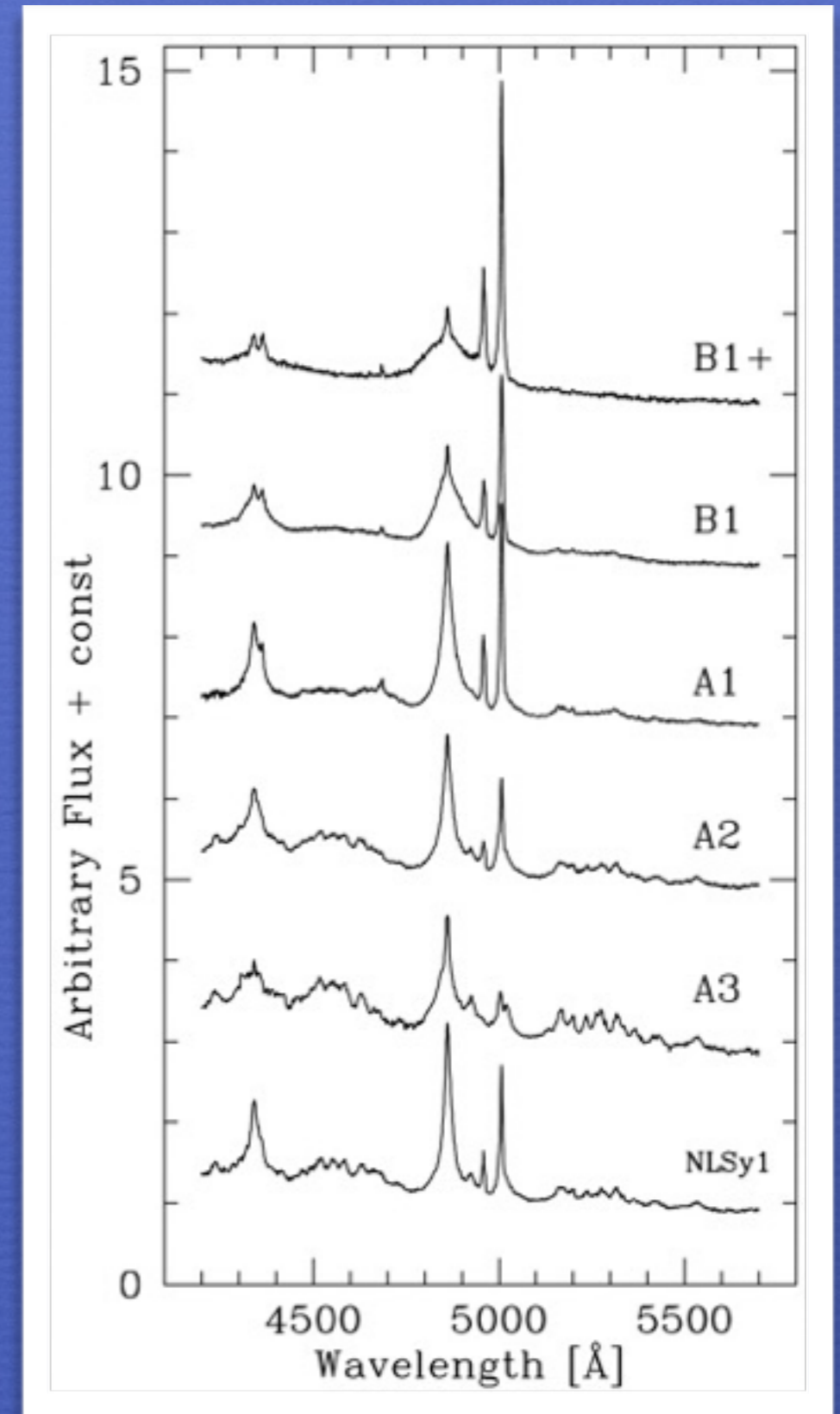
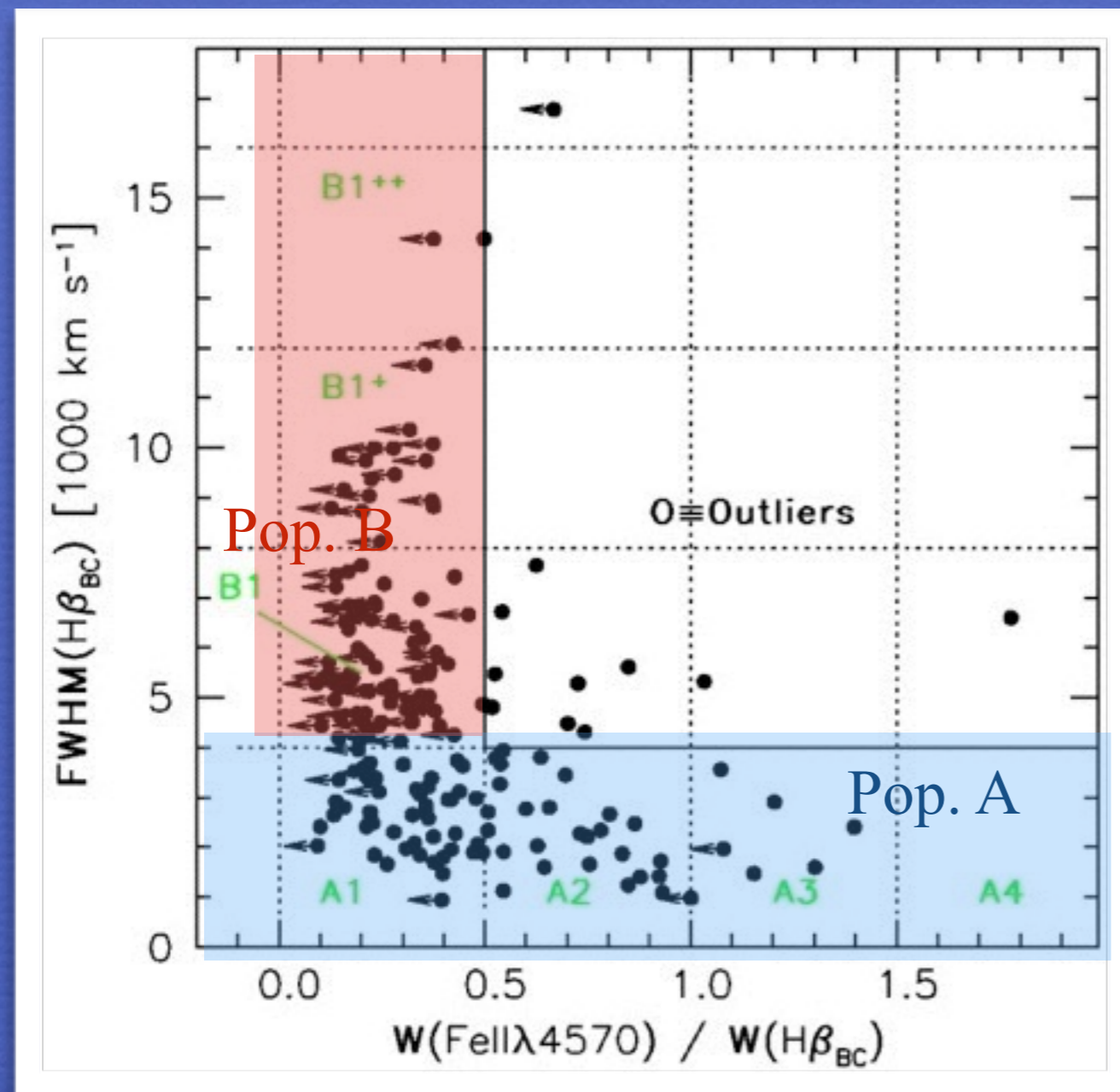
The 4DE1 space of Sulentic et al. includes

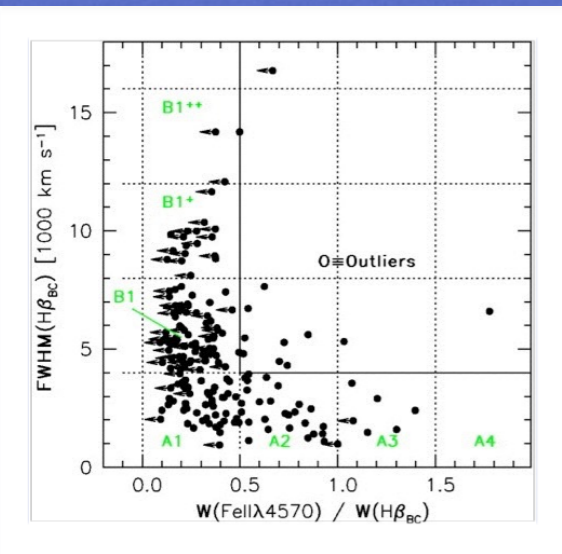
CIV λ 1549 line shift and **soft-X ray photon index**

Eigenvector 2: luminosity effects “Baldwin effect(s)”

e.g. Balwin et al. 1978, Bian et al. 2005

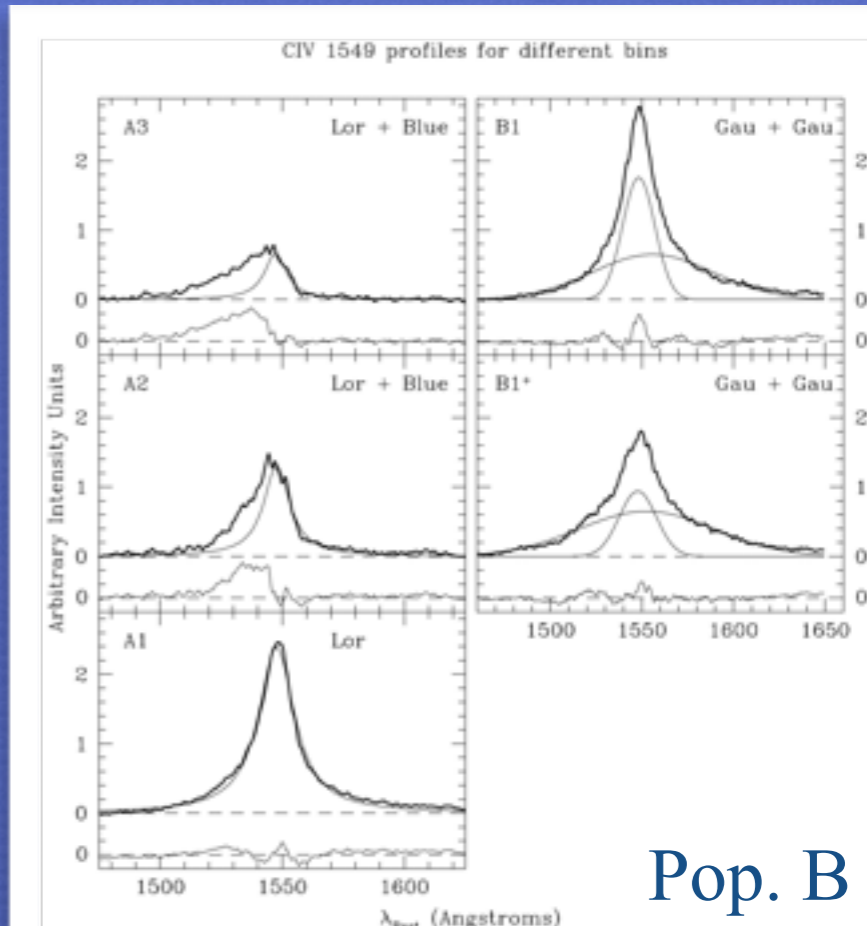
Optical plane of Eigenvector 1: Spectral types in bins along a 1D sequence; Population A and population B



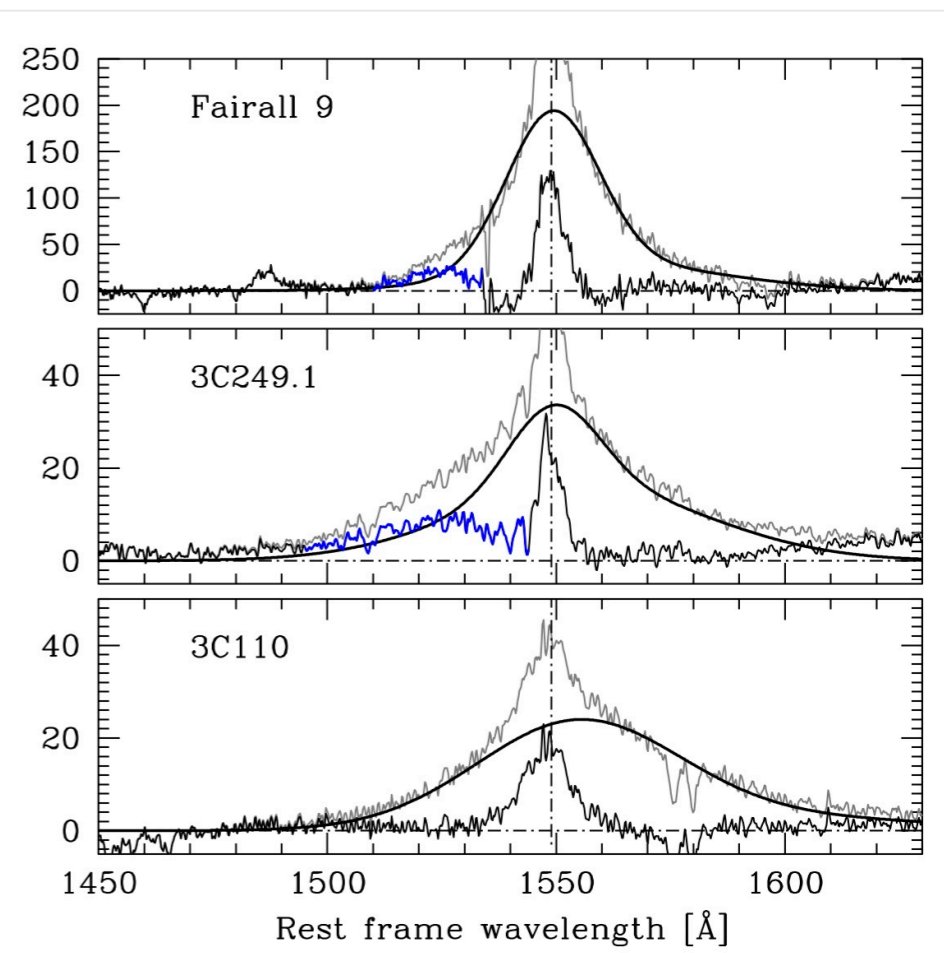
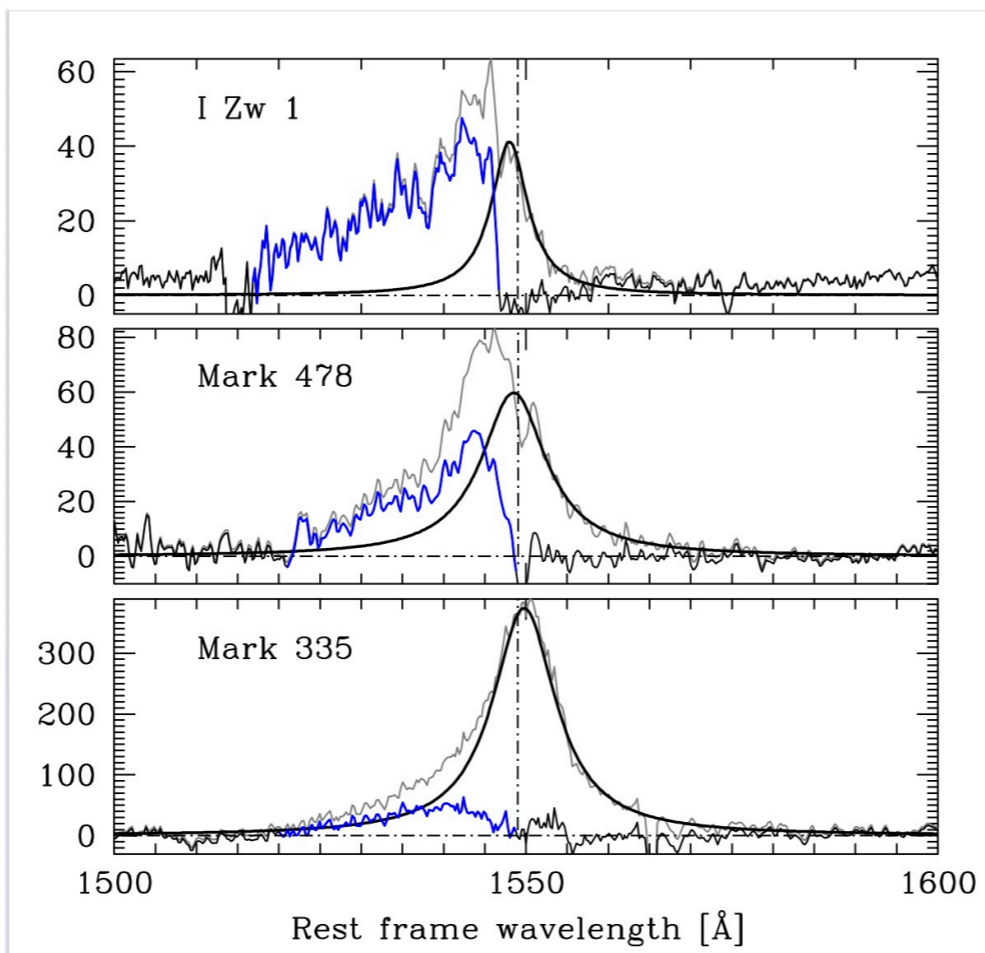
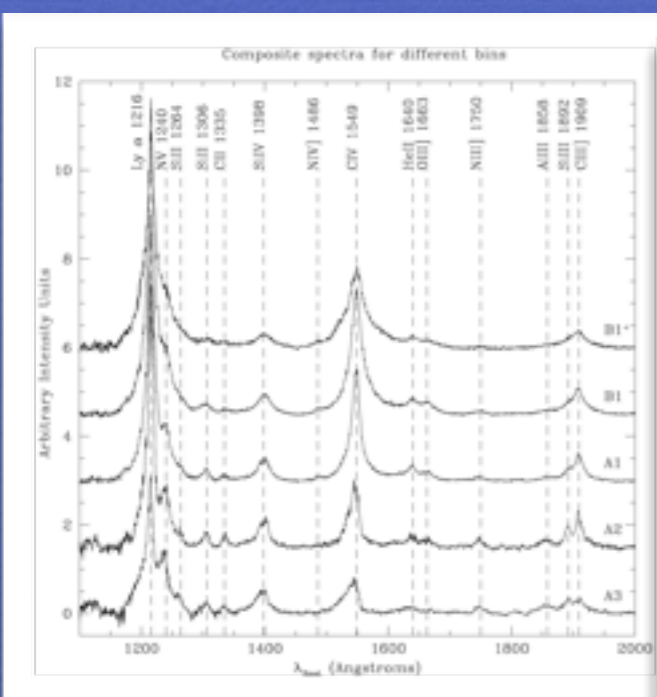


UV correlates of
Eigenvector 1:
UV diagnostic ratios
and CIV 1549 profile:
blueshifted excess

Pop. A



Pop. B



Bachev et al. 2004,
Marziani et al. 2010

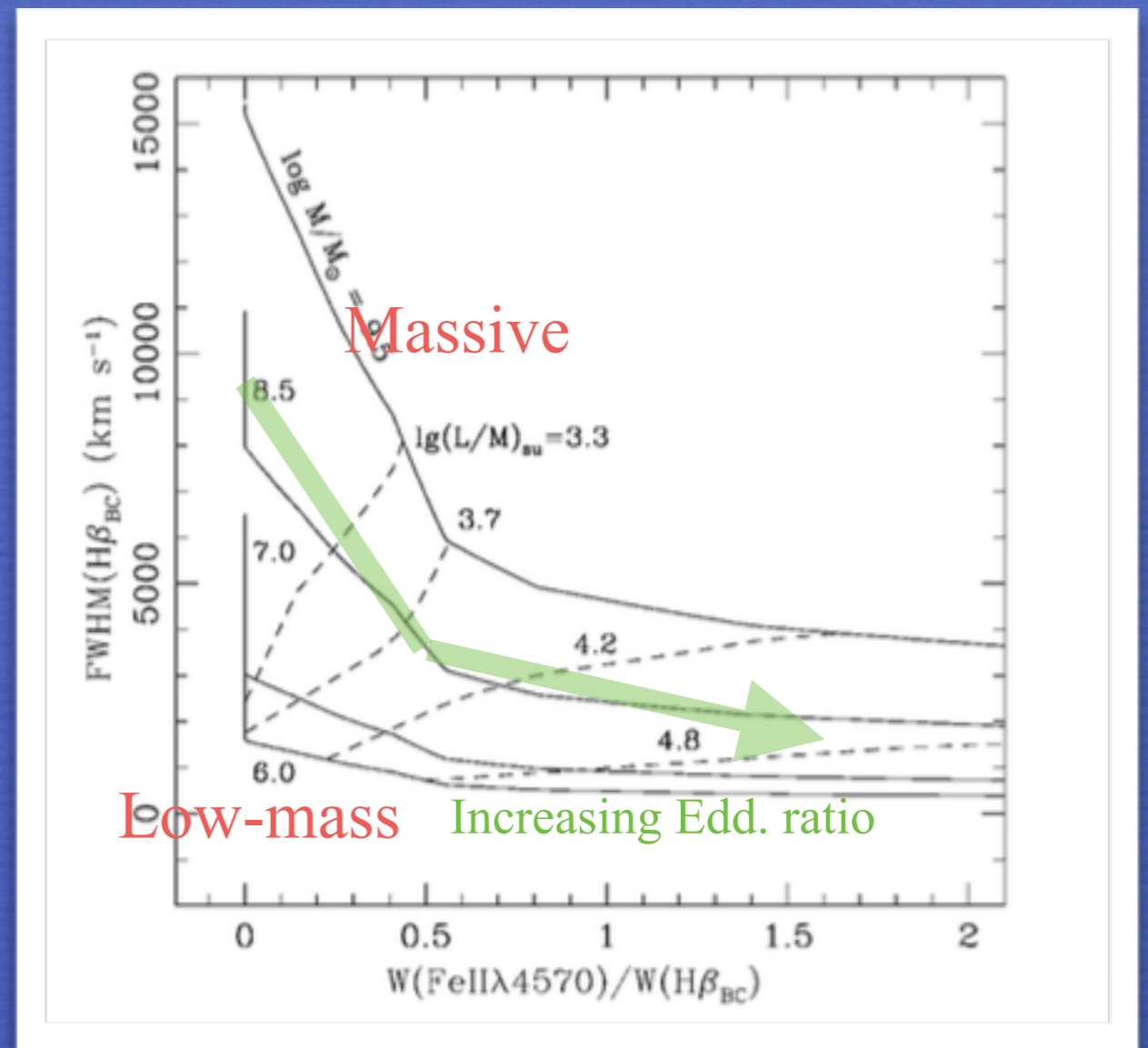
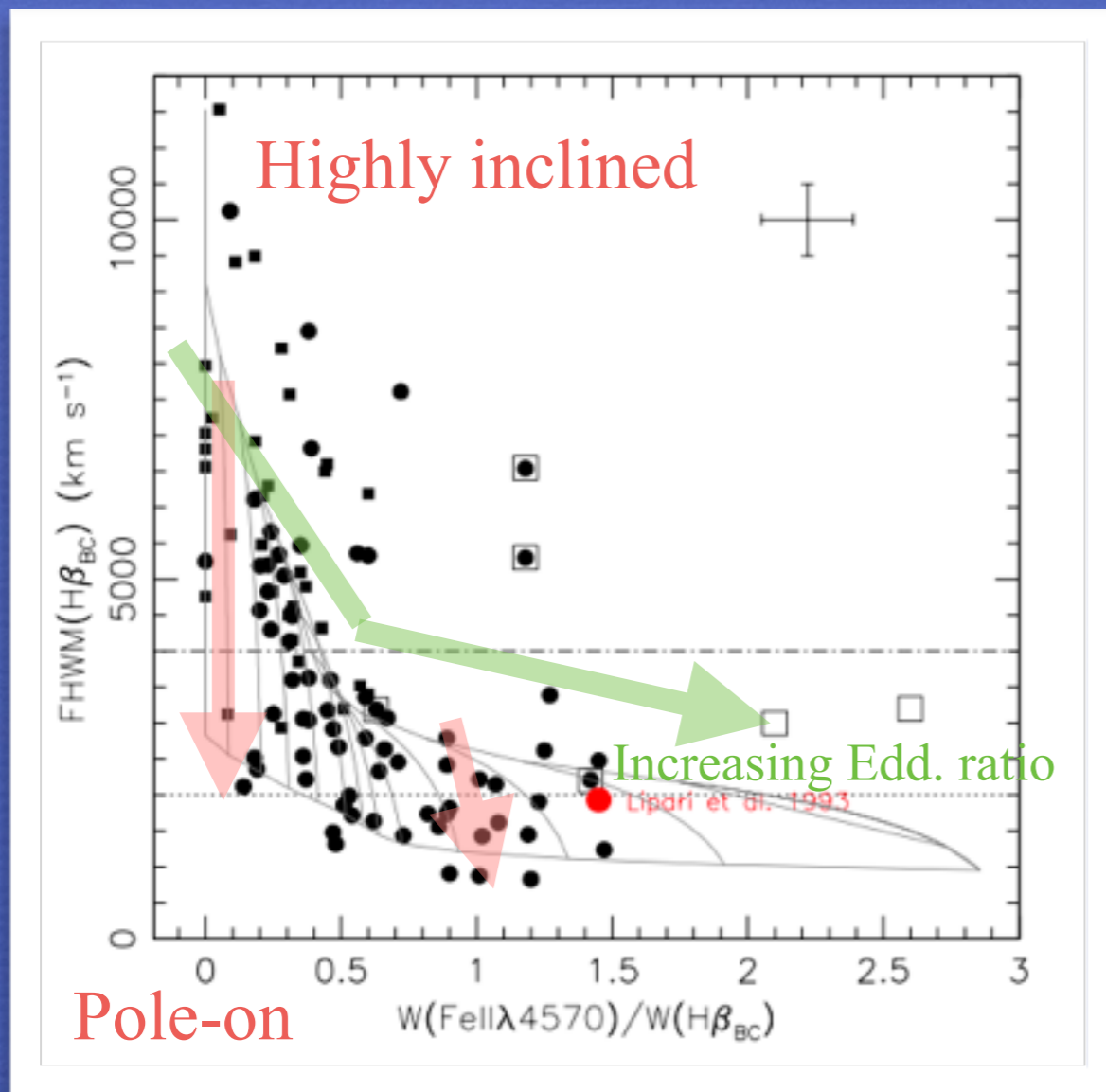
Optical plane of 4DE1: a sequence of Eddington ratio with significant orientation and black hole mass effects

Ionization parameter $U = \frac{\int_{\nu_0}^{+\infty} \frac{L_{\nu}}{h\nu} d\nu}{4\pi r_{\text{BLR}} n_e c}$ written as a function of L/M_{BH} and M_{BH}

assuming virial broadening, FeII and line width orientation dependence, $L \propto r^a$

Fixed black hole mass

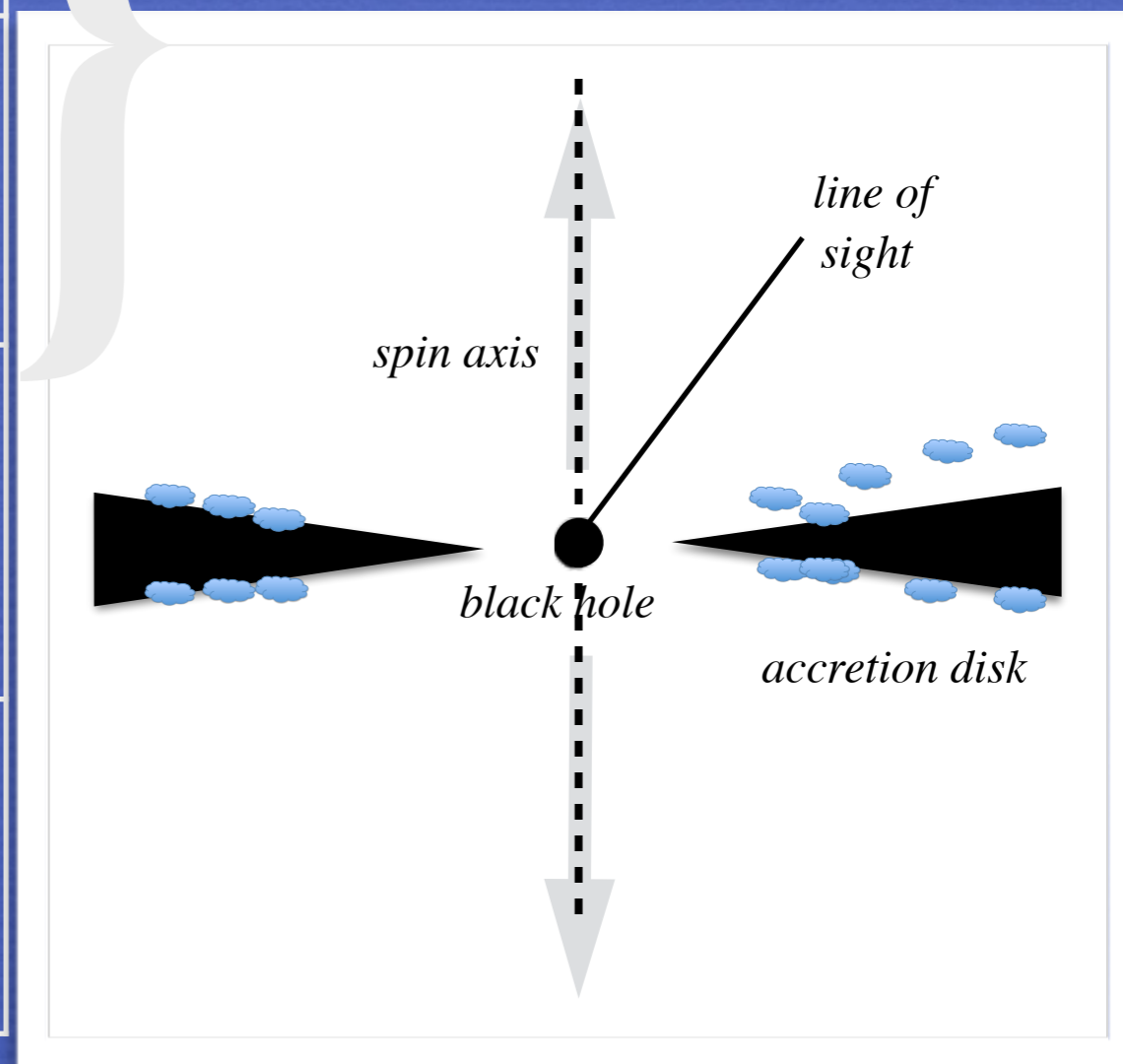
Varying black hole mass, average orientation



The 4D Eigenvector 1 space of quasars

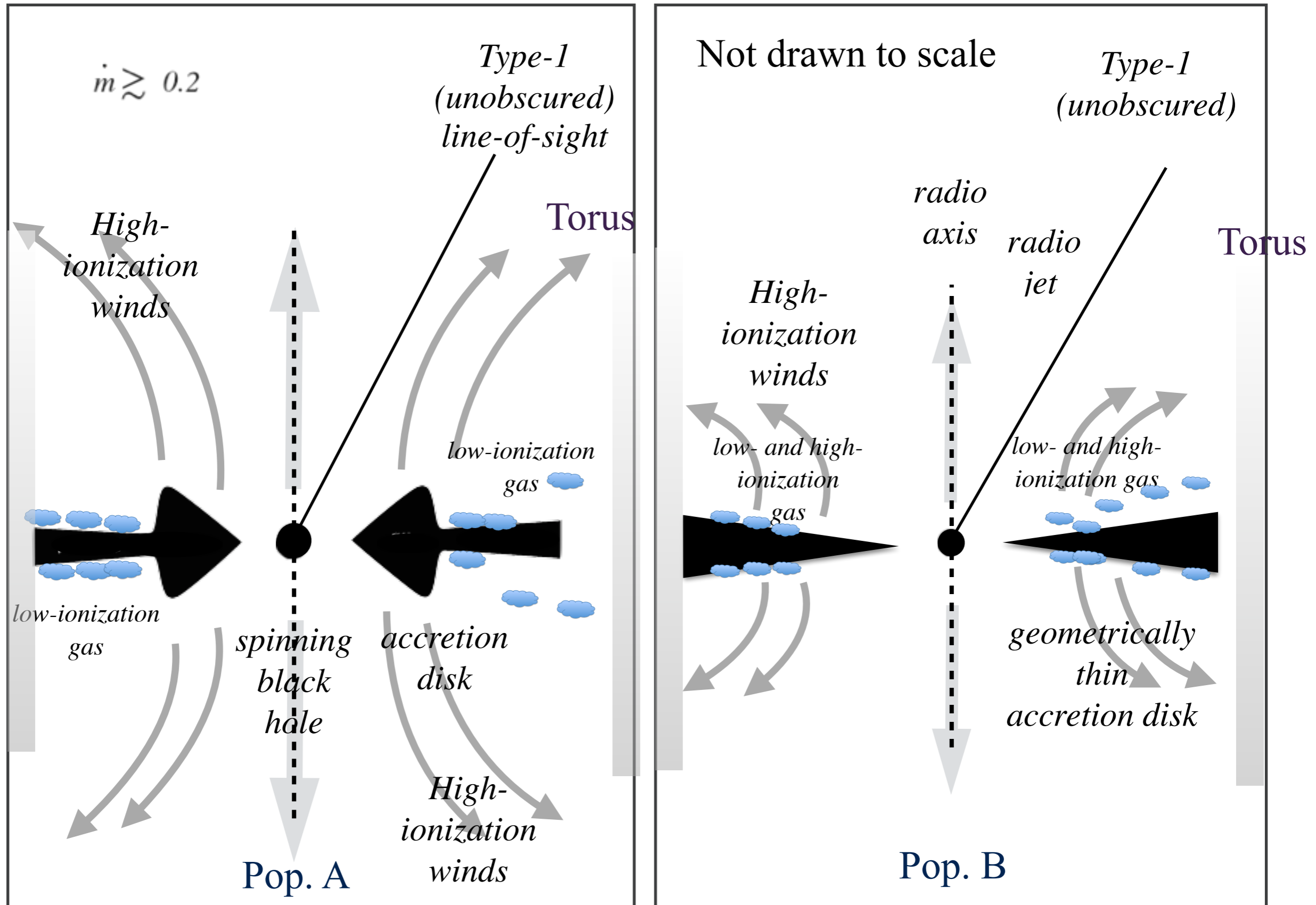
Observed parameter	Physical interpretation	Accretion-related parameters
$R_{\text{FeII}} = I(\text{FeII}) / I(\text{H}\beta)$	ionization degree <i>col. density, Z</i>	L/L_{Edd}
FWHM(H β)	velocity field of low-ionization gas	$L/L_{\text{Edd}}, M_{\text{BH}},$ orientation
CIV λ 1549 Shift	velocity field of high-ionization gas	$L/L_{\text{Edd}},$ orientation
$\Gamma_{\text{soft}} (0.2-2 \text{ KeV})$	Compton thick / accretion disk emission?	L/L_{Edd}

Optical plane of 4DE1



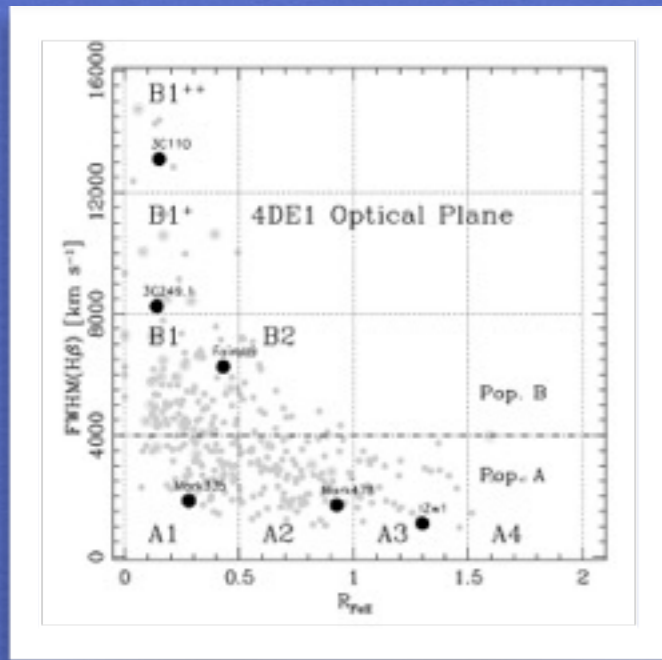
Pop. A/B transition: geometrically thick/thin disk?

Abramowicz et al. 1988, Shakura & Sunyaev 1973



Interpretation of the CIV λ 1549 emission line profile

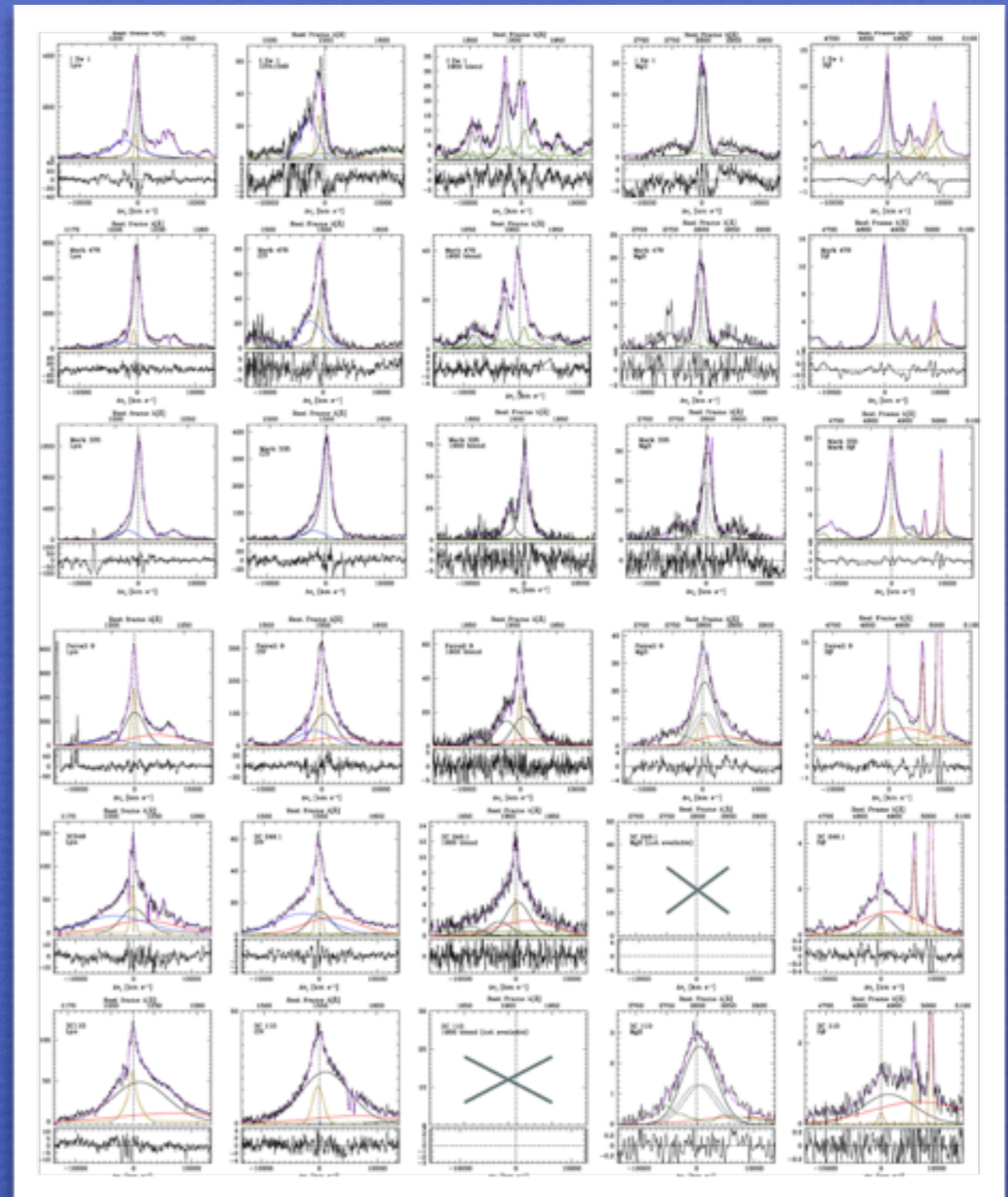
Strongest emission lines along the 4DE1 sequence can be empirically reproduced by three main components



Blueshifted component (BLUE): strong in Ly α , CIV λ 1549, HeII λ 1640

“Broad Component” (BC) strong in all low ionization lines: FeII, MgII λ 2800, H β

“Very Broad Component” (VBC FWHM \sim 10000 km s $^{-1}$) redshifted: strong in Ly α , CIV λ 1549, HeII, Balmer lines absent in FeII



Blueshifted component physical conditions

Results of Cloudy 08.00 (Ferland et al. 1998,2013) simulations as a function of density and ionization parameter U

Table 4. BLUE: FWHM $\sim 7000 \text{ km s}^{-1}$, $\Delta v_r \sim -3000 \text{ km s}^{-1}$.

Sp. T.	Name	Intensity ratio				W^a Lyr
		C iv/ Lyr	He ii/ C iv	H α / H β	Lya/ H β ^b	
A3	IZw 1	0.25	0.41	4.2	~ 18	60
A2	Mrk 478	0.66	0.17	–	~ 46	15
A1	Mrk 335	0.45	0.67	–	~ 32	16
B1	Fairall 9	1.05	0.14	–	~ 46	30
B1 ⁺	3C 249.1	0.59	0.17	–	~ 32	53
B1 ⁺⁺	3C 110 ^c	–	–	–	–	0

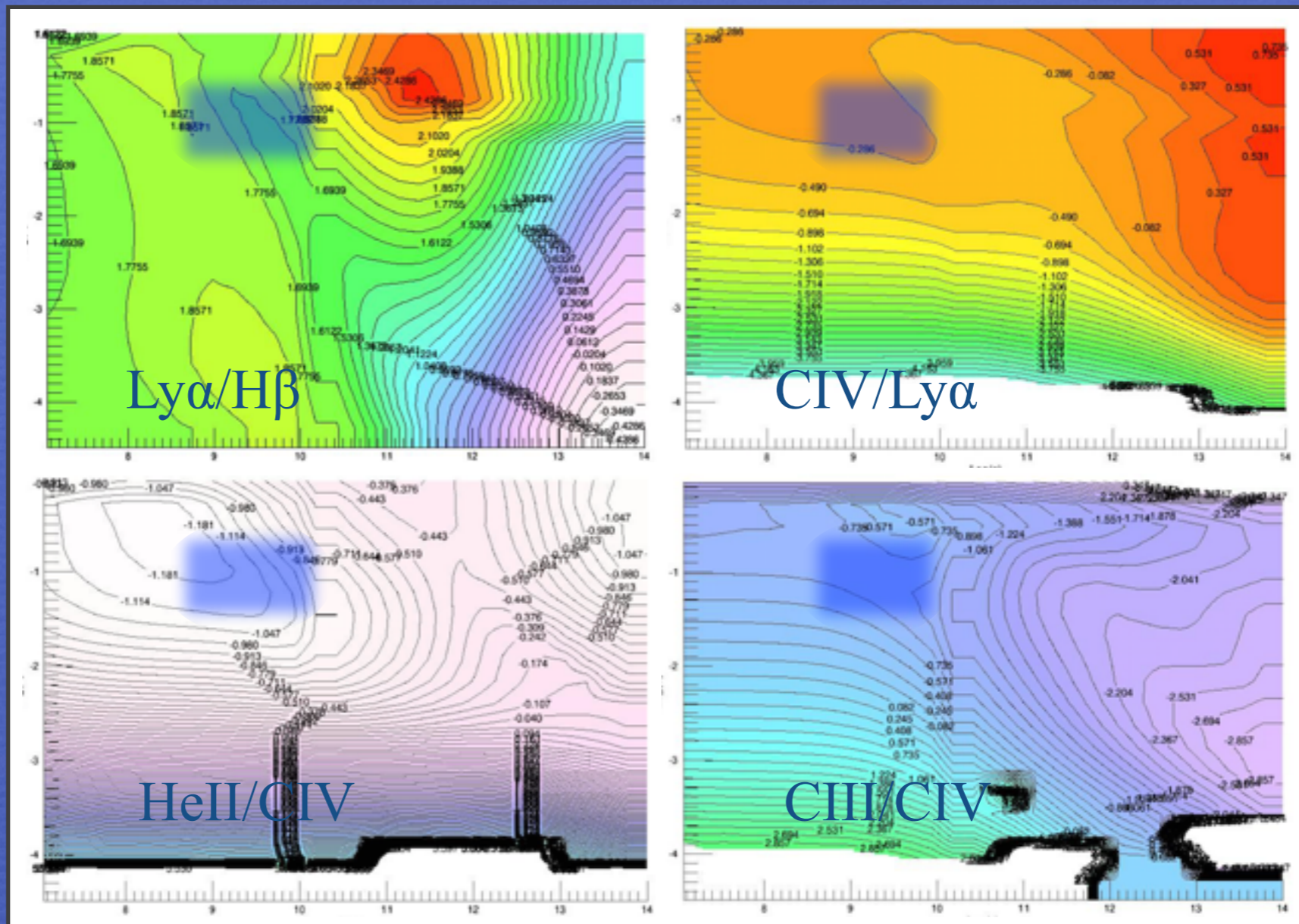
^aEW in Å.

^bLower limits to Lya/H β are estimated by the maximum contribution expected by a component of the same shift and width if peaking at 3 σ the noise level. See the text for a detailed explanation.

^cConsistent with 0 intensity in all lines.

log U

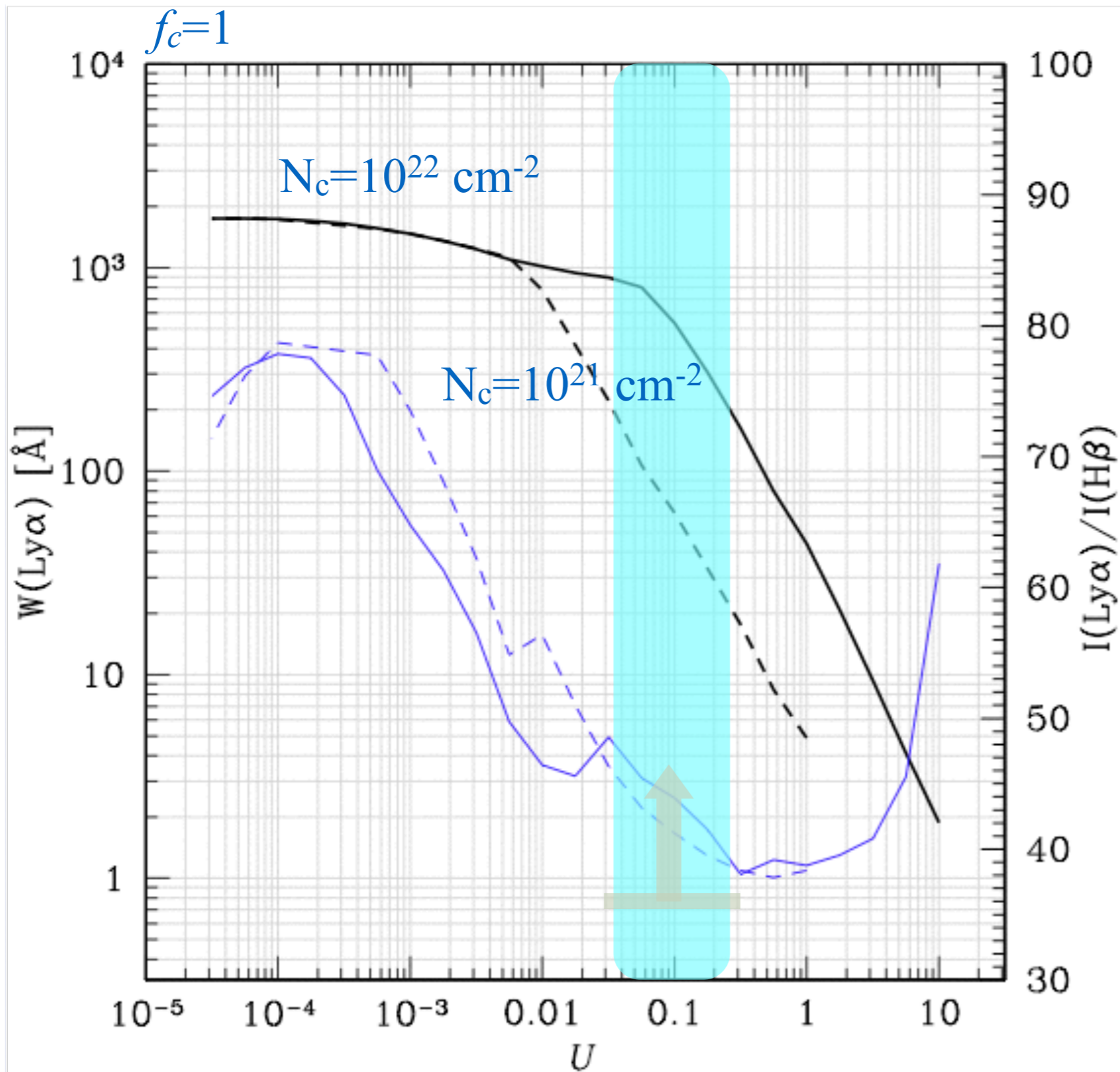
log U



log n

log n

BLUE consistent with high ionization ($U \sim 10^{-1 \pm 0.5}$)
and moderate density ($n_H \sim 10^{9.5 \pm 0.5} \text{ cm}^{-3}$)



Blueshifted
component:
large
 $\text{Ly}\alpha/\text{H}\beta > 30$

Very different from
the other
components for
which
 $\text{Ly}\alpha/\text{H}\beta \sim 5 - 10$

Matter bounded
emitting region?

Interpretation of the heuristic decomposition of the broad profiles: “stratification”

broad component → lower ionization **Broad Line Region**
line broadening predominantly virial; FeII, CaII emission

very broad component →

high-ionization inner **Very Broad Line Region (VBLR)**

emitting no FeII and showing lower continuum responsivity

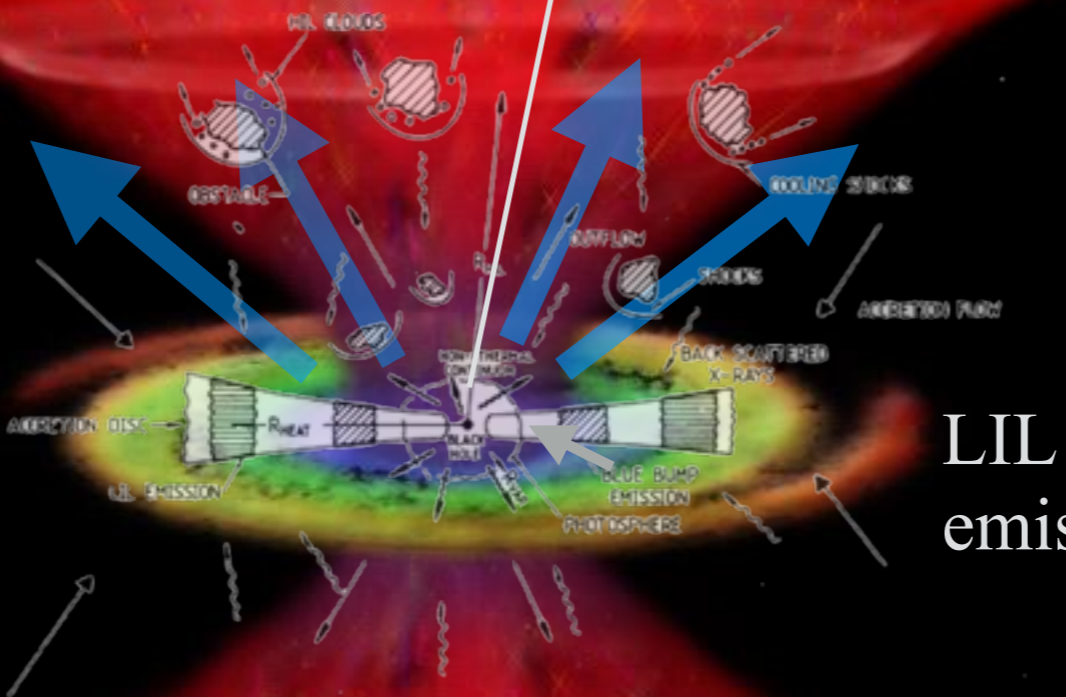
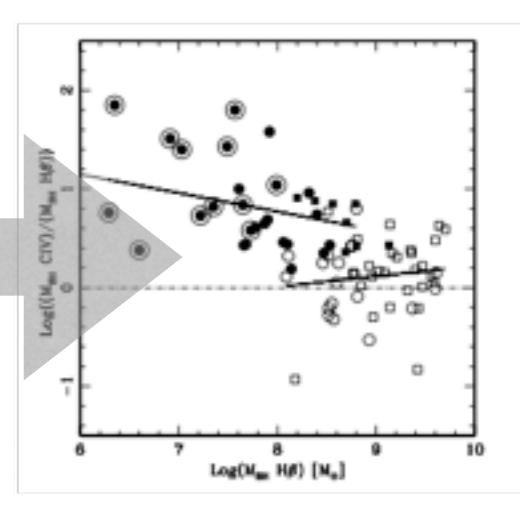
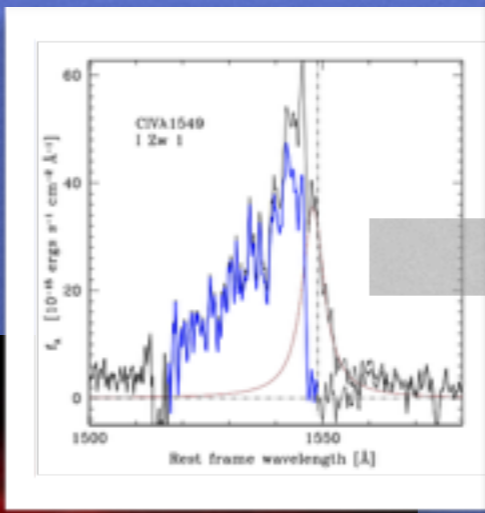
(Snedden & Gaskell 2007; Goad & Korista 2014).

blueshifted component → **outflow/wind**

Heuristic model(s)

line-of-sight

CIV 1549 blueshifted emission

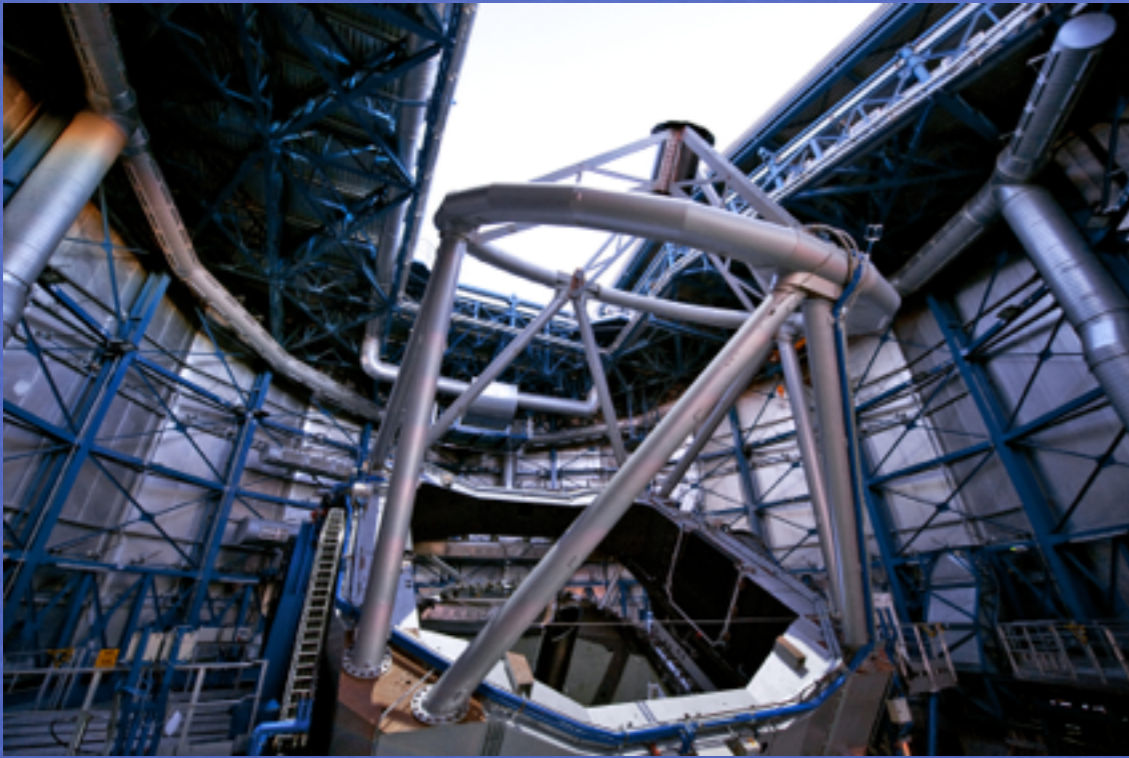


LIL emission

Explains most striking observations of blueshifts in Pop. A sources

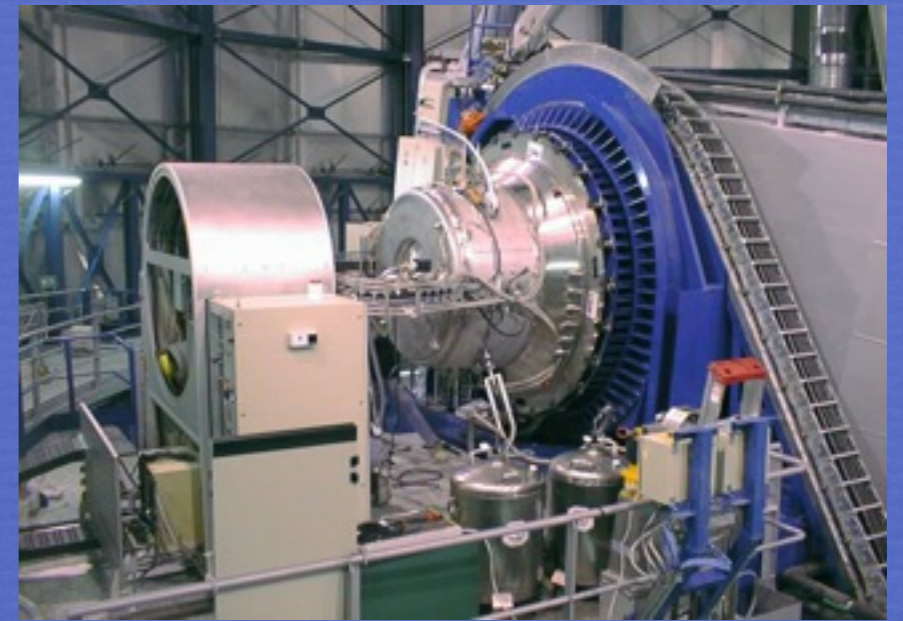
Analysis of CIV λ 1549 at high- z and high- L
maximizing luminosity effects

ESO VLT



ISAAC

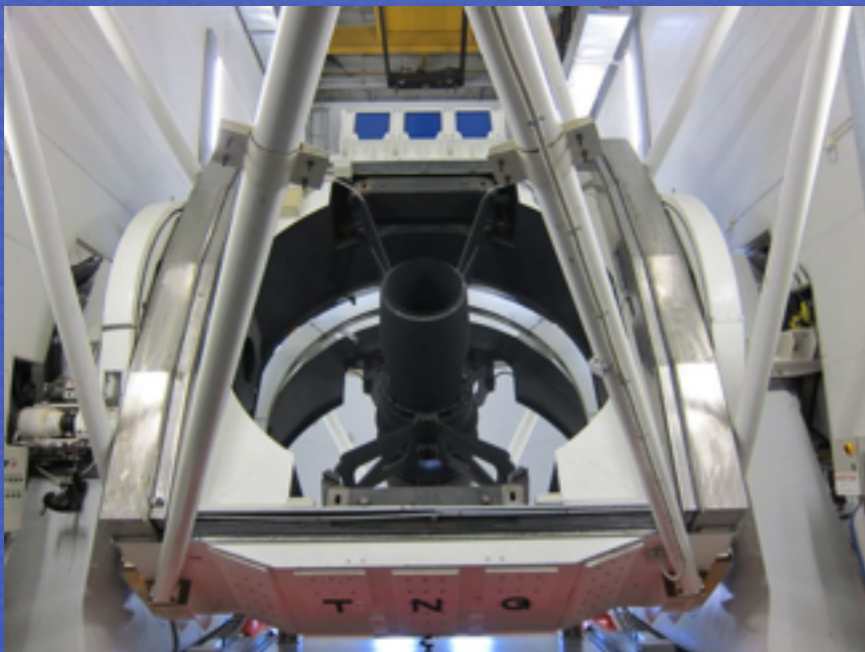
$R = \lambda / \delta\lambda \sim 1000$
sZ,J,H,K



FORS
 $R = \lambda / \delta\lambda \sim 1000 - 1500$
optical



Galileo TNG

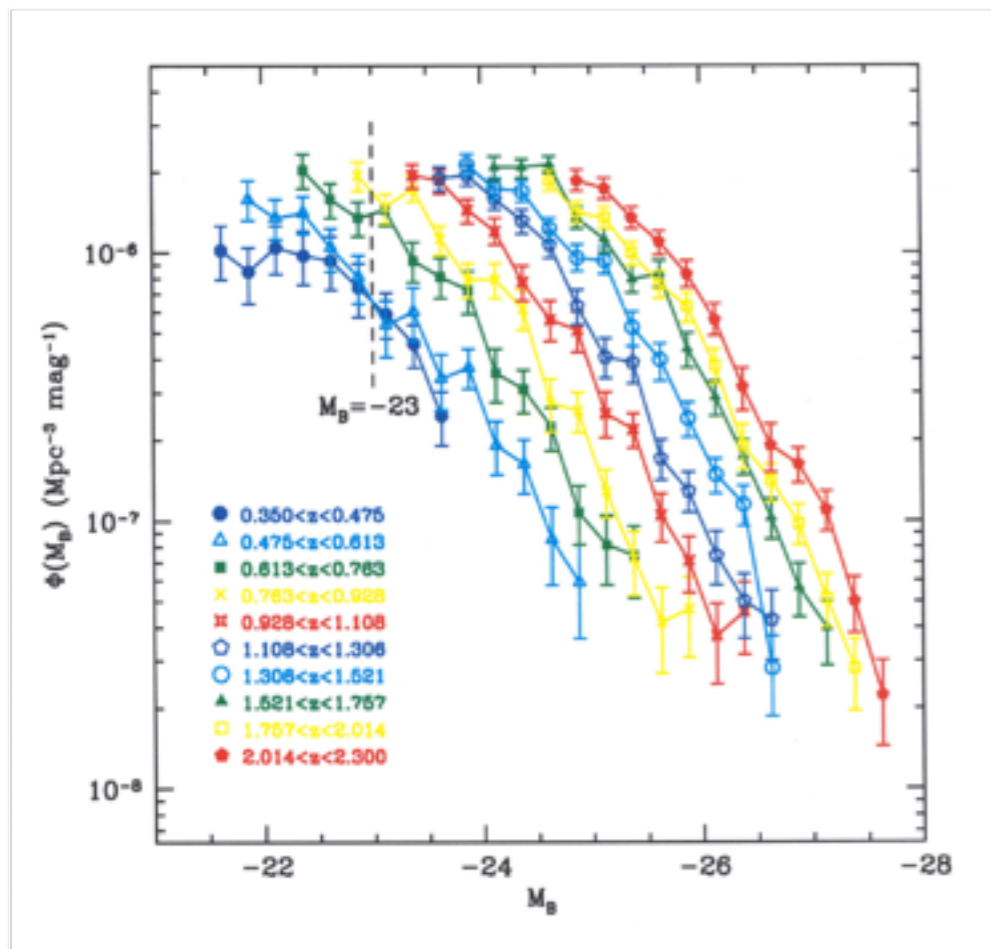


Dolores
 $R = \lambda / \delta\lambda \sim 500$
optical



The sample at high luminosity

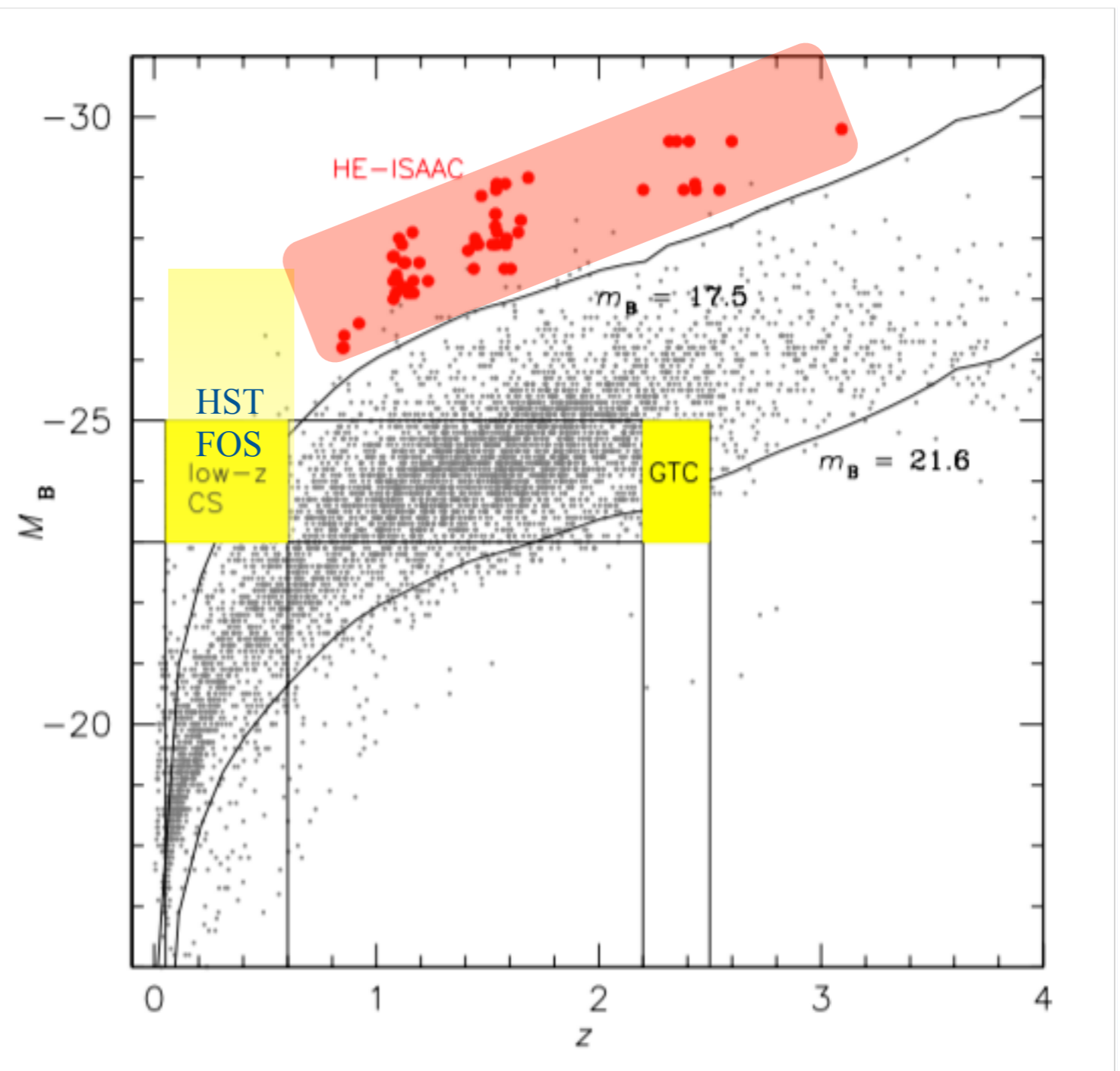
Rare, extremely luminous quasars



Boyle et al. 2000

A control sample
at low z and
luminosity
130 HST/FOS
CIV observations

Sulentic et al. 2007



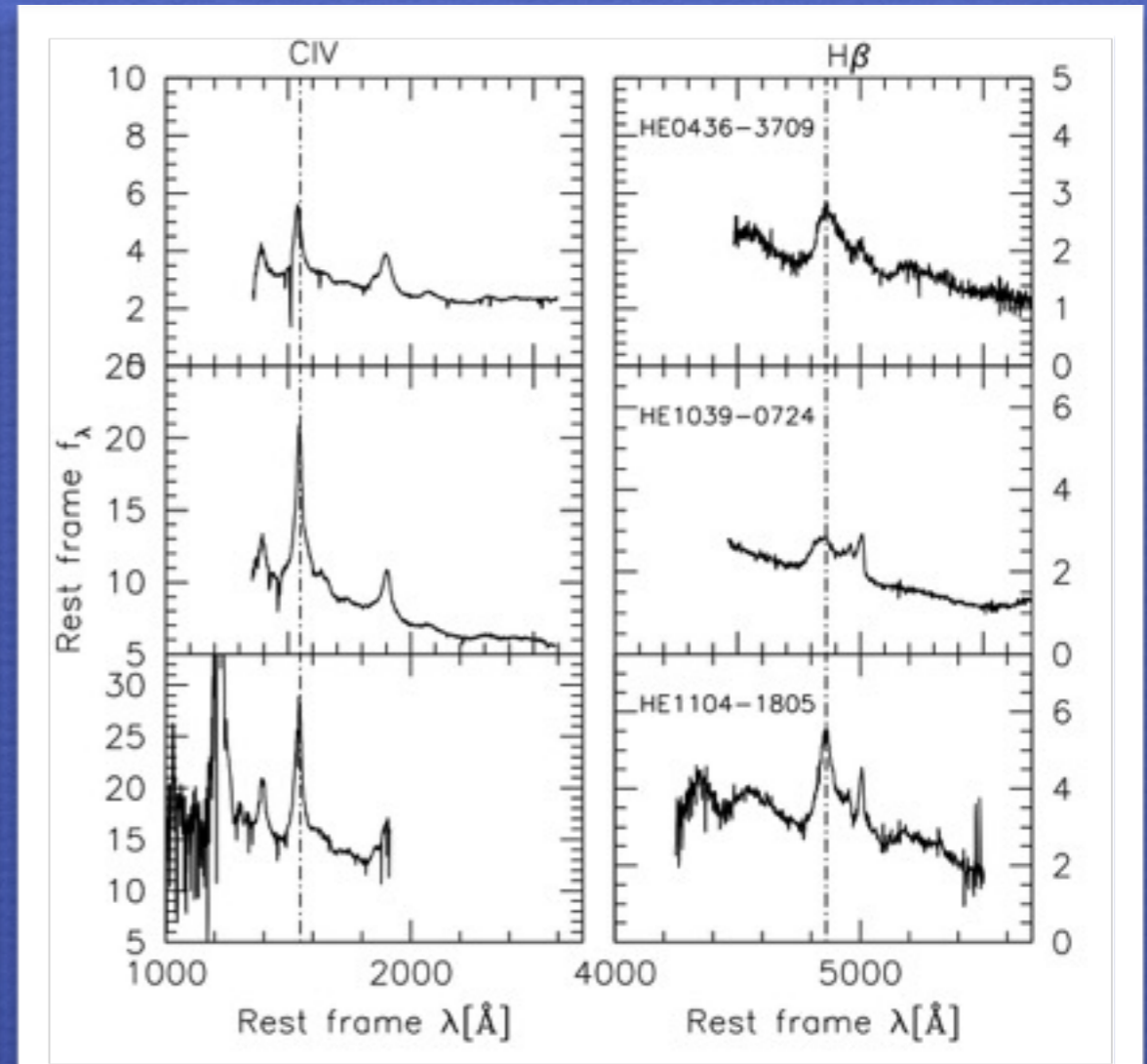
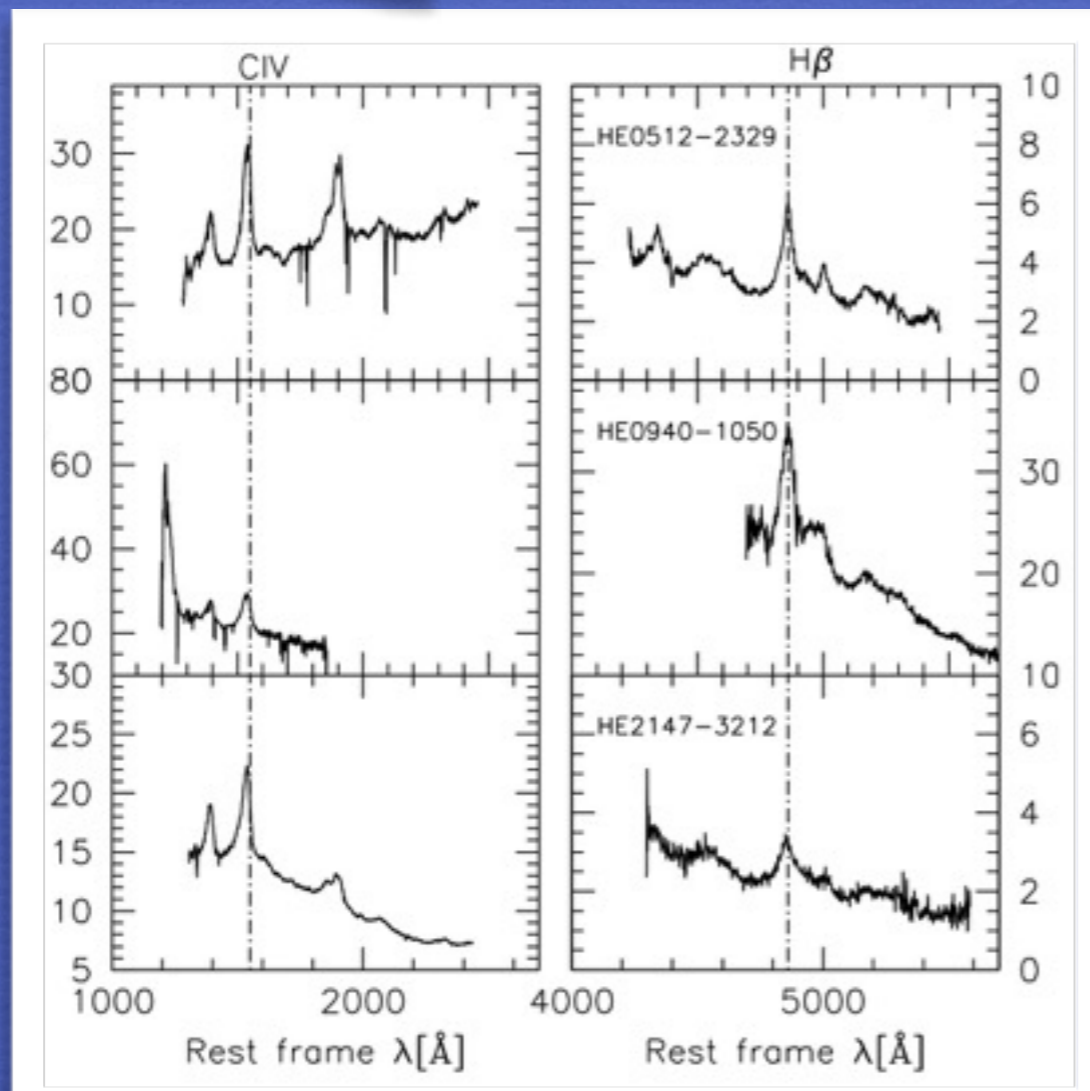
The sample at high luminosity

52 HE quasars observed with ISAAC in the $H\beta$ spectral range (yielding reliable rest frames),
for 32 CIV was observable from ground
(28 actually observed)

Name	m_B	z	M_B	$\log R_K$
HE0035-2853	17.03	1.6377	-28.1	< 0.21
HE0043-2300	17.06	1.5402	-27.9	2.03
HE0058-3231	17.14	1.5821	-27.9	< 0.24
HE0109-3518	16.44	2.4057	-29.6	< -0.04
HE0122-3759	16.94	2.2004	-28.8	< 0.35
HE0203-4627	17.34	1.4381	-27.5	2.07
HE0205-3756	17.17	2.4335	-28.9	1.06
HE0248-3628	16.58	1.5355	-28.4	0.55
HE0251-5550	16.59	2.3505	-29.6	< 0.23
HE0349-5249	16.13	1.5409	-28.9	0.76
HE0359-3959	17.09	1.5209	-27.9	0.22
HE0436-3709	16.84	1.4447	-27.9	< 0.38
HE0507-3236	17.36	1.5759	-27.5	< 0.50
HE0512-3329	17.03	1.5862	-28.0	< 0.36
HE0926-0201	16.23	1.6828	-29.0	< -0.37
HE0940-1050	16.96	3.0932	-29.8	< 0.10
HE1039-0724	17.16	1.4584	-27.9	< 0.20
HE1104-1805	16.45	2.3180	-29.6	< 0.09
HE1120+0154	16.31	1.4720	-28.7	-0.57
HE1347-2457	16.83	2.5986	-29.6	-0.68
HE1349+0007	16.83	1.4442	-28.0	-0.18
HE1409+0101	16.92	1.6497	-28.3	0.40
HE2147-3212	16.84	1.5432	-28.1	< 0.14
HE2156-4020	17.39	2.5431	-28.8	-0.09
HE2202-2557	16.71	1.5347	-28.2	1.56
HE2349-3800	17.46	1.6040	-27.5	1.89
HE2352-4010	16.05	1.5799	-28.9	< 0.25
HE2355-4621	17.13	2.3825	-28.8	< 0.70

Pop. A

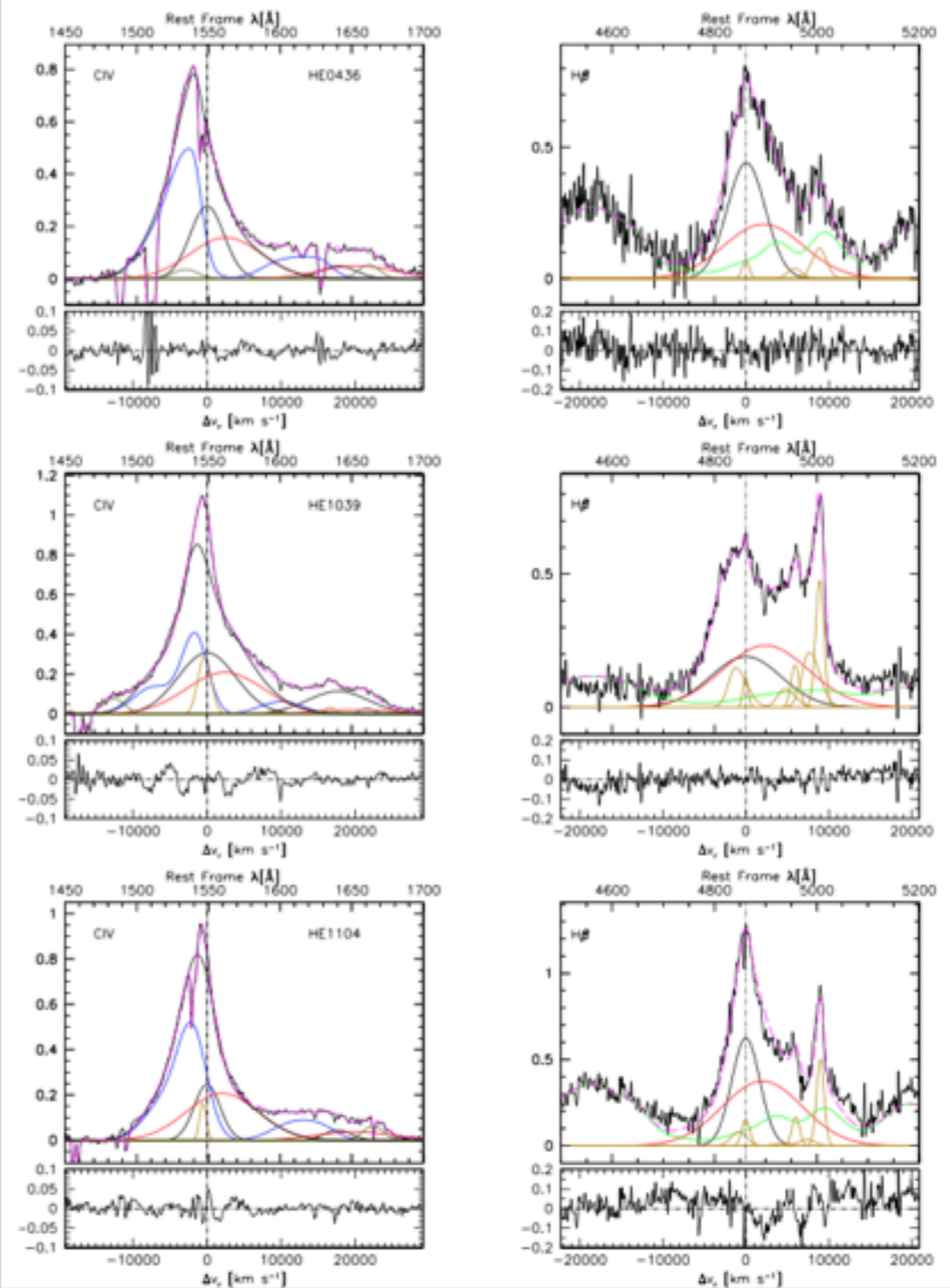
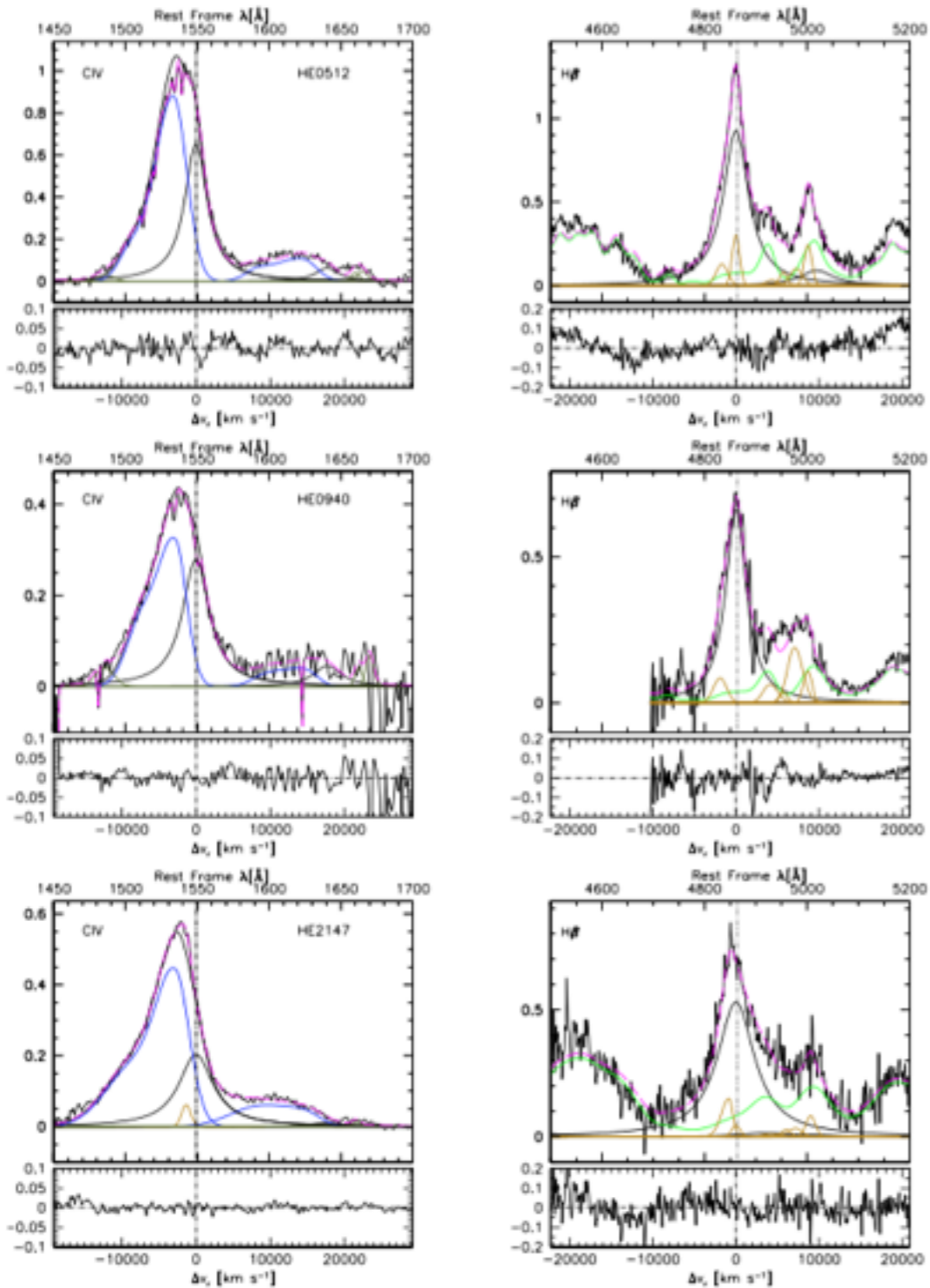
Pop. B



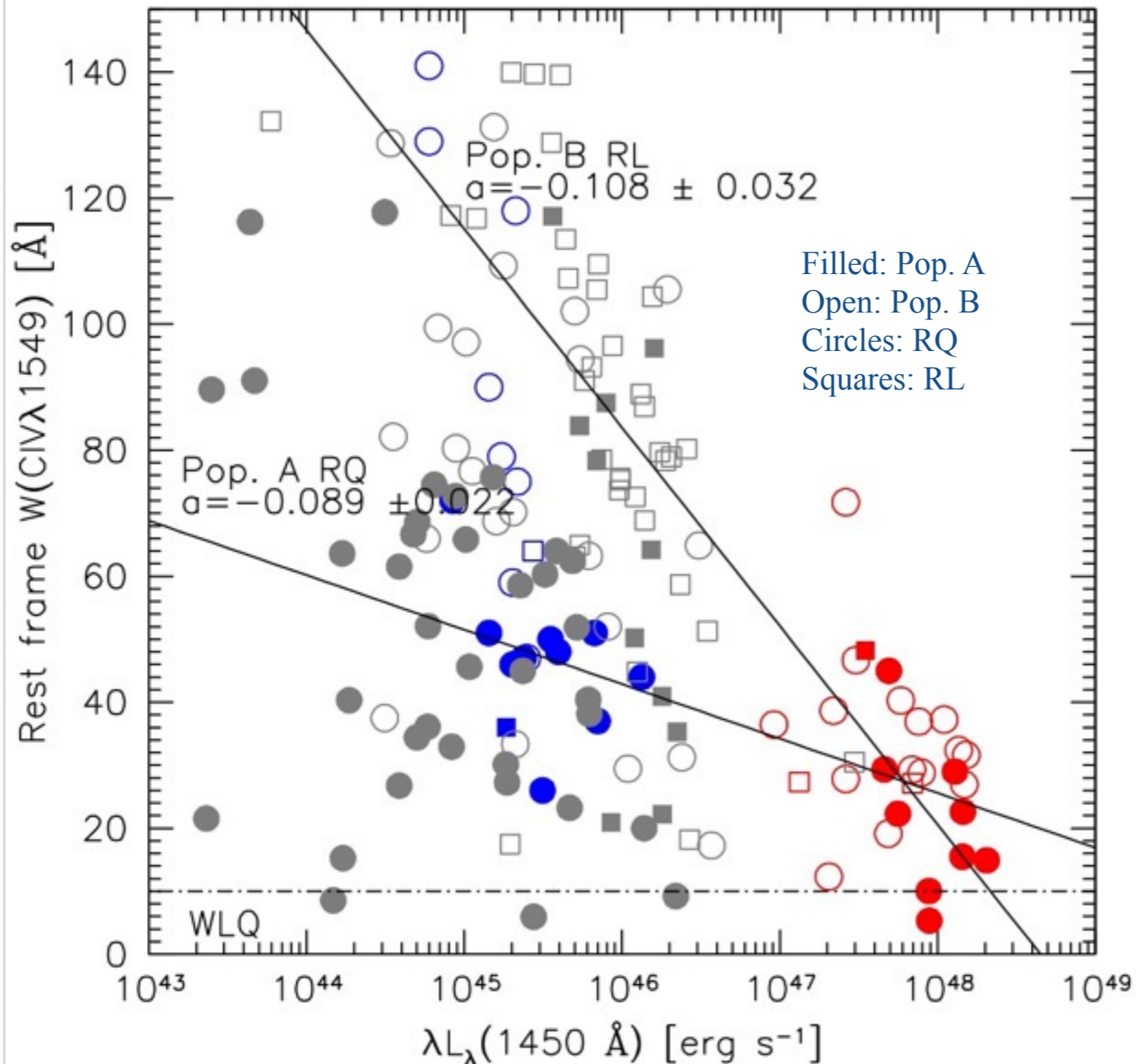
CIV λ 1549: high amplitude blueshifts

Pop. A

Pop. B



The “Baldwin effect”



Consistent with
Bian et al. (2005)

Still explainable
by a dependence
on Eddington
ratio and selection
effects

Bachev et al. 2004; Baskin & Laor 2005
Sulentic et al. 2007; Marziani et al. 2008

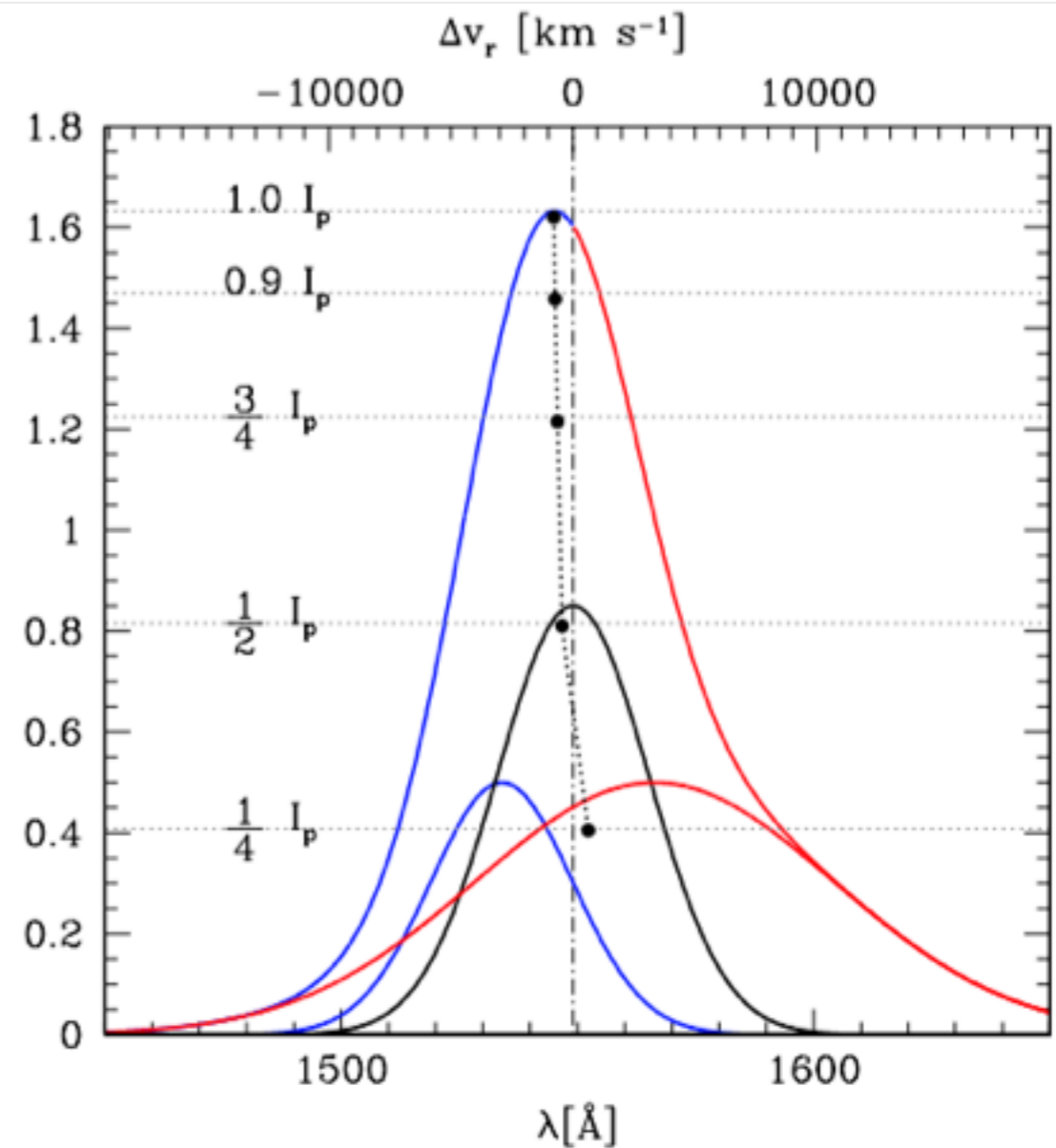
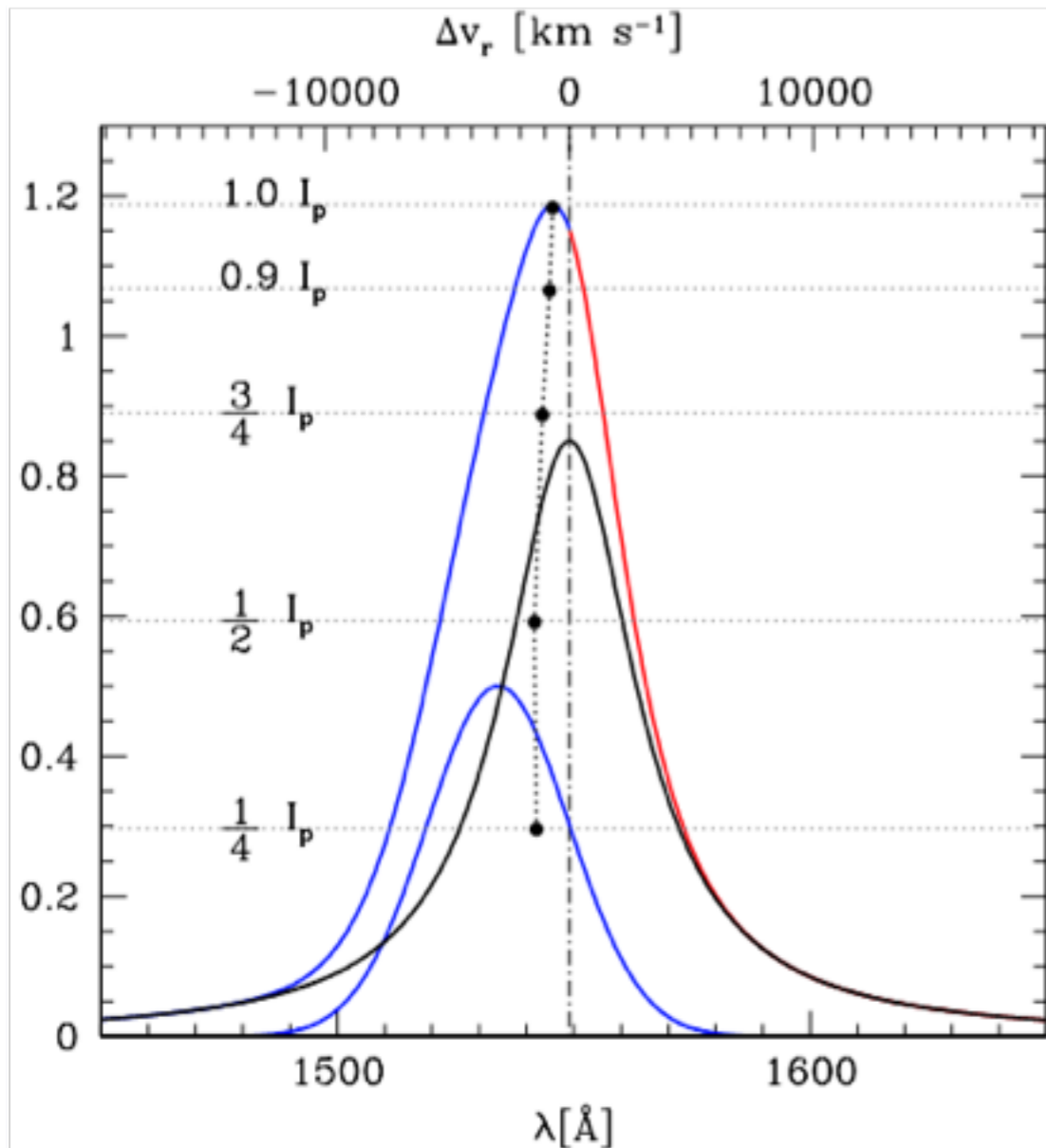
CIV $\lambda 1549$ line profile parameterisation

$$c\left(\frac{i}{4}\right) = \frac{\lambda_B(i/4) + \lambda_R(i/4)}{2} - \lambda_0 \quad \forall i = 0, \dots, 4$$

$$AI\left(\frac{i}{4}\right) = \frac{\lambda_B(i/4) + \lambda_R(i/4) - 2 \cdot \lambda_P}{\lambda_R(i/4) - \lambda_B(i/4)} \quad \forall i = 0, \dots, 4$$

Pop. A

Pop. B

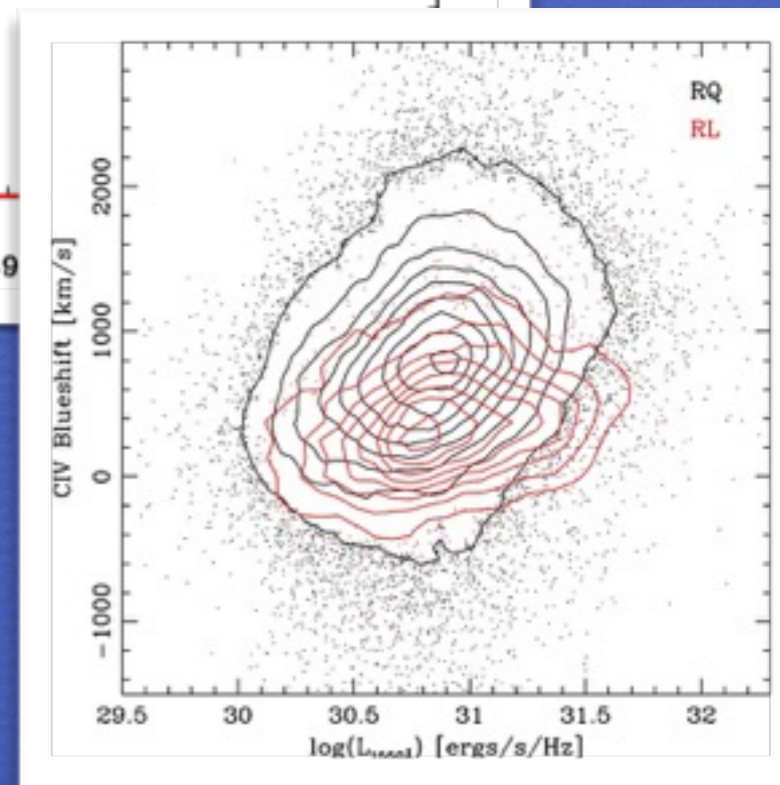
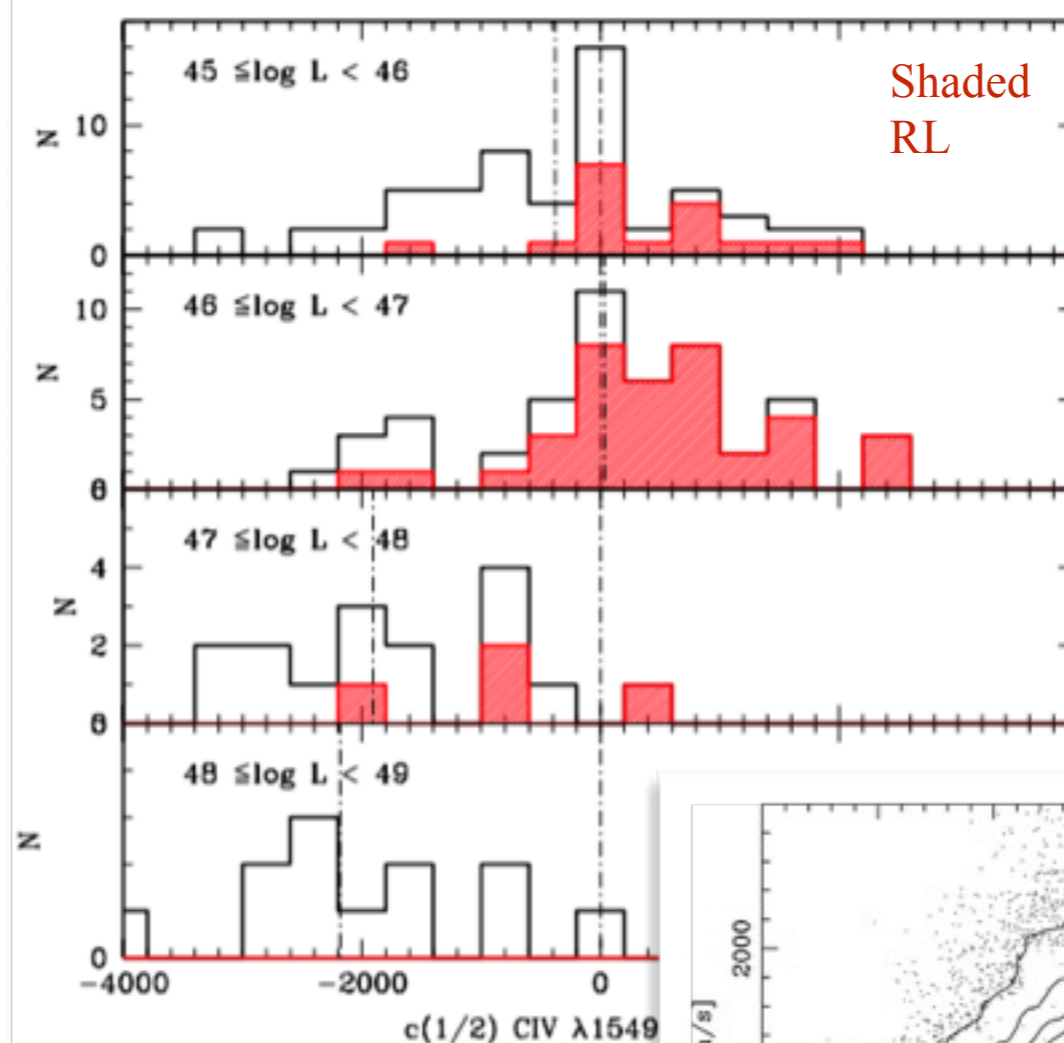
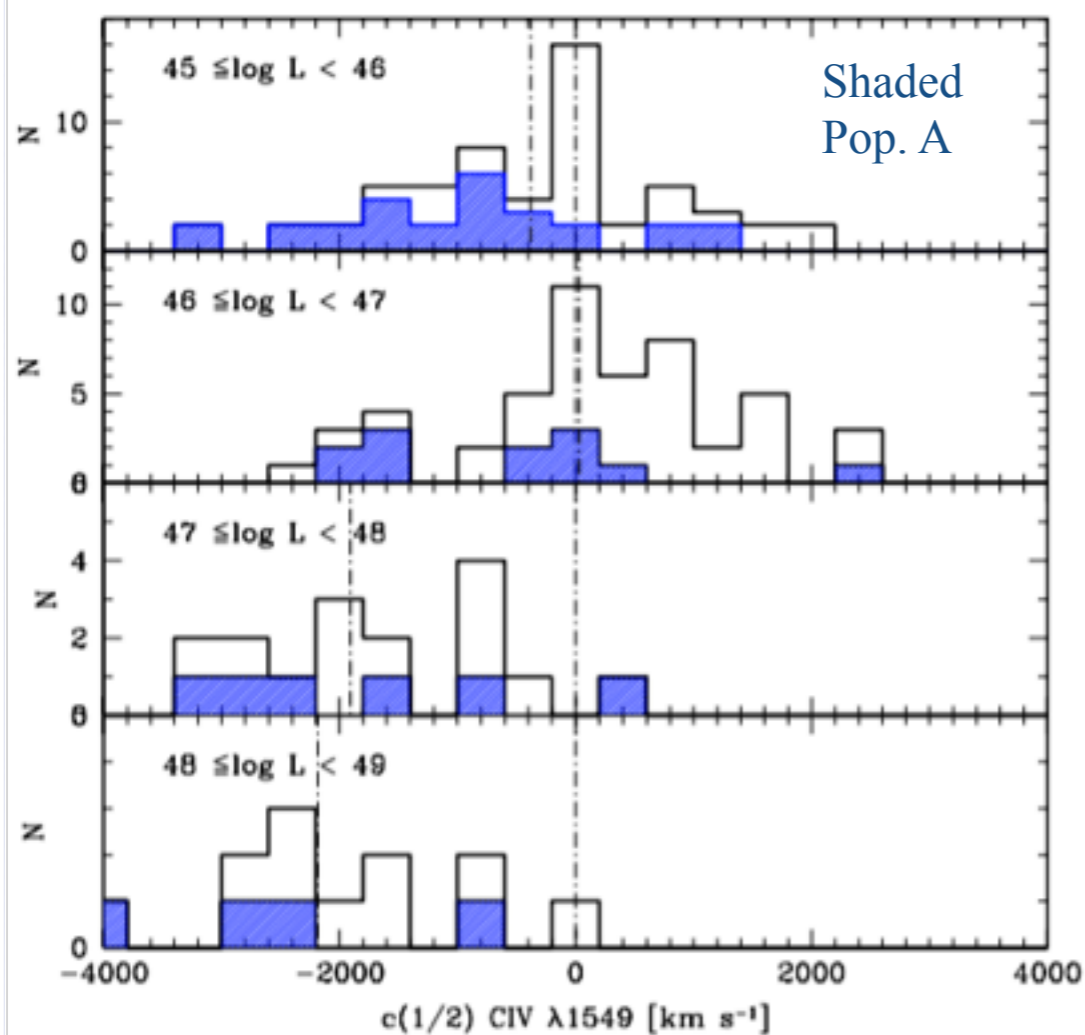


line centroids at fractional intensity
independent from multi-component decomposition

Blueshift distribution as a function of luminosity

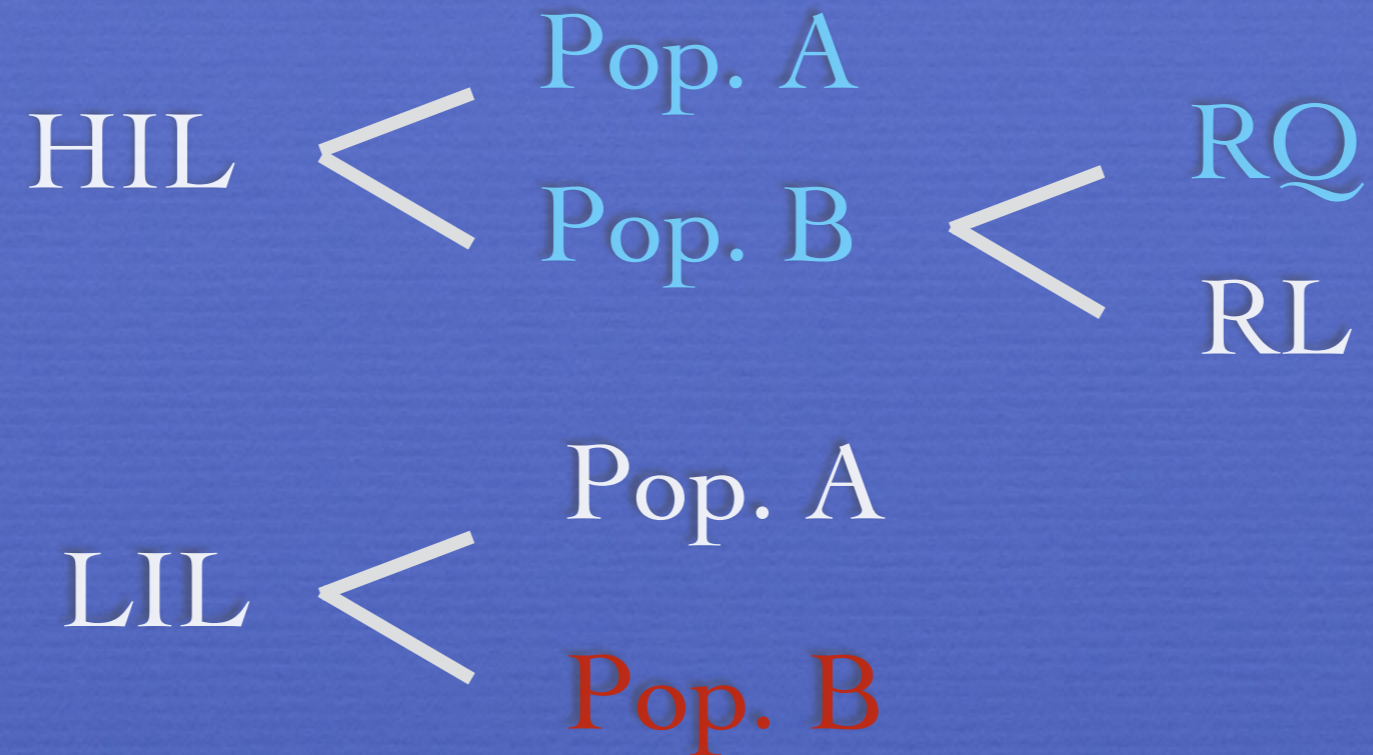
All and Pop. A; FOS + HE

All and RL; FOS + HE

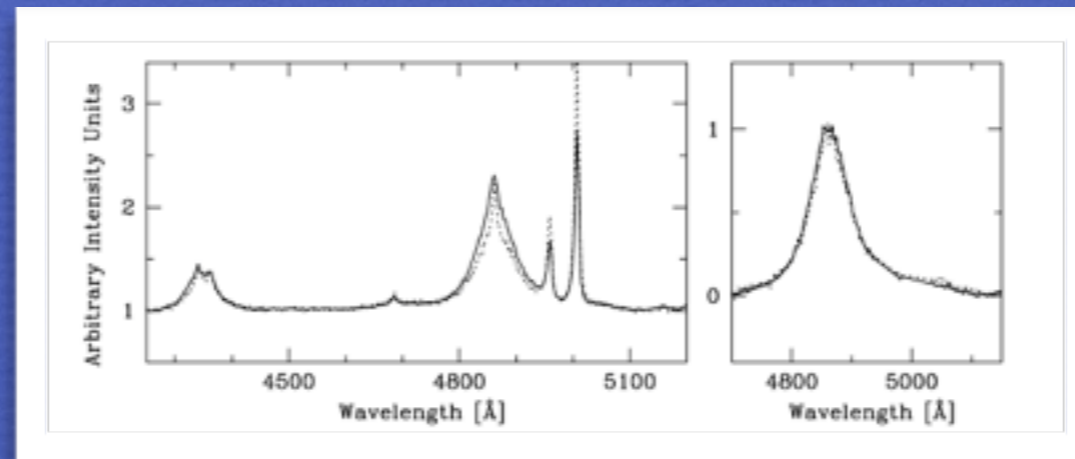


Consistent with result from SDSS

Contextualization for High Ionization Lines



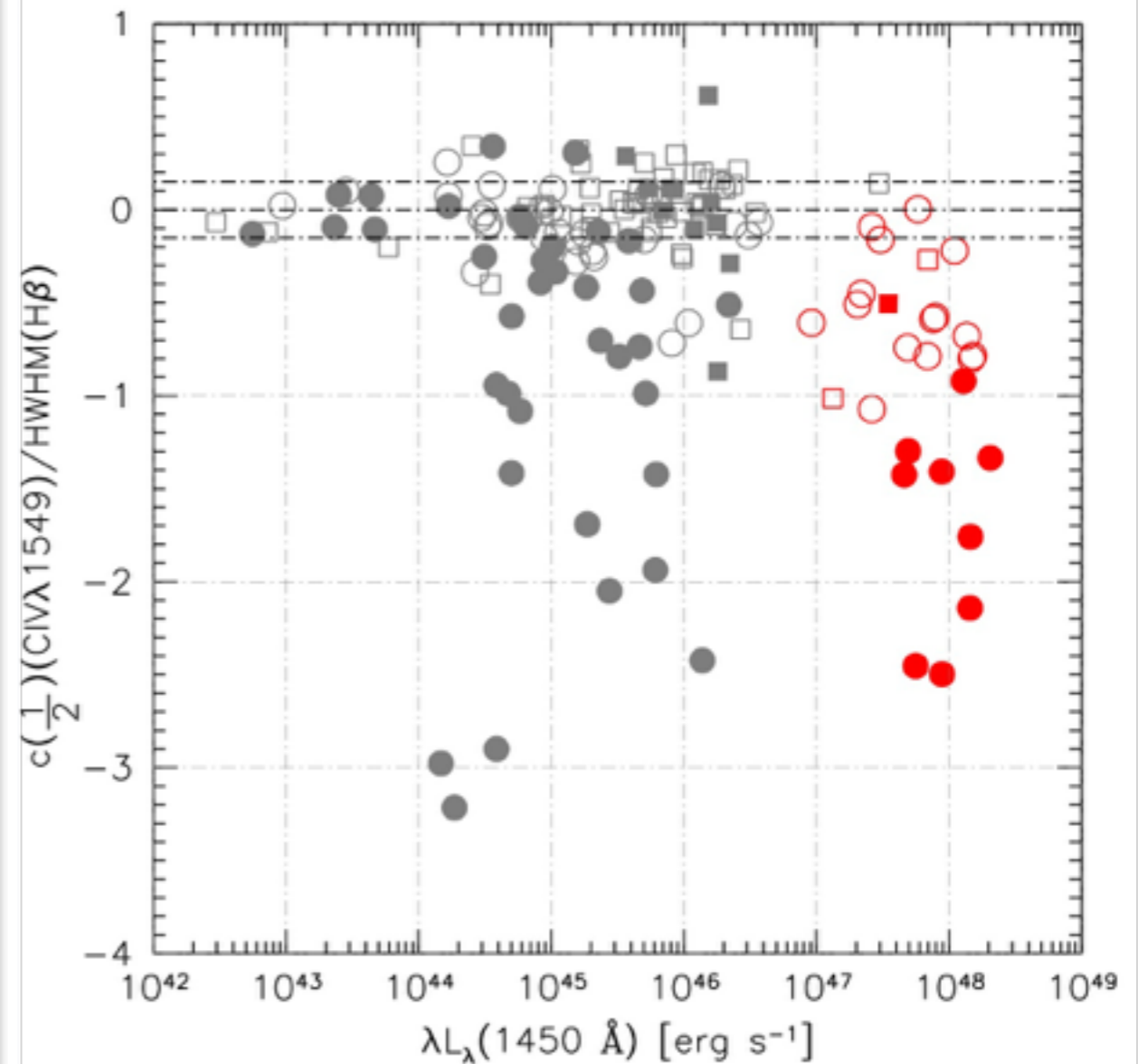
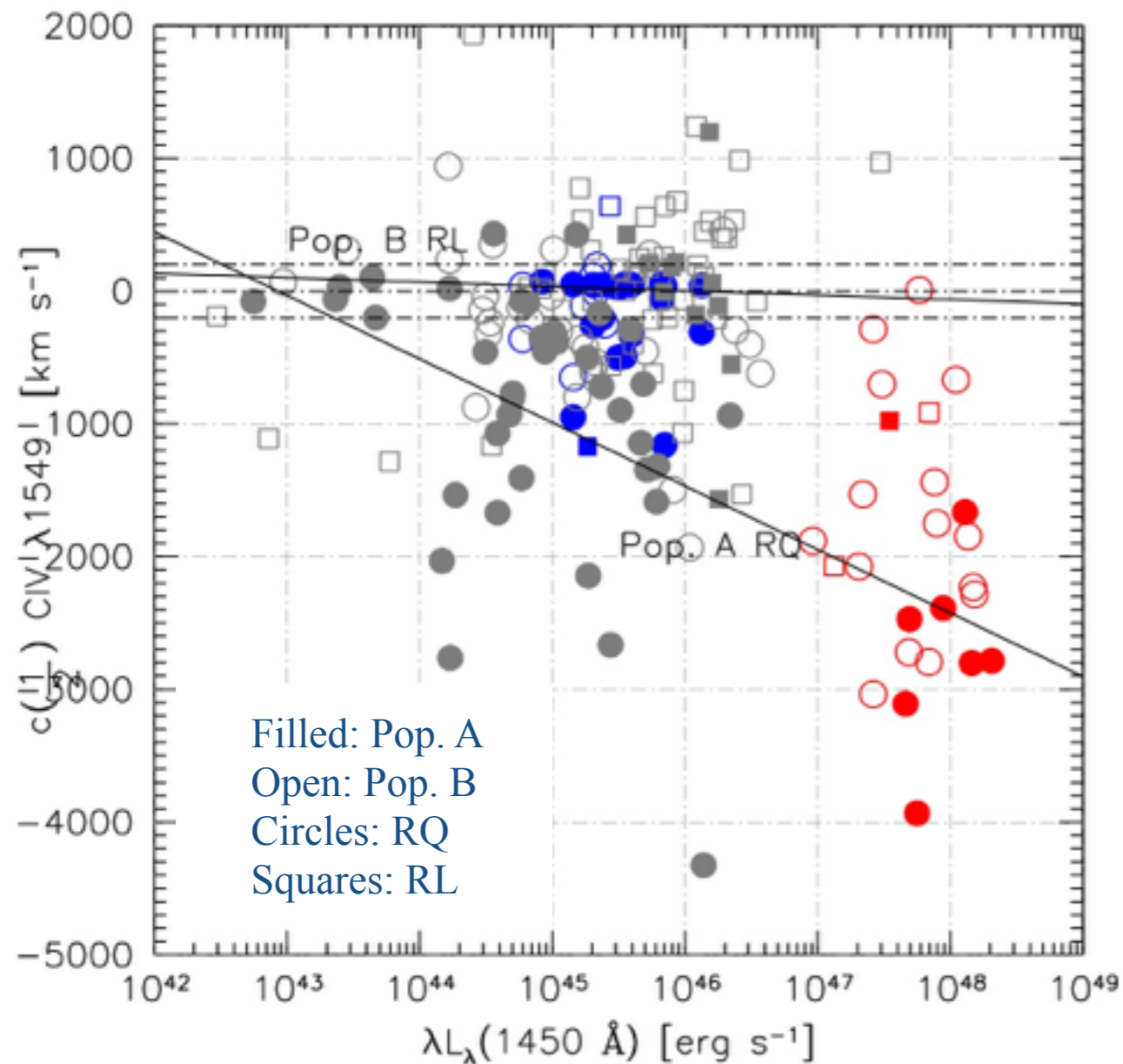
No strong effect of Radio Loudness on LIL profiles, only on HILs.



H β RL vs RQ
Pop. B

Large blueshifts are apparently more frequent at high L but shift amplitudes at lower L are comparable

$$\frac{c\left(\frac{1}{2}\right)}{HWHM(H\beta)} \quad \text{“Dynamical relevance” of CIV}\lambda 1549 \text{ shift}$$



Blueshift trends are consistent with a radiation-driven wind

Using $2 \times c(1/4)$ as a proxy of terminal velocity

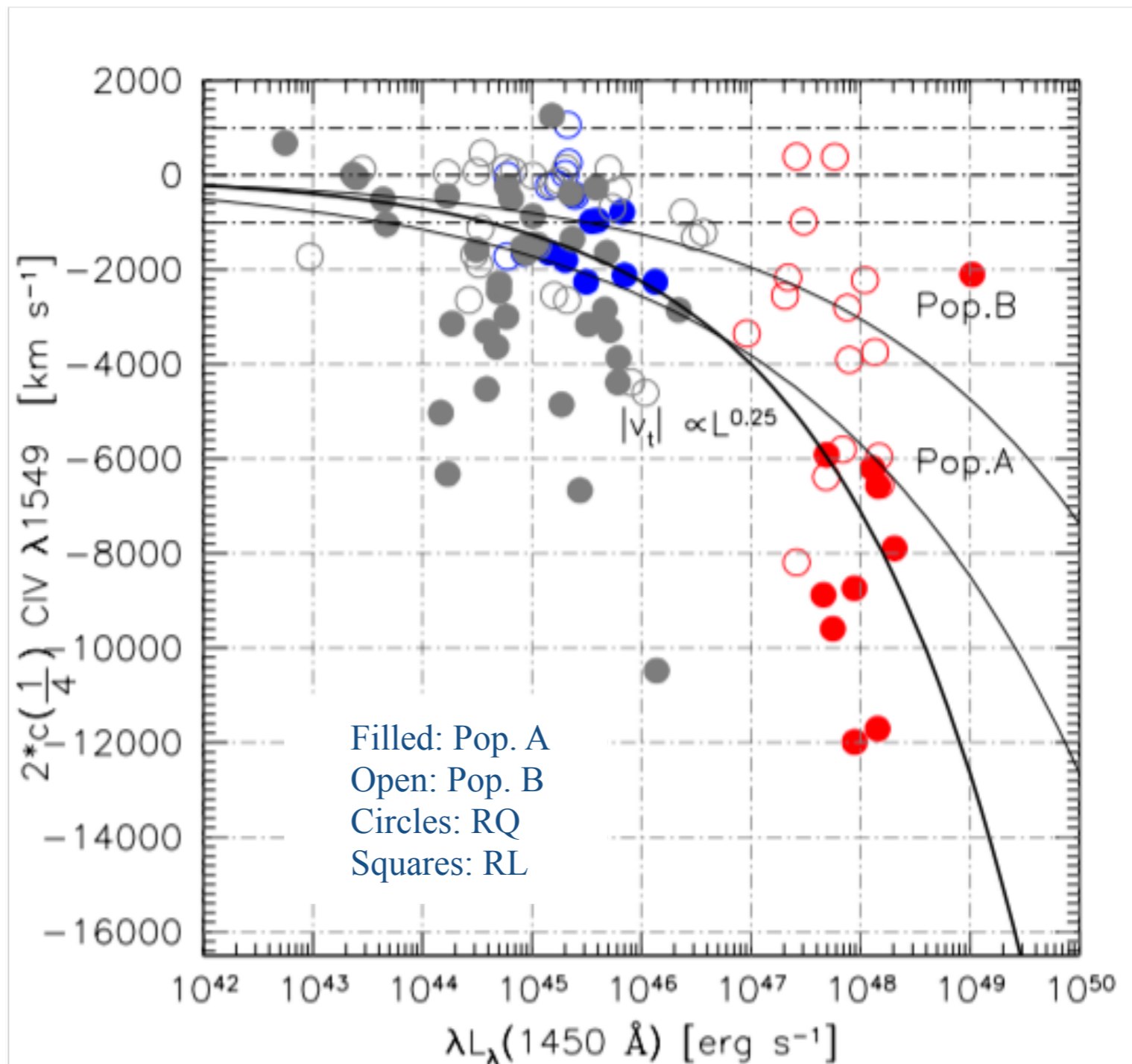
Assuming:

$$v_t \sim v_K \sqrt{\mathcal{F} \frac{L}{L_{\text{Edd}}}}$$

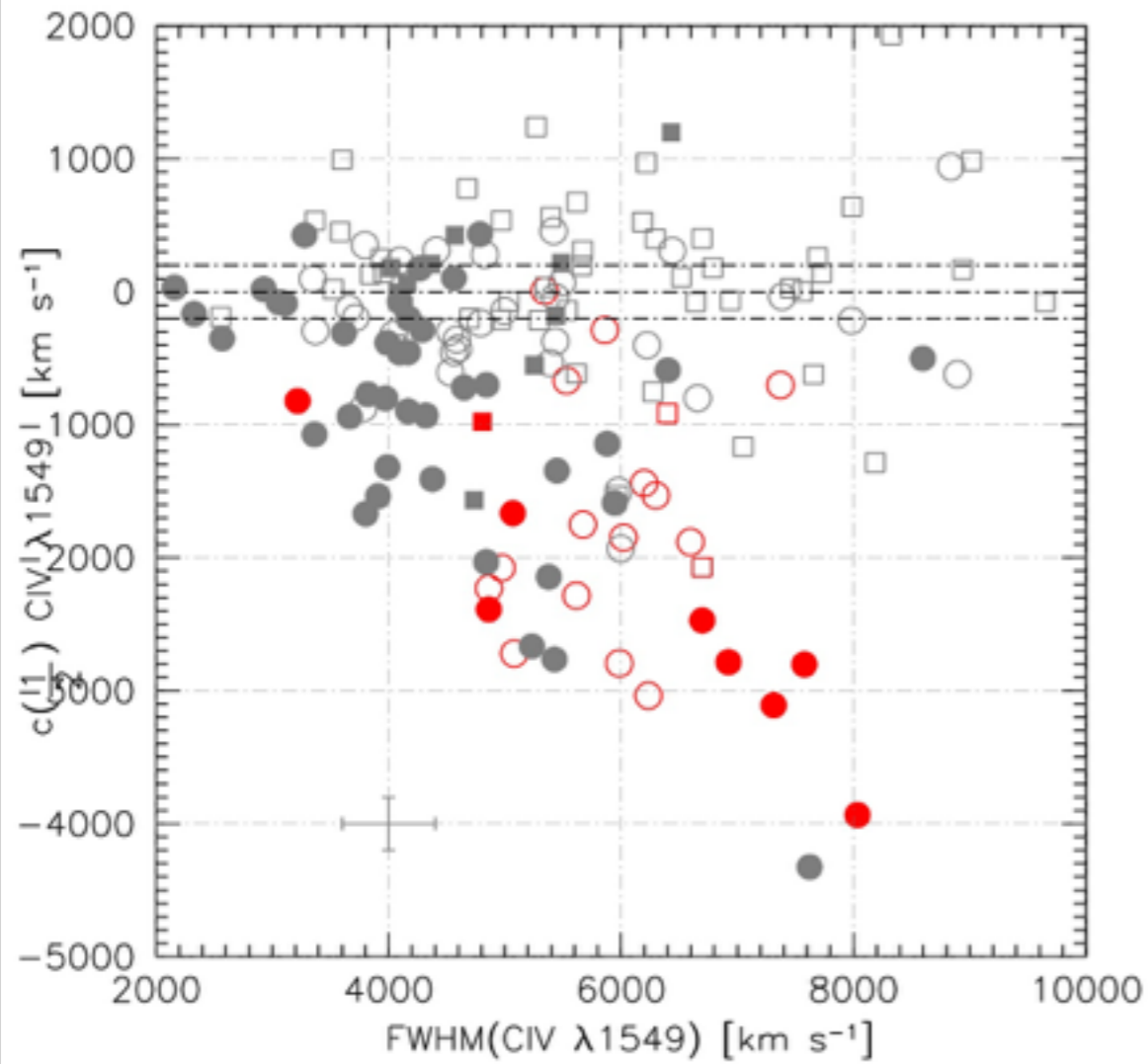


$$v_t \propto L^{1/4}$$

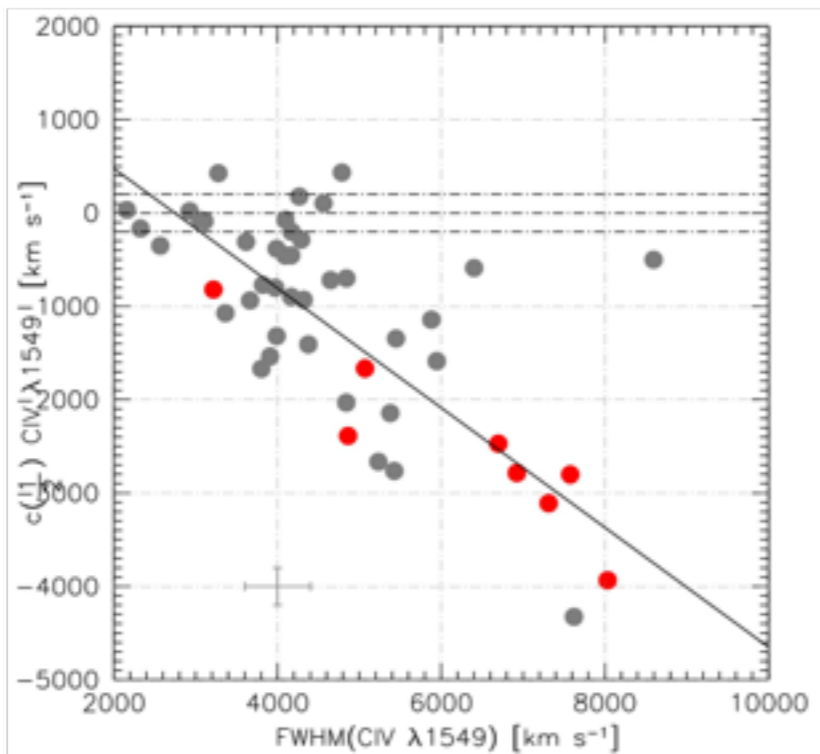
Laor & Brandt 2002



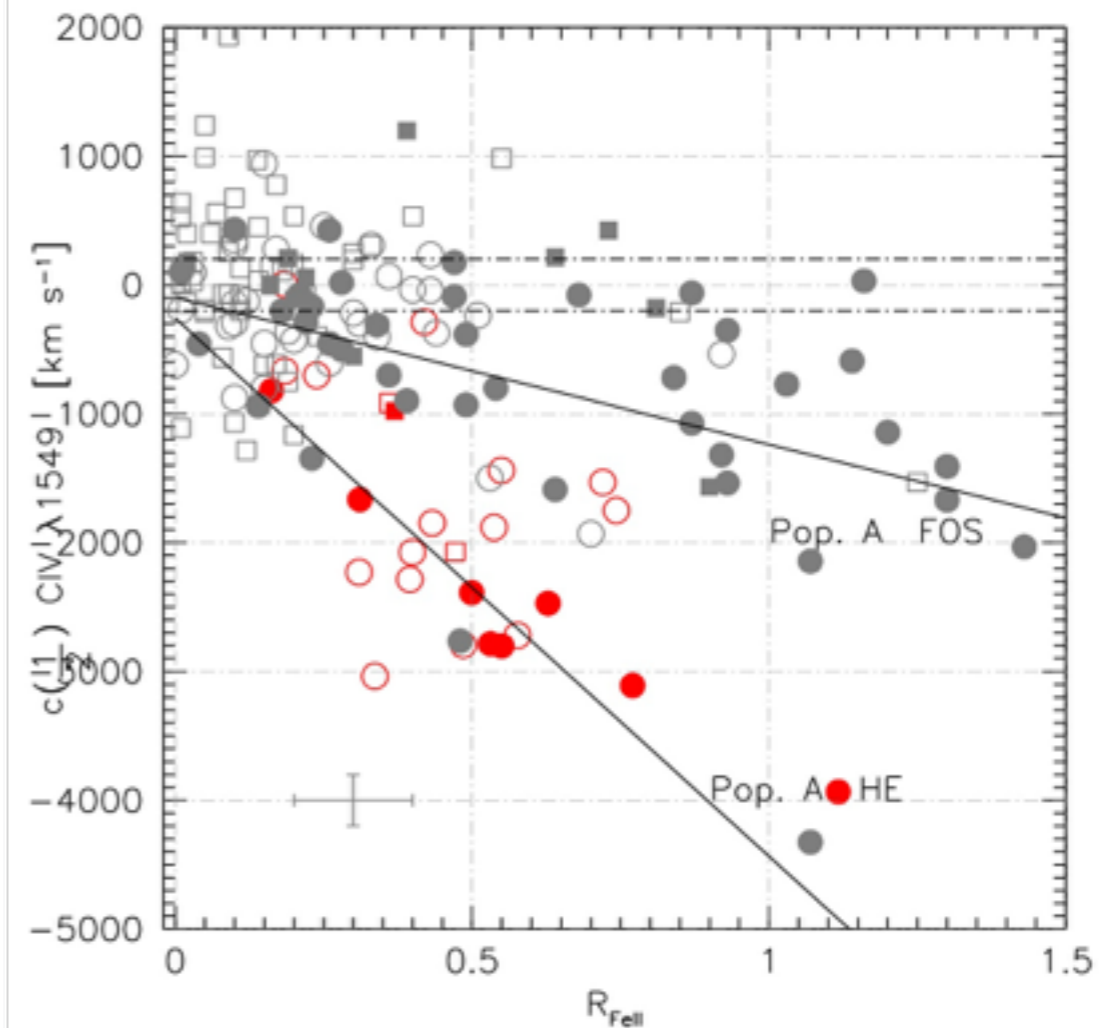
Correlations with 4DE1 parameters FWHM(H β) $R_{\text{FeII}} = F(\text{FeII}\lambda 4570) / F(\text{H}\beta)$



Filled: Pop. A
Open: Pop. B
Circles: RQ
Squares: RL



Pop. A
RQ
only



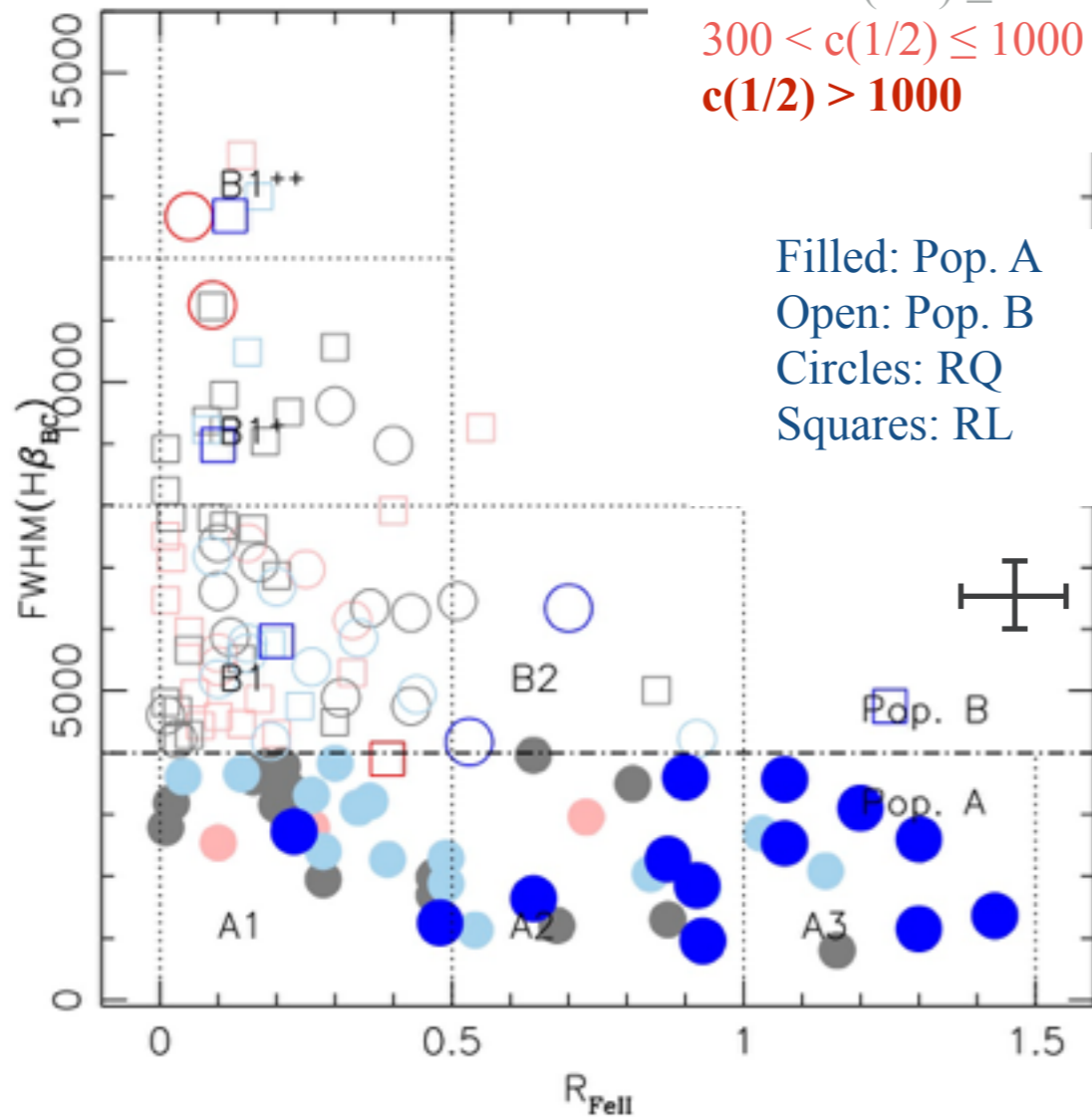
High-L HE quasars in the optical plane of the 4DE1

Luminosity (Mass) effect visible in a systematic increase of the minimum FWHM possible for a sub-Eddington radiator

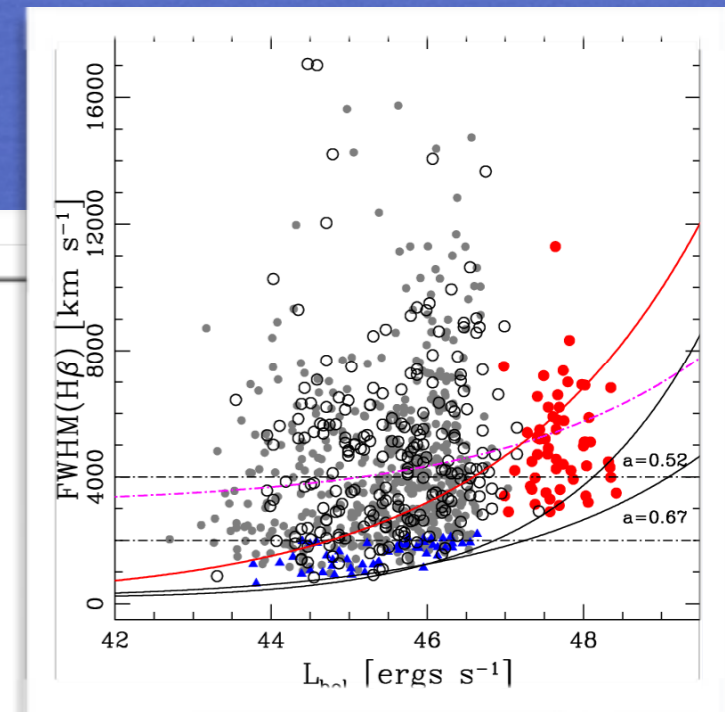
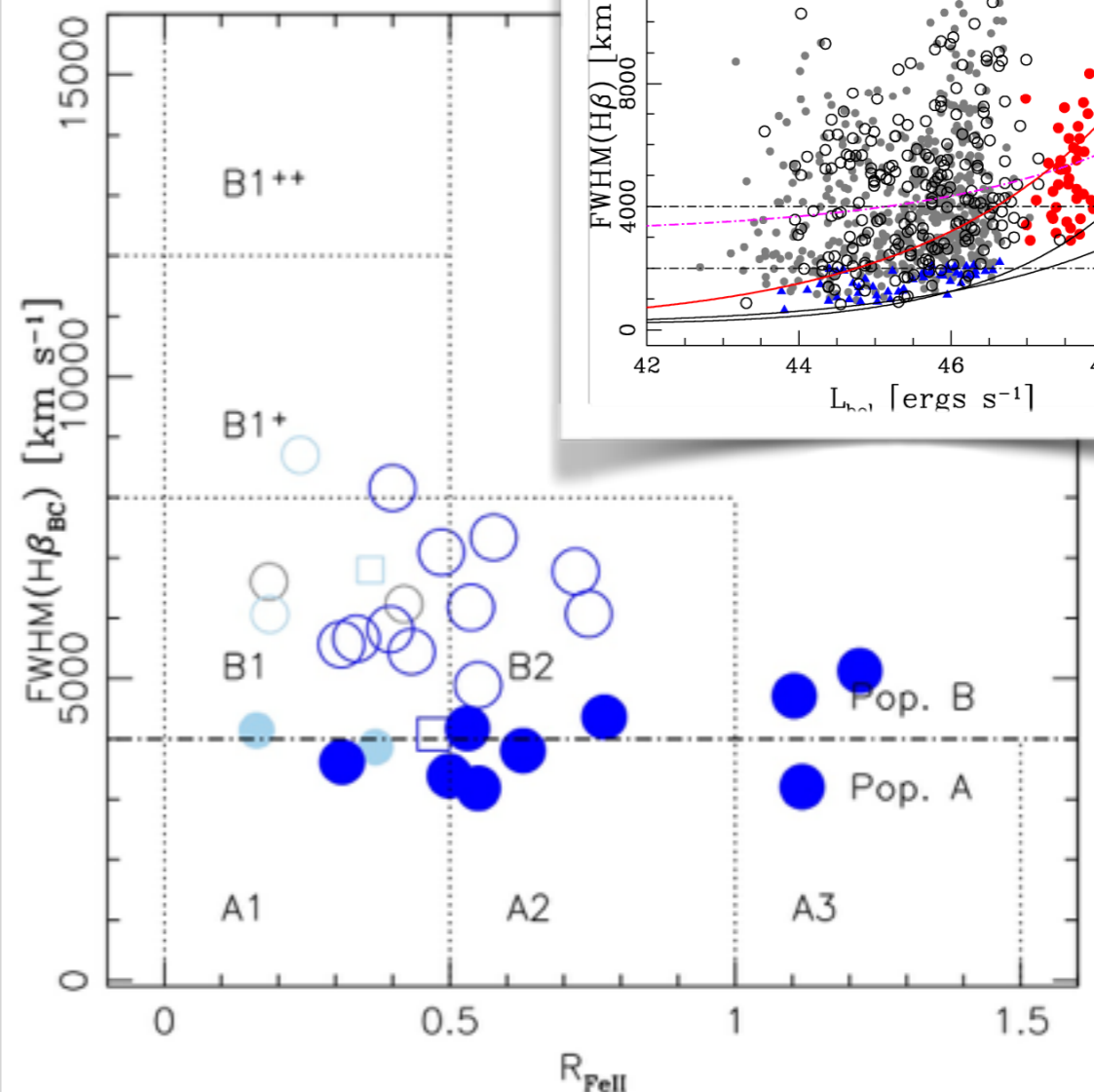
FOS

$c(1/2) \leq -1000$
 $-300 \geq c(1/2) > -1000$
 $-300 < c(1/2) \leq 300$
 $300 < c(1/2) \leq 1000$
 $c(1/2) > 1000$

Filled: Pop. A
 Open: Pop. B
 Circles: RQ
 Squares: RL



HE



Virial Black Hole Mass & Eddington ratio

geometry
dynamics

Keplerian velocity field: the BLR dynamics dominated by the gravity of a central mass; $v \propto r^{-1/2}$

$$M_{\text{BH}} = \frac{f r (\delta v)^2}{G}$$

r_{BLR}

FHWM
 σ
FWZI

valid for low-ionization lines
H β and MgII λ 2800

$$M_{\text{BH}}(\text{H}\beta) = 1.05 \times 10^8 \left[\frac{L_{5100}}{10^{46} \text{ ergs s}^{-1}} \right]^{0.65} \left[\frac{\text{FWHM}(\text{H}\beta)}{10^3 \text{ km s}^{-1}} \right]^2 M_{\odot}$$

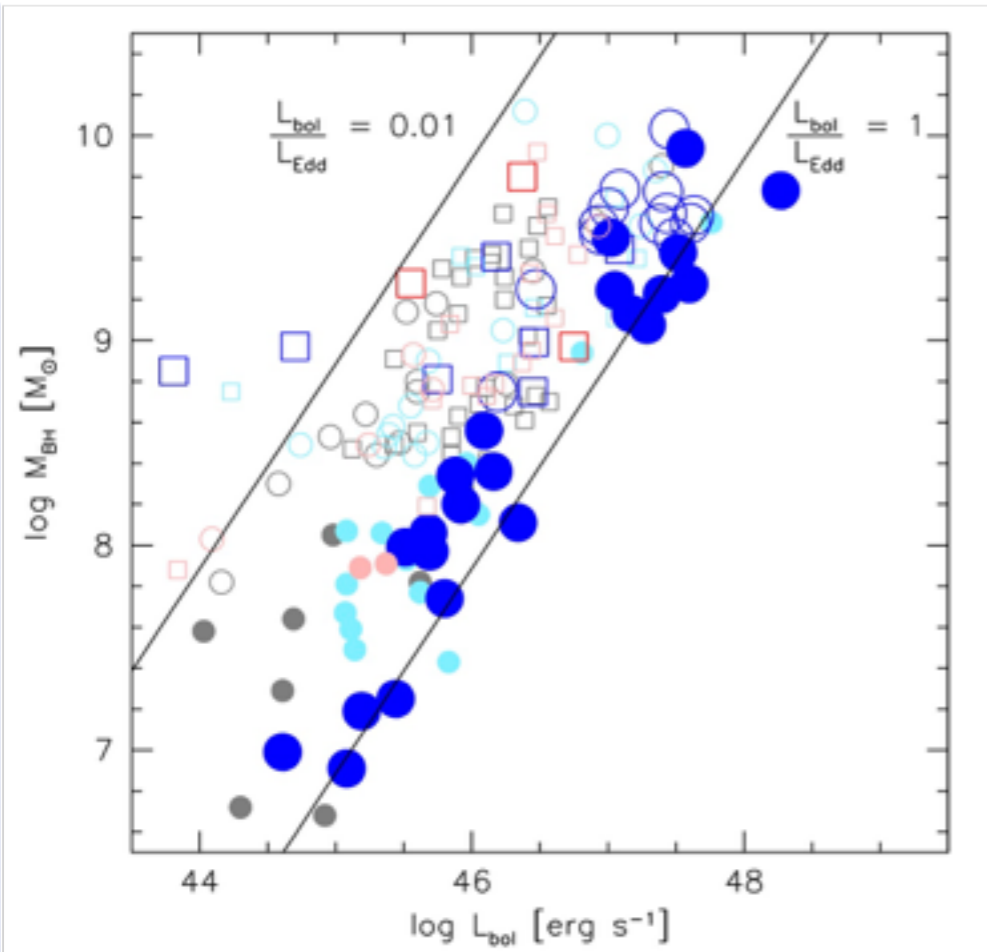
for large samples: $r \propto L^{1/2} \rightarrow M_{\text{BH}} = M_{\text{BH}}(L, \text{FWHM})$

(Vestergaard & Peterson 2006; Trakhtenbrot & Netzer 2012)

$$\text{Eddington ratio} = \frac{L_{\text{bol}}}{L_{\text{Edd}}} \propto \frac{\lambda L_{\lambda} \times \text{B.C.}}{M_{\text{BH}}}$$

Bolometric correction not trivial especially at high L

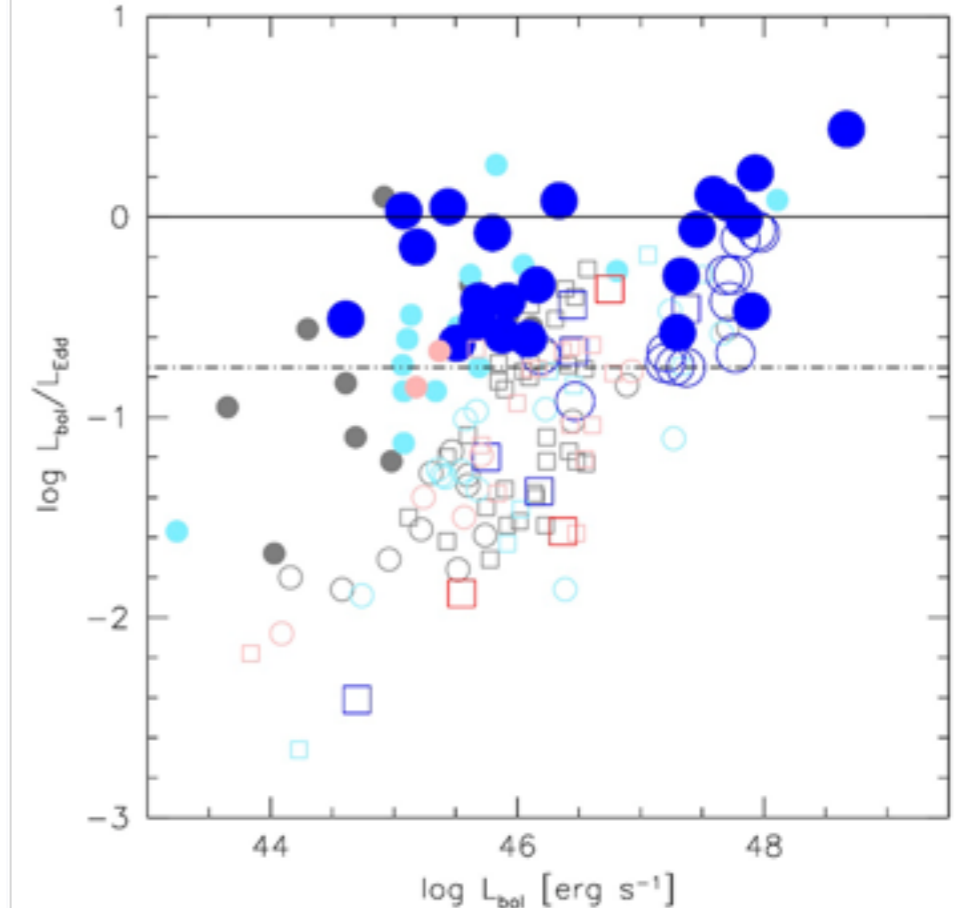
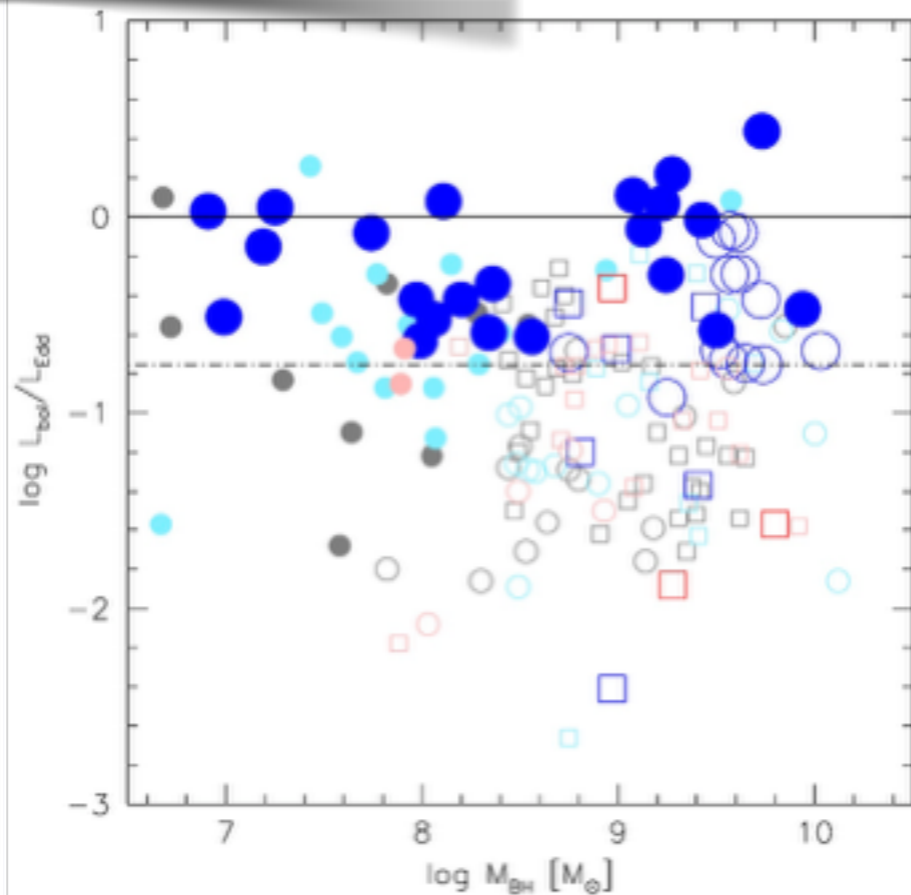
(Richards et al. 2006; Runnoe et al. 2013)



Largest CIV λ 1549 blueshifts
 are observed at high L/L_{EDD}
 but not necessarily at high
 M_{BH} or high L

$c(1/2) \leq -1000$
 $-300 \geq c(1/2) > -1000$
 $-300 < c(1/2) \leq 300$
 $300 < c(1/2) \leq 1000$
 $c(1/2) > 1000$

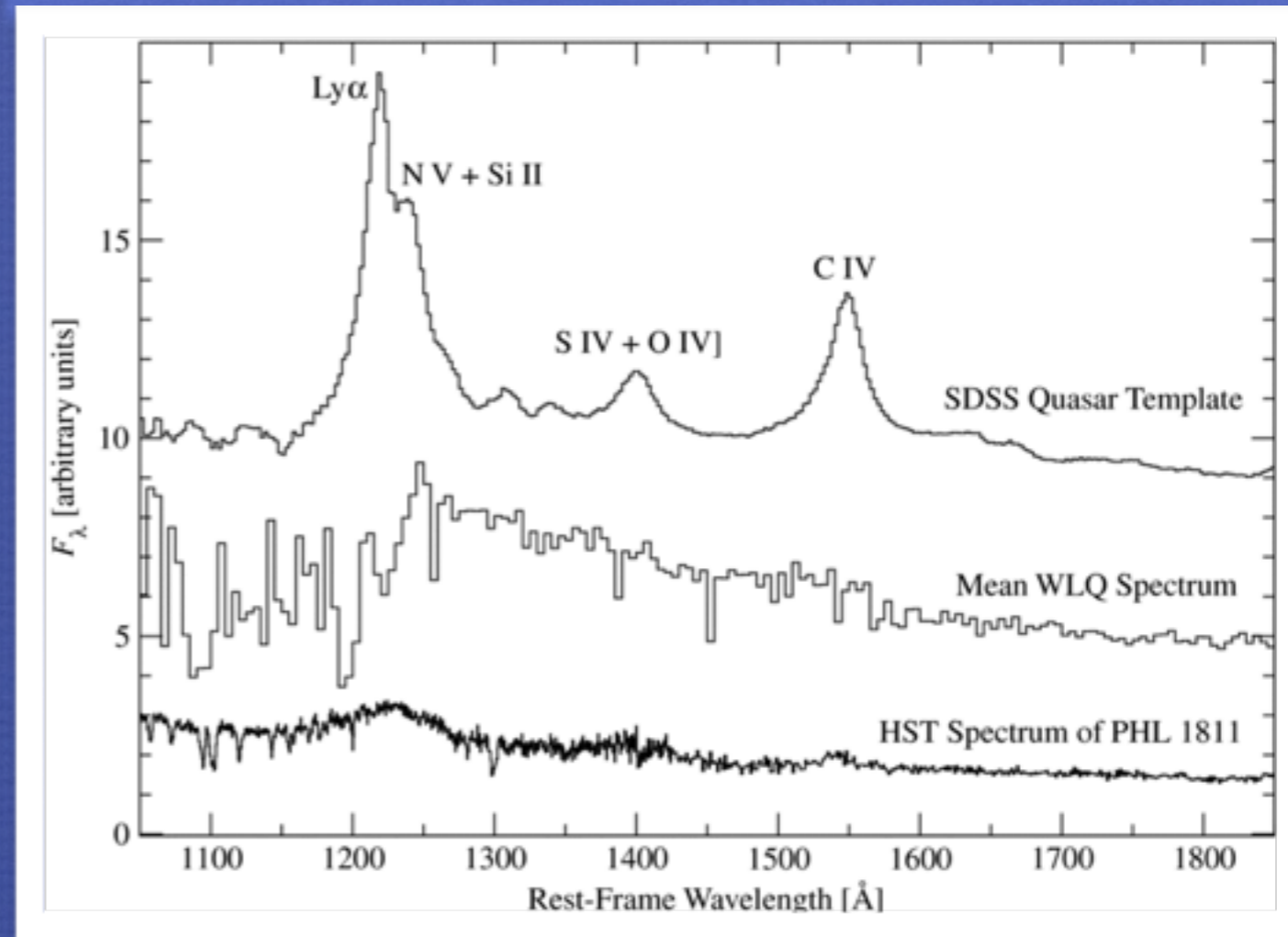
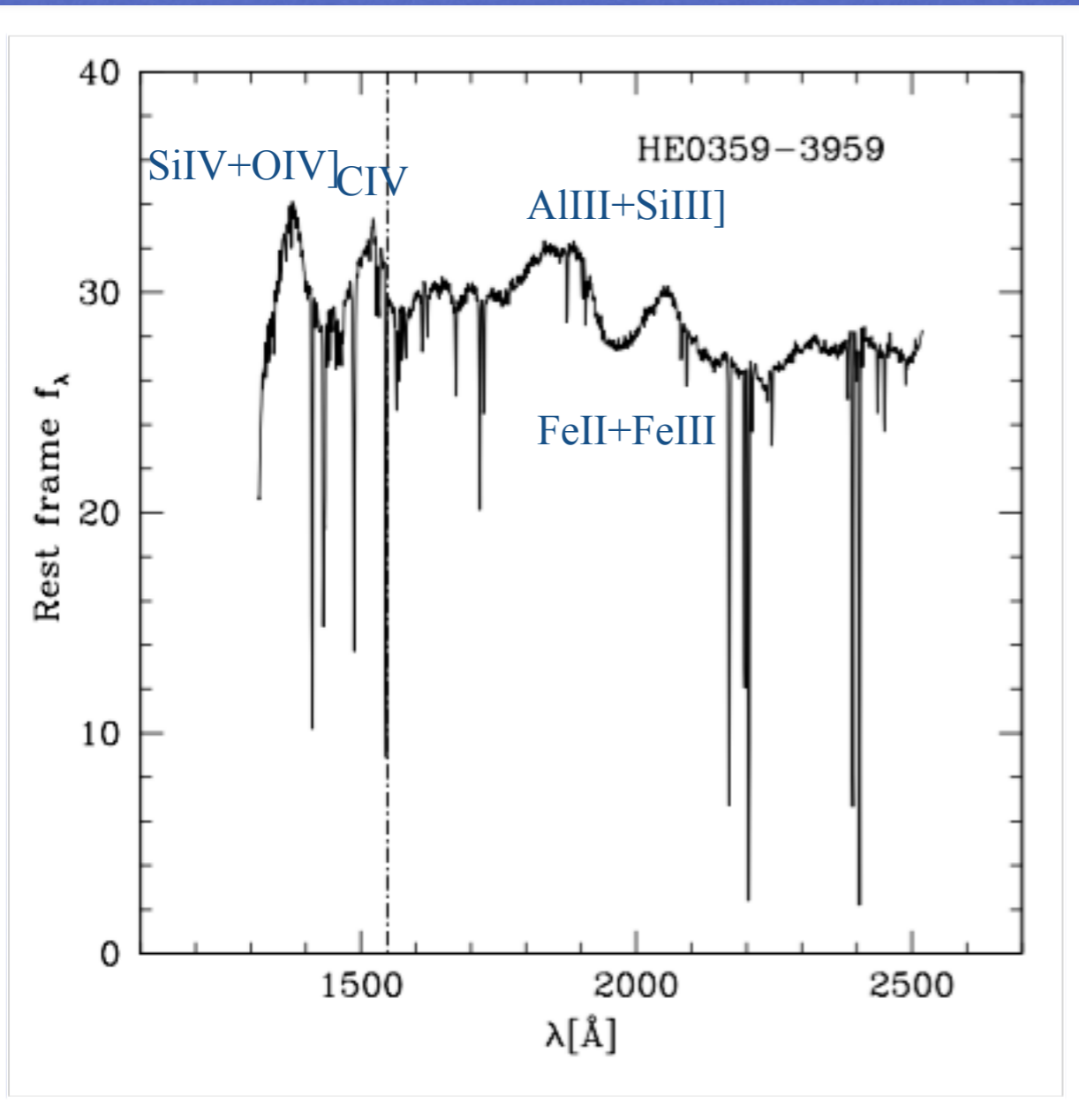
Filled: Pop. A
 Open: Pop. B
 Circles: RQ
 Squares: RL



Weak Lined Quasars (WLQs)

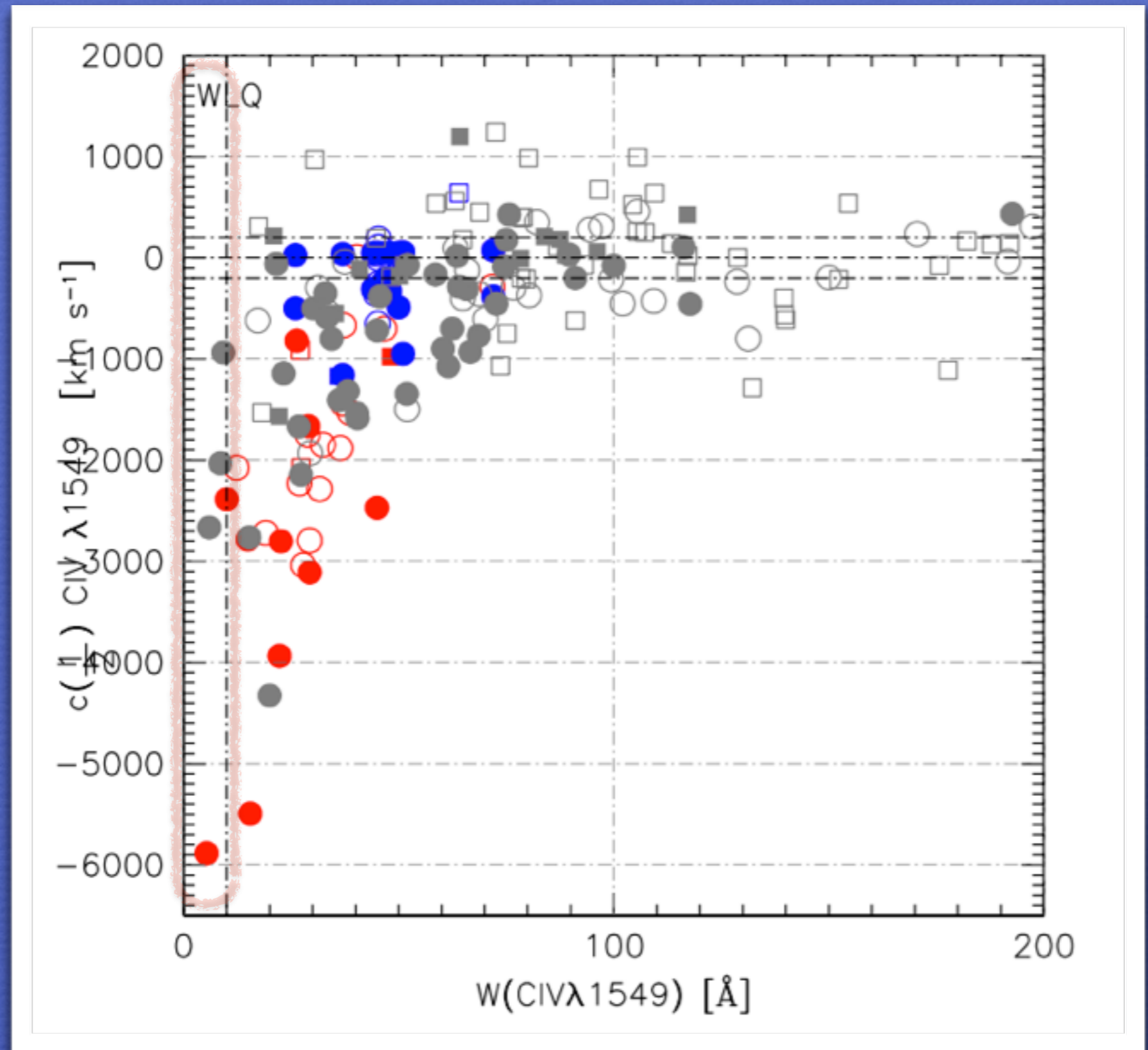
Low equivalent width of CIV λ 1549 ($\leq 10 \text{ \AA}$) and Ly α ($\leq 16 \text{ \AA}$)

Diamond-Stanic et al. 2009



Shemmer et al. 2009

$W(\text{CIV}\lambda 1549)$ vs CIV shift



$c(1/2) \leq -1000$

$-300 \geq c(1/2) > -1000$

$-300 < c(1/2) \leq 300$

$300 < c(1/2) \leq 1000$

$c(1/2) > 1000$

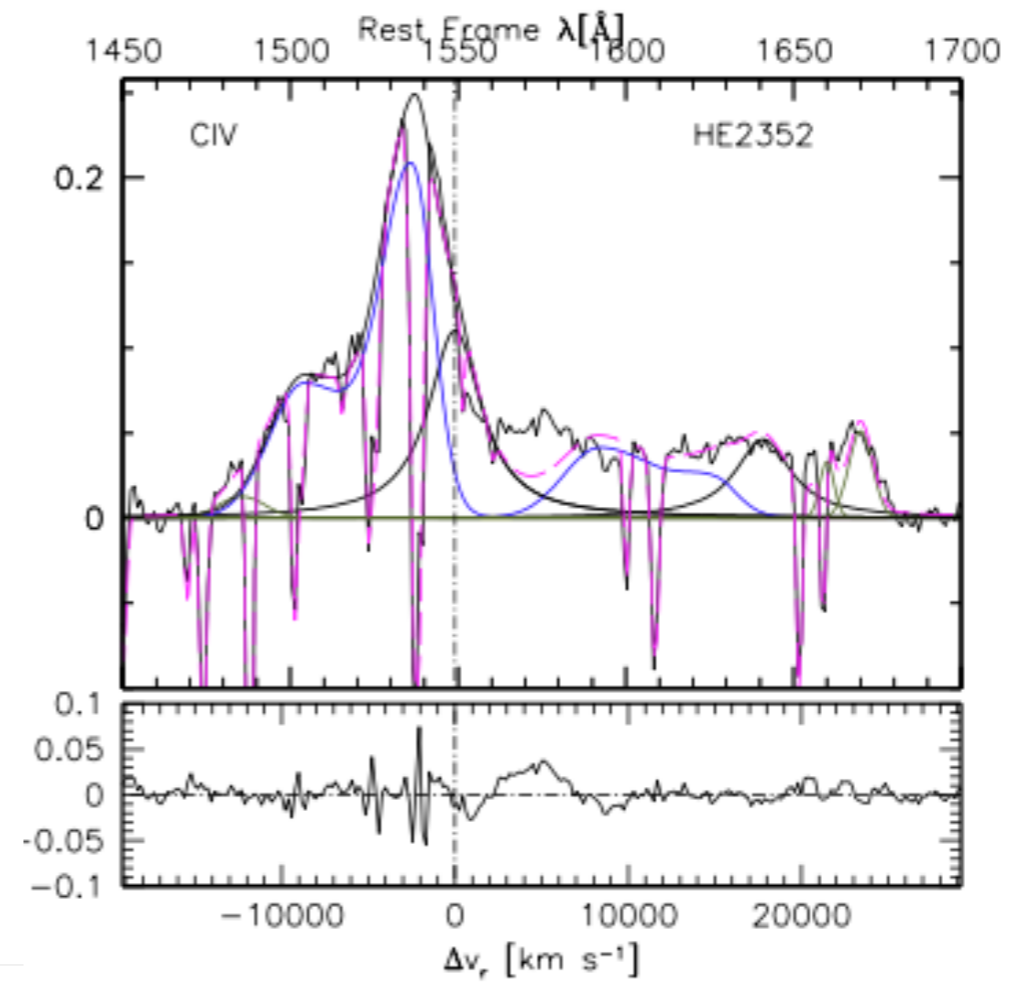
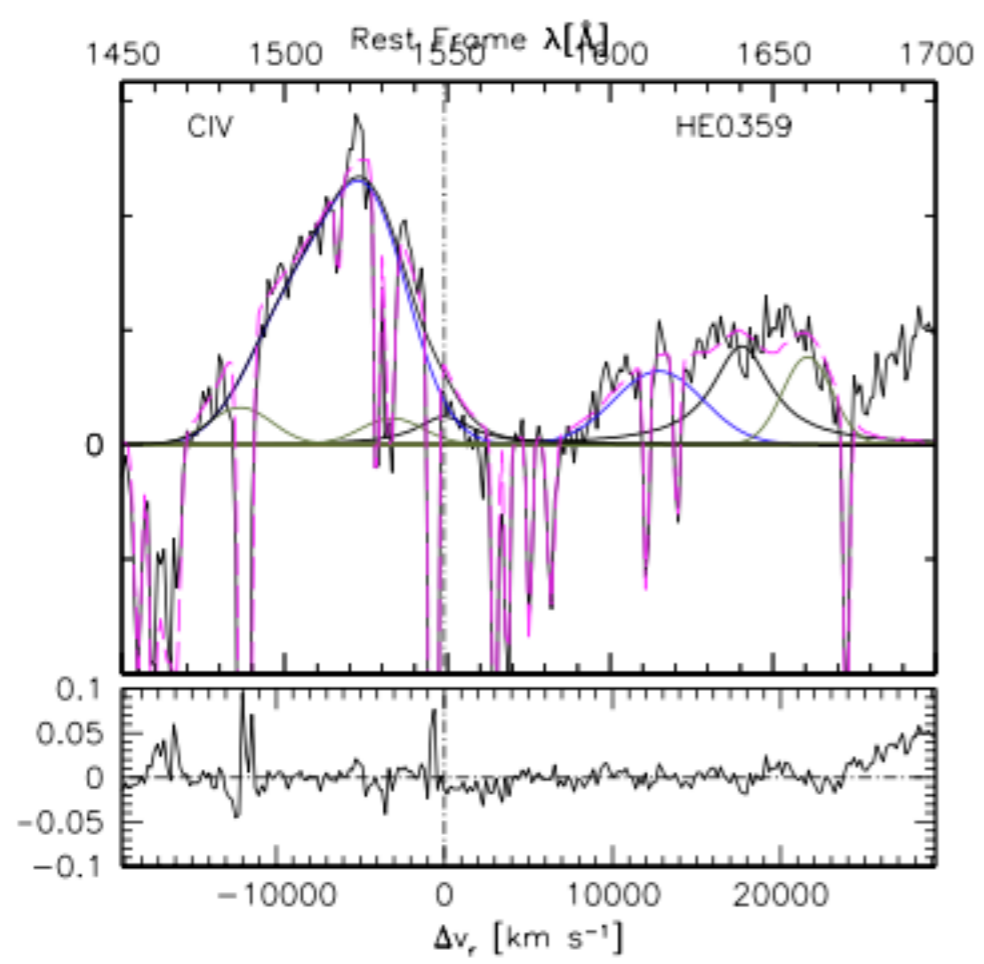
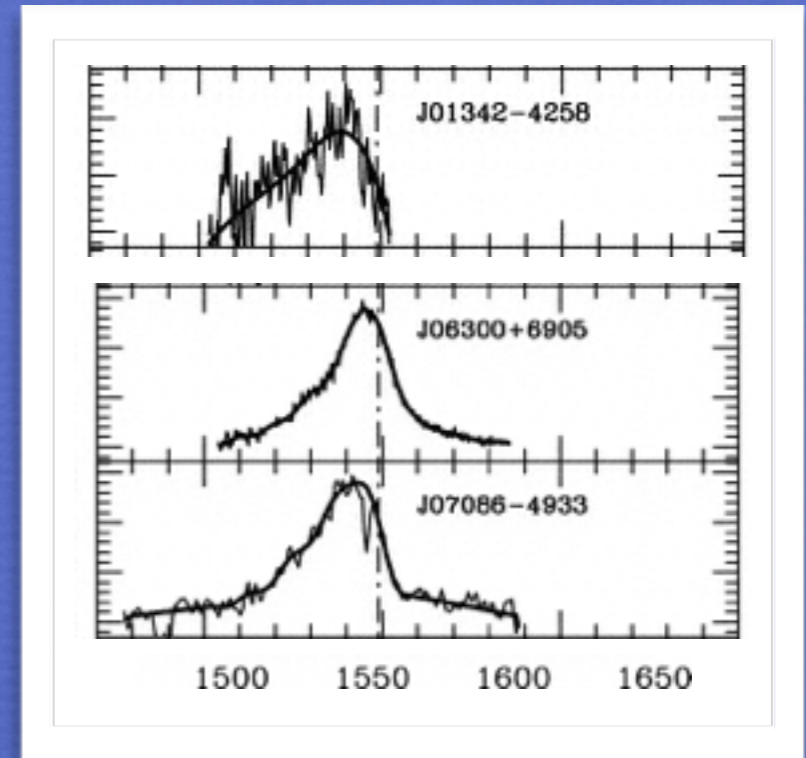
Filled: Pop. A

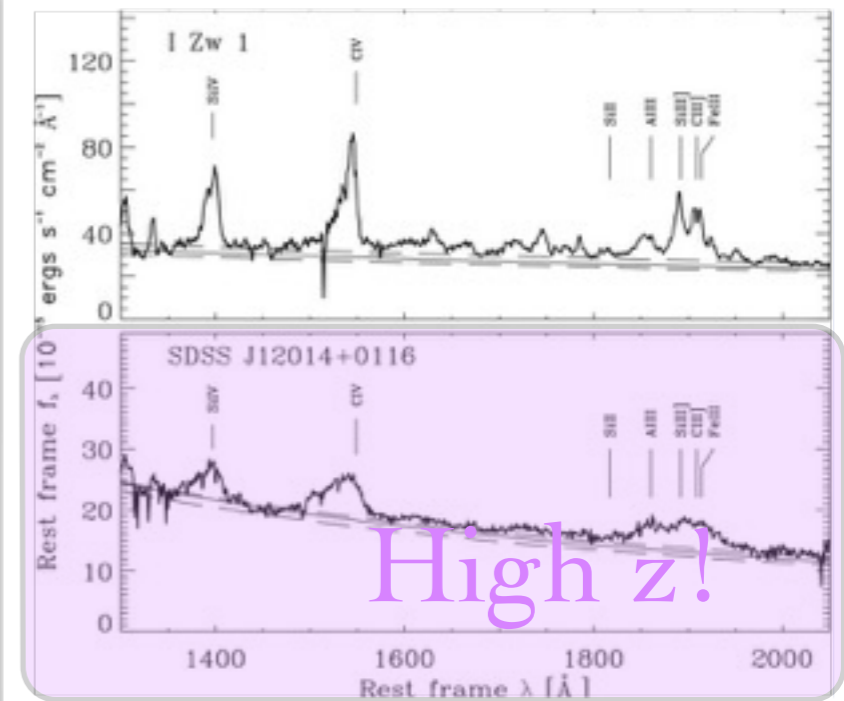
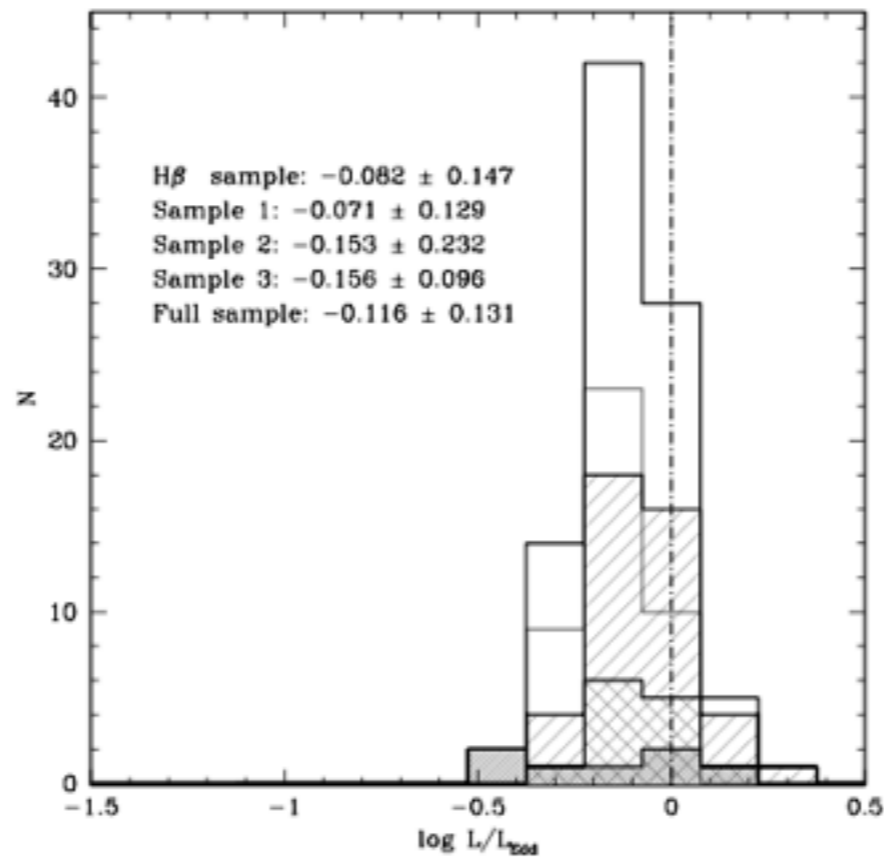
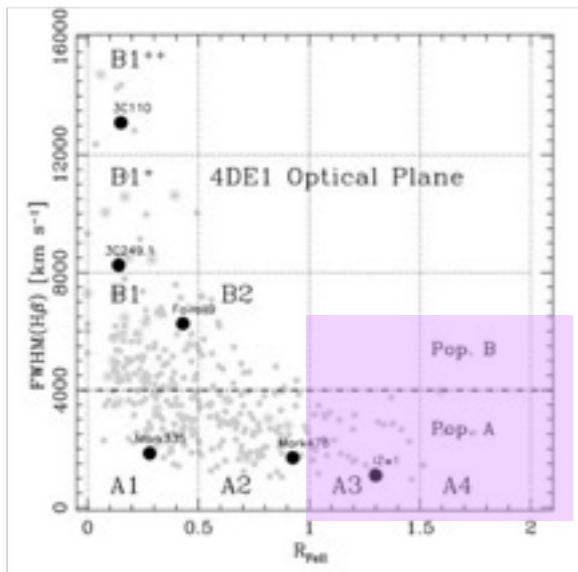
Open: Pop. B

Circles: RQ

Squares: RL

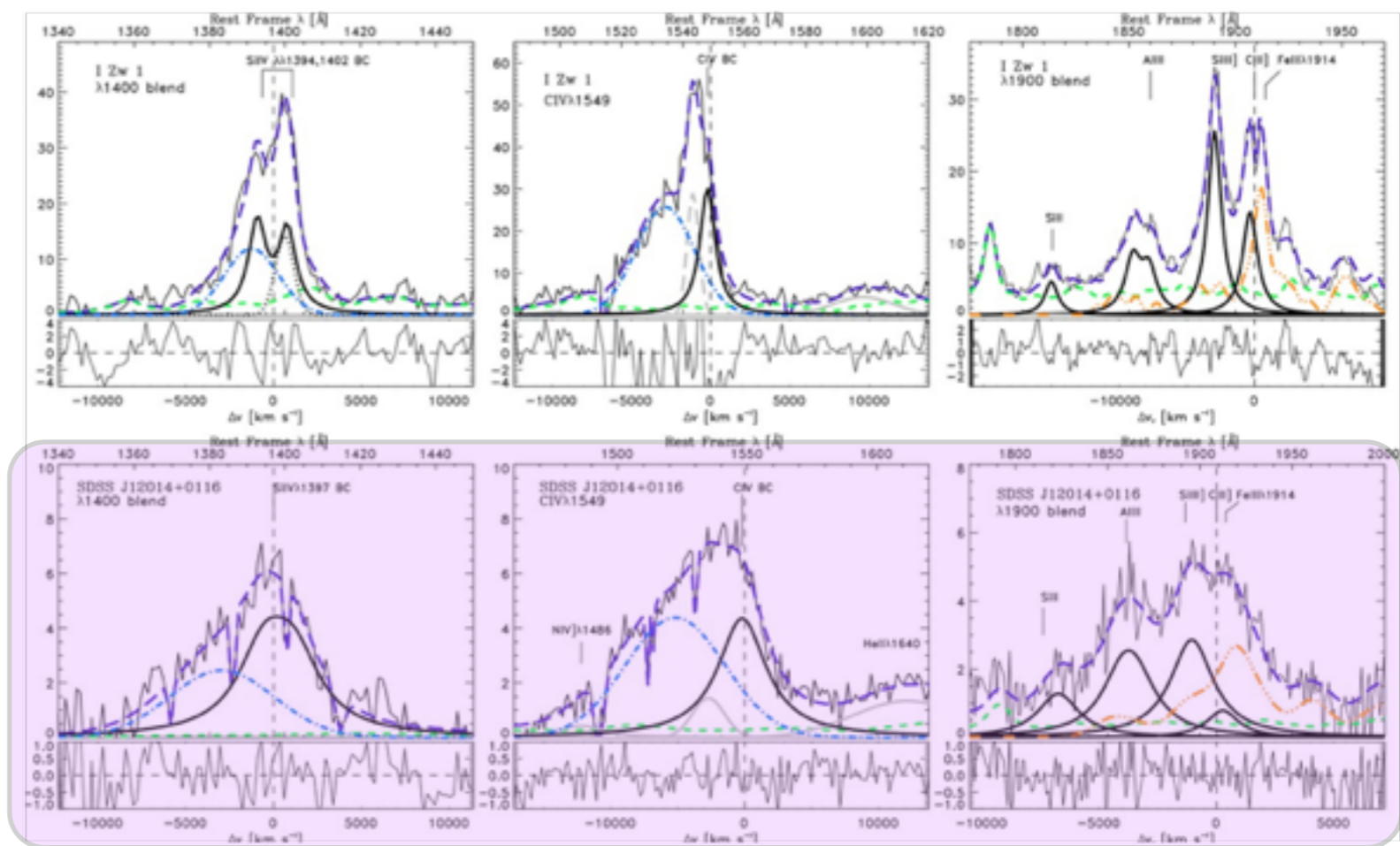
CIV $\lambda 1549$ profiles show extreme blueshifts





UV spectrum
consistent with
extreme A quasars
revealed at both high
and low luminosity,
radiating at high
Eddington ratio

(Dultzin et al. 2011; Negrete et al. 2012
Marziani & Sulentic 2014)



WLQs in the optical plane of 4D Eigenvector 1

Most —all of the ones at high- z — are extreme Pop. A sources with $R_{\text{FeII}} > 1$, with CIV showing extreme outflow velocities

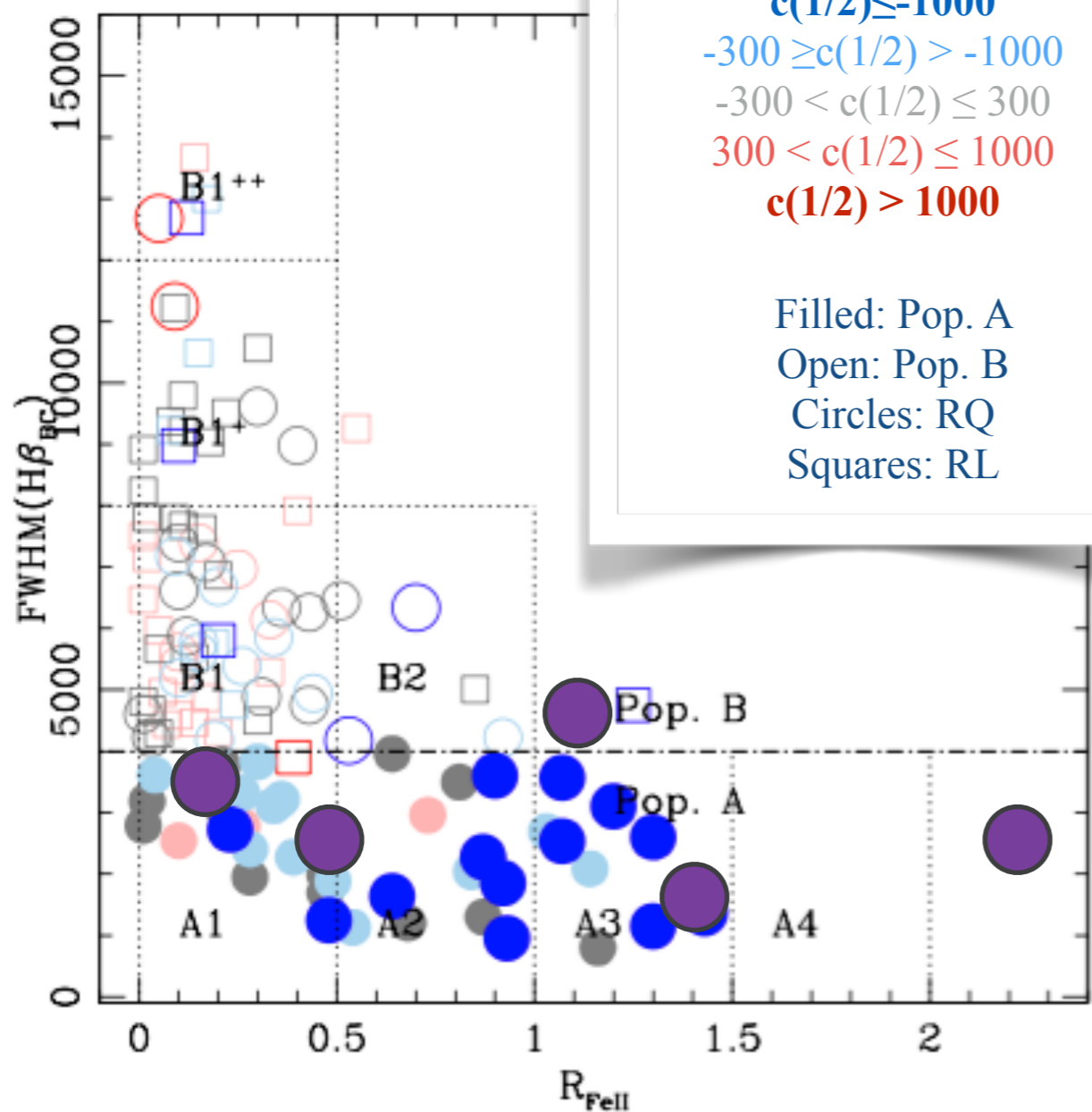
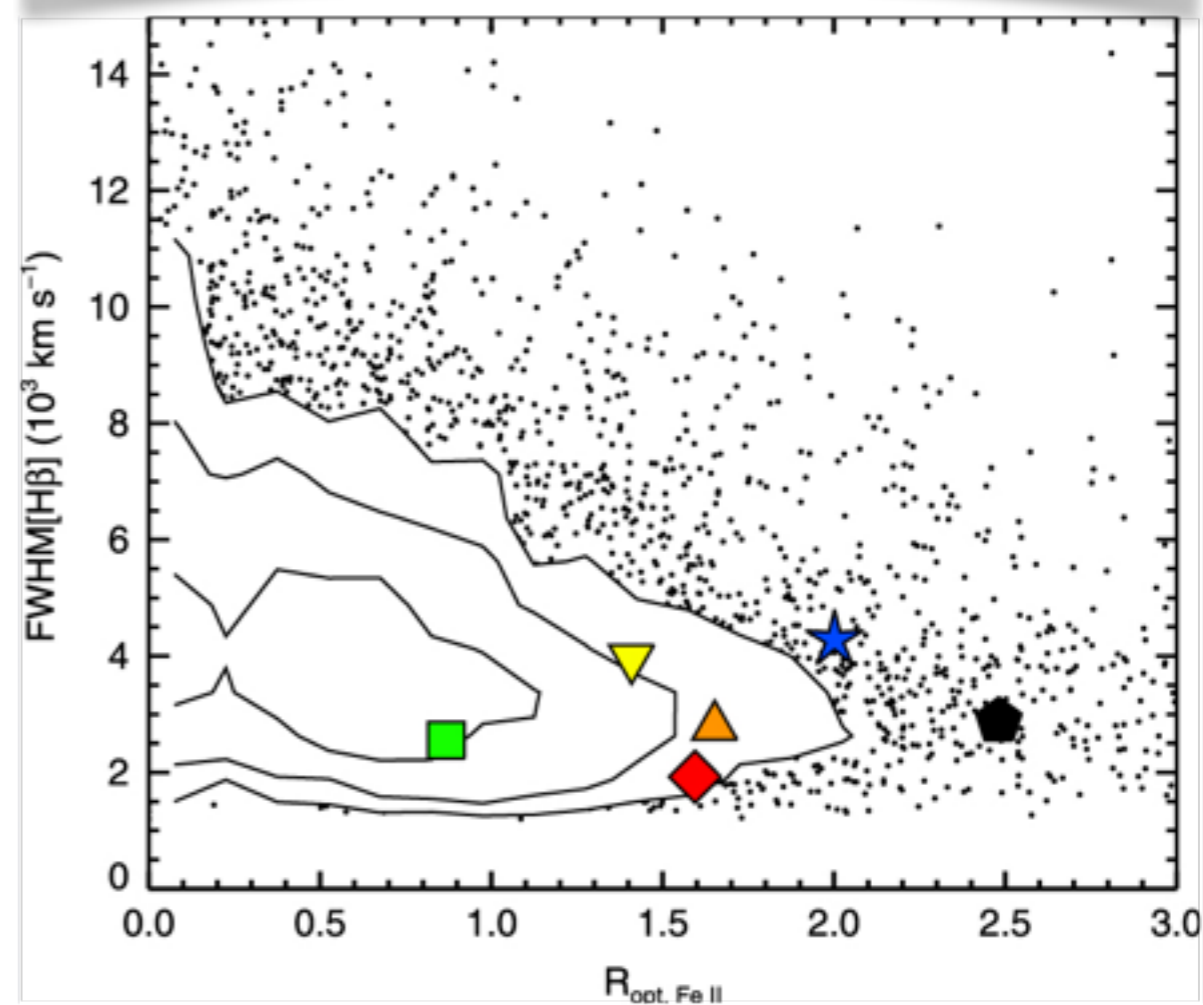


Table 4
Line Luminosities and Blueshifts

Name	$\log L[\text{H}\alpha]$ (erg s^{-1})	$\log L[\text{H}\beta]$ (erg s^{-1})	$\log L[\text{Mg II}]$ (erg s^{-1})	$\log L[\text{C IV}]$ (erg s^{-1})	$\Delta v[\text{Mg II}]$ (km s^{-1})	$\Delta v[\text{C IV}]$ (km s^{-1})
J0836	$44.29^{+0.11}_{-0.06}$	$43.71^{+0.09}_{-0.09}$	$43.56^{+0.09}_{-0.06}$	43.54 ± 0.07	197 ± 216	2266 ± 191
J0945	44.64 ± 0.05	44.02 ± 0.08	44.29 ± 0.02	43.75 ± 0.12	1281 ± 183	5485 ± 380
J1321	$43.89^{+0.07}_{-0.04}$	$43.32^{+0.09}_{-0.06}$	$43.48^{+0.11}_{-0.03}$	$43.95^{+0.08}_{-0.06}$	202 ± 188	396 ± 189
J1411	$44.03^{+0.05}_{-0.06}$	43.52 ± 0.20	43.34 ± 0.06	$43.60^{+0.08}_{-0.08}$	-136 ± 181	3142^{+129}_{-208}
J1417	$44.15^{+0.07}_{-0.03}$	43.45 ± 0.11	43.88 ± 0.02	$43.55^{+0.08}_{-0.05}$	624 ± 180	5321^{+417}_{-612}
J1447	$43.99^{+0.07}_{-0.03}$	$43.41^{+0.11}_{-0.03}$	$43.56^{+0.09}_{-0.02}$	$43.89^{+0.09}_{-0.15}$	1 ± 185	1319^{+129}_{-381}

Note. $\Delta v[\text{Mg II}]$ and $\Delta v[\text{C IV}]$ are line of sight blueshifts of the peaks of the Mg II and C IV profiles, respectively. Δv is based on the observed wavelength of each line center (expected to be at rest-frame 2800 Å for Mg II and 1549 Å for C IV) compared to the systemic redshifts in Table 1. Blueshifts are defined to be positive for unambiguous motions.



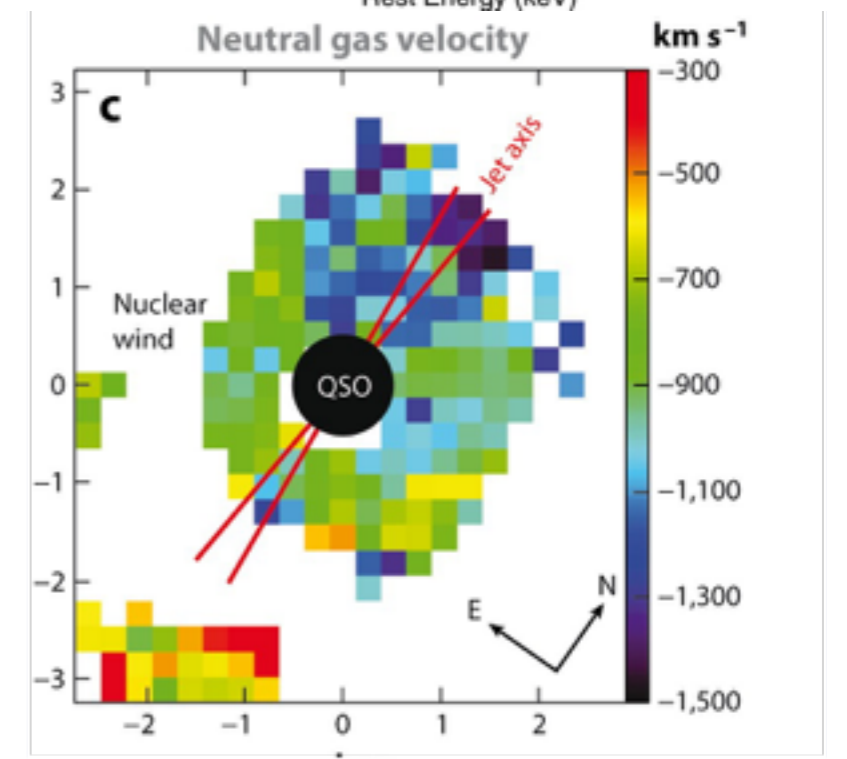
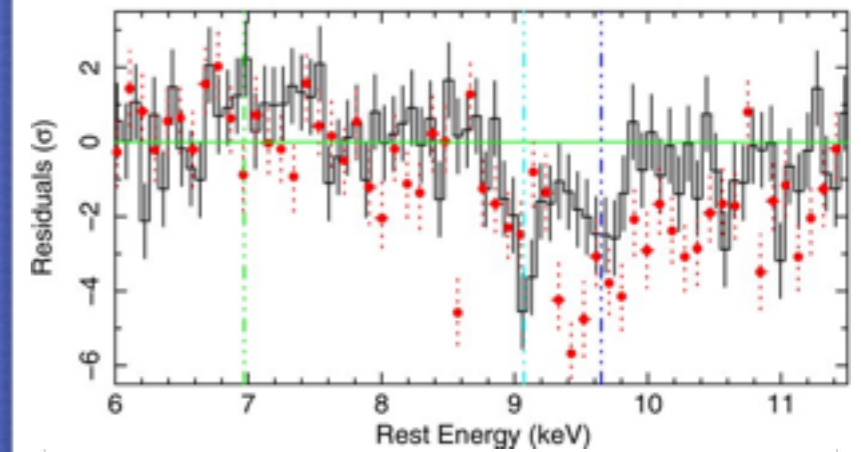
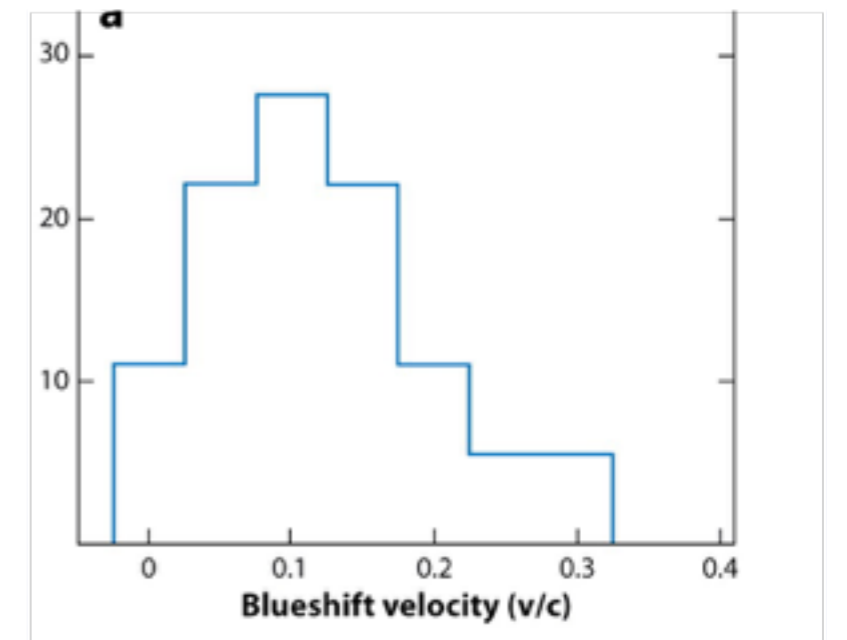
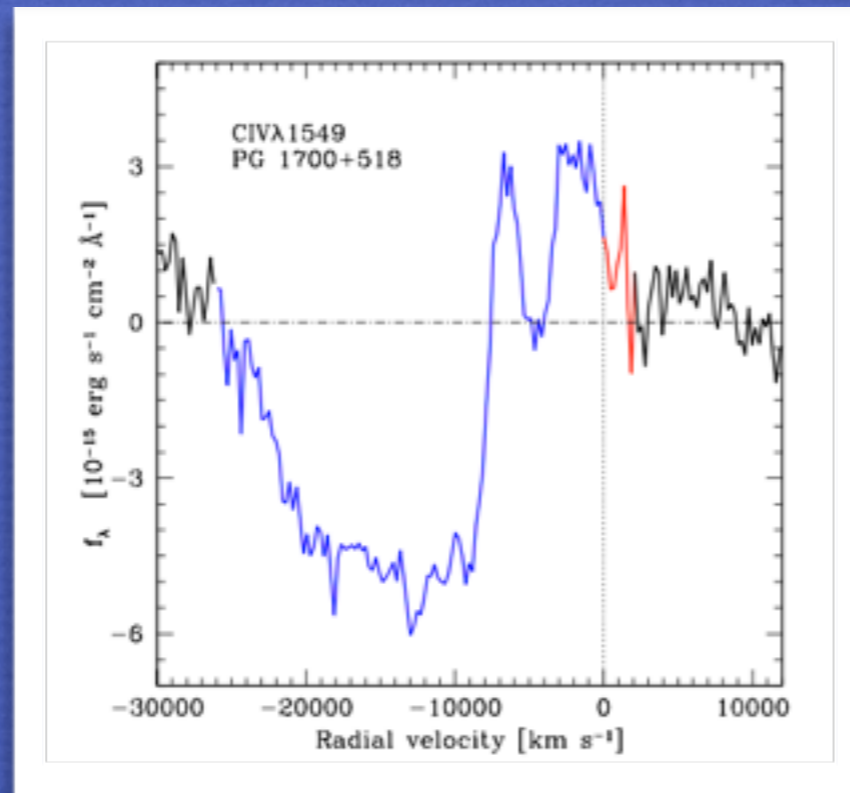
The observational evidence of the active nucleus feedback is still debated

UFO

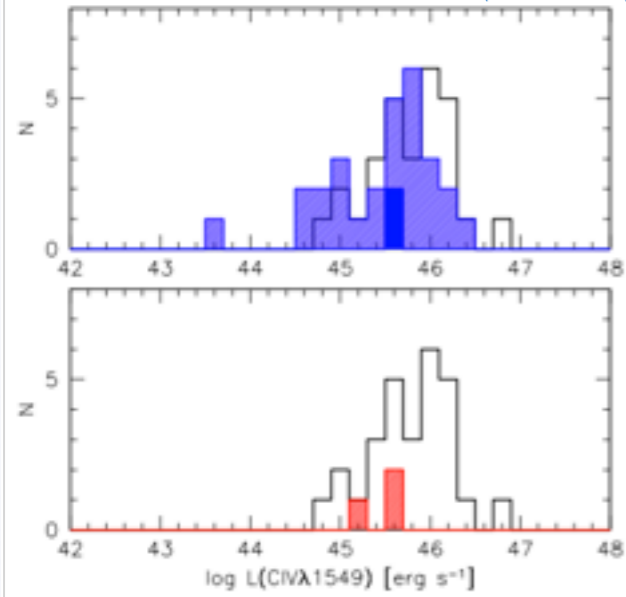
Table 1 Observational evidence for AGN feedback

Evidence	Quality
High-velocity broad absorption lines in quasars	Strong
Strong winds in AGN	Strong
1,000 km s ⁻¹ galactic outflows	Strong
Bubbles and ripples in brightest cluster galaxies	Strong
Giant radio galaxies	Strong
Lack of high star-formation rate in cool cluster cores	Indirect
<i>M</i> - σ relation	Indirect
Red and dead galaxies	Indirect
Lack of high lambda, moderate N_H , quasars	Indirect
Steep <i>L</i> - <i>T</i> relation in low <i>T</i> clusters and groups	Indirect

Large Balnicity index BAL QSOs are a minority of quasars

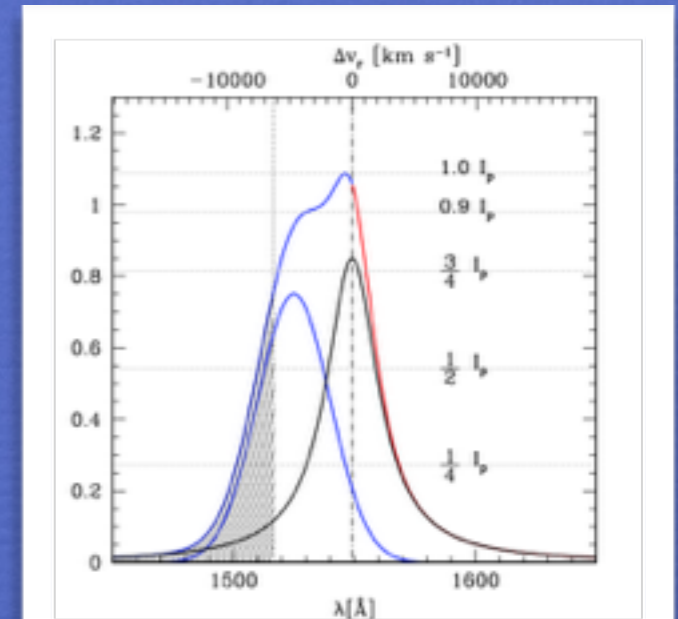


Full and BLUE line L (shaded)



CIV $\lambda 1549$ blue component

a fraction of the line emitting gas is above the expected projected escape velocity at $r \sim 1000 R_g$.



King & Pounds 2015; Fabian 2012; Cano.Diaz et al. 2014

The mass of ionised gas emitting CIV $\lambda 1549$ can be written as, under the assumption of constant density:

$$M_{\text{out}}^{\text{ion}} = 9.5 \cdot 10^2 L_{45}(\text{CIV}) \left(\frac{Z}{5Z_{\odot}} \right)^{-1} n_g^{-1} M_{\odot}$$

The mass outflow rate at a distance r (1 pc) can be written as, if the flow is confined to a solid angle of Ω :

$$\dot{M}_{\text{out}}^{\text{ion}} = \rho \Omega r^2 v = \frac{M_{\text{out}}^{\text{ion}}}{V} \Omega r^2 v \approx 15 L_{45} v_{5000} r_1^{-1} M_{\odot} \text{ yr}^{-1}$$

The outflow kinetic power, with outflow v in units of 5000 km s^{-1} , is:

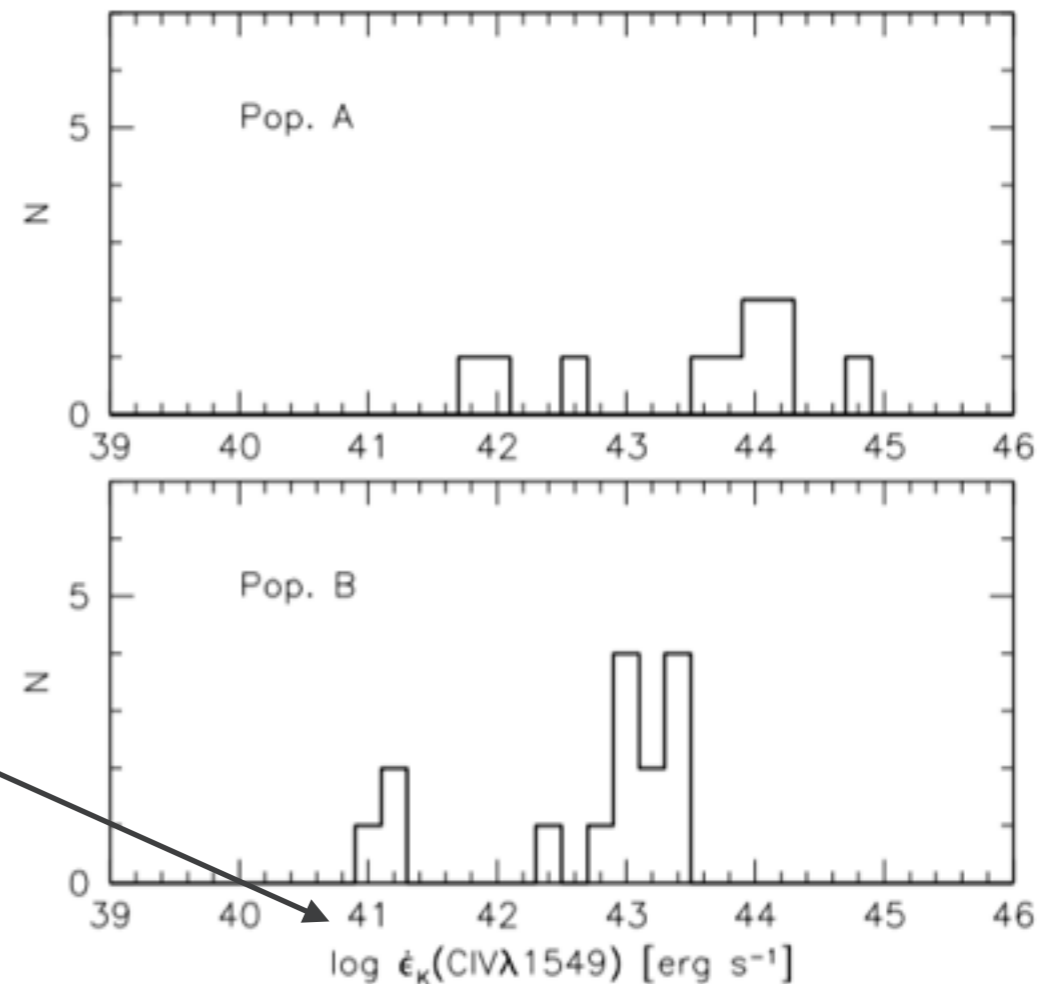
$$\dot{\epsilon} = \frac{1}{2} \dot{M}_{\text{out}}^{\text{ion}} v^2 \approx 1.2 \cdot 10^{44} L_{45} v_{5000}^3 r_1^{-1} \text{ erg s}^{-1}.$$

The total energy expelled over a duty cycle of 10^8 yr is

$$\int \dot{\epsilon} dt \approx 3.6 \cdot 10^{59} L_{45} v_{5000}^3 r_1^{-1} \tau_8 \text{ erg}.$$

This value can be compared to the binding energy of the gas in a massive bulge/spheroid:

$$U = \frac{3GM_{\text{sph}}^2 f_g}{5R_e} \approx 2 \cdot 10^{59} M_{\text{sph},11}^2 f_{g,0.1} R_{e,2.5\text{kpc}}^{-1} \text{ erg}$$



Conclusions

4DE1 provides an interpretation framework at extreme luminosity.

The CIV analysis reveals blueshifted emission associated with quasars outflows in RQ quasars, with high amplitude shifts being frequent at high L .

“Unexpected” luminosity effects are not seen: larger CIV shifts are expected for a radiation driven wind. The outflow phenomenology is self-similar over a wide range of L .

The CIV blueshift-dominated profile in the most luminous sources supports the idea that the outflow may be at the origin of galactic-scale feedback effects.